INTEGRATED PERFORMANCE BASED DESIGN OF COMMUNITIES AND DISTRIBUTED GENERATION

A Thesis
Presented to
The Academic Faculty

by

Michael A. Street

In Partial Fulfillment
of the Requirements for the Degree
Doctor of Philosophy in the
College of Architecture

Georgia Institute of Technology
December 2016

INTEGRATED PERFORMANCE BASED DESIGN OF COMMUNITIES AND DISTRIBUTED GENERATION

Approved by:

Godfried Augenbroe, Advisor
College of Architecture
Georgia Institute of Technology

Jason Brown
College of Architecture
Georgia Institute of Technology

Roderick K. Jackson
Building Technology Research and Integration Center
Oak Ridge National Laboratory

Michael Stadler
Grid Integration Group
Lawrence Berkeley National Laboratory

Santiago Grijalva
School of Electrical and Computer Engineering
Georgia Institute of Technology

Date Approved: August 26, 2016

DEDICATION

To Dallas H. Green, may you be inspired to always reach for your dreams.

ACKNOWLEDGEMENTS

I can do all this through Him who gives me strength. - Phillipians 4:13

I would like to thank my committee for their support and guidance throughout the development of this work. Thank you to Professors Godfried Augenbroe and Jason Brown for their critical role in bringing me to the Georgia Institute of Technology and their coursework, which truly allowed me to develop a more complete understanding of the role that physics and engineering plays in the design of architectural systems, spaces and experiences. Thank you to Dr. Roderick Jackson for his continued mentoring and his belief in my abilities to pursue research both at the Oak Ridge National Laboratory and the Georgia Institute of Technology. A special thank you to my dissertation readers Dr. Michael Stadler and Prof. Santiago Grijalva for their thought provoking comments and additions. This dissertation would not have been possible without Dr. Stadler's support and work to produce and license the DER-CAM tool for use in this context.

Thank you to my grandfather Llyod Street, Ph.D. without whom the idea and dream of advancing scientific knowledge through the pursuit of a doctoral degree may never have materialized. Thank you to my friends and family and their never-ending love and support that has allowed me to concentrate so deeply on the task at hand.

Finally, I would especially like to thank my lab mates in the High Performance Buildings Lab in particular Gustavo, Qinpeng, Jenny and Yuna. Your conversation and insight have contributed greatly to my development and understanding of the core problems addressed both by our lab and within this dissertation.

This material is based upon work supported by the National Science Foundation Graduate Research Fellowship under Grant No. 0946809. Any opinions, findings, and conclusions or recommendations expressed in this material are those of the author(s) and do not necessarily reflect the views of the National Science Foundation.

Onwards and upwards.

TABLE OF CONTENTS

LIST OF TABLES

LIST OF FIGURES

SUMMARY

The vertically integrated utility market within the U.S. is undergoing rapid changes due to the rise of small-scale distributed power generation known as microgrids, which are local networks of power generation and distribution typically serving a demand less than 40 MW. Primary drivers for microgrid investment are the performance benefits these systems return to their owners, which include increased reliability, reduced emissions and reduced operating costs. We define a novel modeling methodology to represent the microgrid as an integrated system of the demand and supply. Previous work to develop an integrated system model does not adequately model the building thermal demand, incorporate a modelers knowledge of the grids availability or allow for a user to model their tolerance for unmet demand. To address these modeling issues, we first demonstrate a technique for representing a building stock as a reduced order hourly demand model. Next, as demand side measures are typically defined at the building level as discrete options, we demonstrate a technique for converting a large discrete optimization problem into a simplified continuous variable optimization problem through the use of Pareto efficient cost functions. The reduced problem specification results in 90% fewer function evaluations for a benchmark optimization task. Then, we incorporate two new features into the Distributed Energy Resource Customer Adoption Model (DER-CAM) developed by Lawrence Berkeley National Laboratory (LBNL) that allow users to define grid outage scenarios and their limit of expected energy demand not served. Applying the integrated model to a microgrid design scenario return solutions that exhibit on average an 8% total annual cost reduction and 18% reduction in CO_2 emissions versus a *Supply Only* case. Similarly, the results on average reduce total annual cost by 5% and annual emissions by 17% for a *Demand First* case. In summary, we present a modeling methodology with application to joint decision making that involve renewable power supply, building systems and passive building design measures and recommend this model for performance based microgrid design.

CHAPTER I

PROBLEM FORMULATION

1.1 Challenges of Energy Service Provision

Energy services play a pivotal role in modern society such as heat for cooking, compressor work for air conditioning, pump work for moving chilled water, etc. Deriving energy services, however, has a variable cost both to the end user and society at large. End user costs generally refer to the rate paid for a specific energy carrier while societal costs may refer to abstract costs such as the increased risk of illness in areas near to large power plants. This cost variability is because energy carriers come in a variety of forms. For instance, cooking heat may be derived by either burning biomass, natural gas in a grid connected home or via electric resistance.

The U.S. electric grid efficiently and reliably links distributed sources of generation to millions of residential, commercial and industrial end-users at a near global standard of quality, adequacy and reliability. The U.S. grid is a continuously operating, interstate transmission system subject to both federal and state laws managed and monitored by more than 3000 organizations (Kassakian et al., 2011). The scale of the grid, however, is both benefit and obstacle (Razanousky and Hyams, 2010). Benefits of scale include the ability to deploy large, high-efficiency power generation plants such as megawatt scale coal-fired steam generators, which account for approximately 25% of U.S. primary energy consumption (EIA, 2011). Obstacles of scale include the inability to rapidly improve grid telecommunications technology, the cost to upgrade transmission and distribution infrastructure and the cost of regular maintenance (Razanousky and Hyams, 2010). Razanousky and Hyams (2010) note that the cost to maintain the current level of electric power consumption is $200 billion per year, with approximately $10 billion per year in damages due to unplanned outages.

The U.S. electric grid also produces a number of societal costs due to the use of fossil fuels, which has numerous environmental impacts such as contributing to global warming and pollution of air, water and land (Hansen et al., 2016). Fossil fuels consumption also contributes to increased global and political conflict because nations compete for better access and control over these limited

resources. Renewable power generation is a viable alternative to fossil fuel consumption, but integrating renewable power into national energy supply systems is difficult as these resources are often at odds with existing infrastructure due to their variable production output (McGlade and Ekins, 2015).

1.2 What is the importance of microgrids?

Distributed generation (DG) and distributed energy resources (DERs) have emerged in response to the challenges of energy service provision mentioned in Section 1.1. Ackermann et al. (2001) defines distributed generation as:

> **Distributed Generation:** *A source of active electric power connected either directly to the distribution network or on the customer side of the meter.*

Examples of DG include photovoltaics, wind power generators, conventional fuel powered generators, combustion turbines and fuel cells. DG's primary purpose is active power generation for local consumption. DERs incorporate DG, but broadens the scope to include energy storage technologies and control devices and communications (Razanousky and Hyams, 2010).

Microgrids are aggregations of DERs and loads into larger systems. A physical microgrid aggregates these systems via real distribution equipment such as wires, cabling and pipes. In contrast, a virtual microgrid coordinates DERs and building demand with the extant macro-grid across multiple end-users via existing distribution networks and software. Virtual microgrids are outside the scope of this dissertation and instead we focus on investment decisions regarding physical microgrids (Razanousky and Hyams, 2010):

> **Physical Microgrid:** *A small (<40 MW), local energy system with integrated loads (i.e., demand from multiple sources) and distributed energy resources - producing electric or both electric and thermal energy - which can operate connected to the traditional centralized electric grid or autonomously from it, in an intentional island mode.*

A key characteristic of a microgrid is the ability to intelligently coordinate the thermal and electric power flows between a number of energy end-users and distributed generation resources. This coordination is often capable of bi-directional flow, electric power sales and energy storage.

Microgrids encourage the use of more renewable power generation due to their advanced power electronics and help to alleviate stress on the external grid at times of high demand through the ability to operate in an islanded mode. In general, microgrids function to increase power reliability, decrease power purchases during times with adverse pricing, reduce environmental impact of power consumption and generate revenue through renewable power sales to the grid.

Reliability alone has driven a great deal of the interest in microgrids especially in the wake of large-scale grid outages (Campbell, 2012; Halverson and Rabenhorst, 2013; Wood, 2016b). The demand for high performing microgrids continues to grow and market reports project a $20B investment in microgrids globally and $3.5B in the U.S. by 2020 (Wood, 2015). Yet this growing market still faces challenges during the design phase. For example, predicting the performance of a microgrid based on measures of reliability has proven difficult and as a result few to no insurance products exist that insure or guarantee performance outcomes of microgrids (Jones, 2015). Section 1.3 describes several of the reasons why evaluating microgrid performance is difficult and reviews steps taken in the microgrid design literature to improve aspects of microgrid performance prediction and analysis.

1.3 Why are microgrid investment decisions difficult?

Hazelrigg (2012) defines a rational decision as an allocation of resources to achieve an aim that does not result in a sure loss, but rather maximizes the utility of the outcome to the decision maker. Hence the decision to purchase the technology that realizes a particular microgrid system design is an investment decision. While the objectives of microgrid design appear simple, rationally evaluating microgrid design options is difficult; decision makers must evaluate system performance in terms of reliability as well as economic and environmental value. Two important characteristics of microgrid systems that contribute to the difficulty of designing these systems are: (1) the number of uncertainty sources that affect system performance and (2) the technical system of interest is composed of interacting sub-systems that generate both demand and supply.

Fundamentally, systems and engineering design involves complex decision making in reference to physical systems with non-intuitive behavior. To achieve rational decisions then requires the introduction of a performance based approach to design that ensures expected outcomes align with the

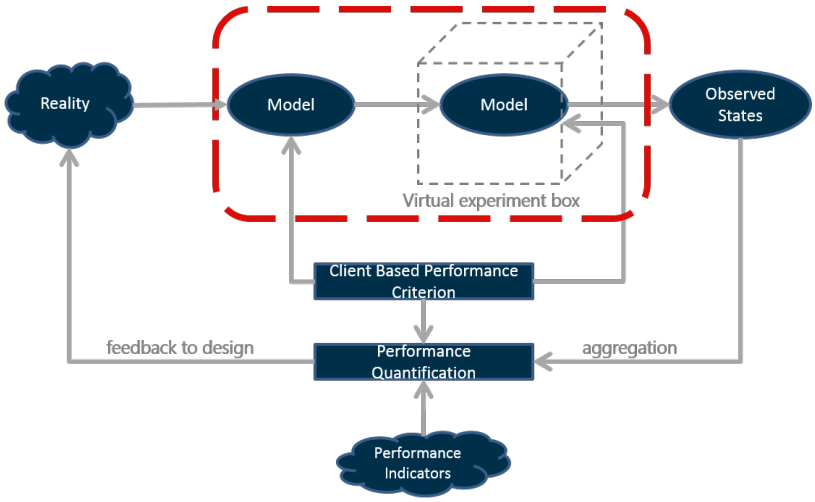

Figure 1: The performance based design framework focuses on the development of models whose outputs serve as estimates of reality. Model output is then used to quantify the performance of the systems represented in accordance with a client's preference. Adapted from (Hensen and Lamberts, 2012, Ch. 2)

preferences of the decision maker. A decision maker must predict outcomes of the technical system of interest via an abstract model that captures the idealized design specifications. This idealized model is then interrogated through a "virtual experiment" designed to elicit the underlying system's performance (Fig. 1). Observed states of the model under a specified experimental scenario are aggregated into metrics of performance in accordance with indicators that reflect the desired functional criteria (Hensen and Lamberts, 2012, Ch. 1). Current methods for predicting microgrid system performance, however, are insufficient as they neither account for major sources of uncertainty nor do they model the interacting sub-systems of supply and demand simultaneously.

During the design phase, the actual performance of the system can not be known as it will happen in the future and is therefore uncertain. Sources of uncertainty in reality include: thermal and electric power demand profiles, the utility's reliability (i.e., failure frequency and duration), power generation from renewable sources, reliability of DERs, control system reliability, construction issues and maintenance. Performance based modeling can never remove all sources of uncertainty as some of these sources are not included in idealized design models because they either do not warrant addition relative to other technical aspects being modeled or their effects and occurrences can not be predicted. Accounting for sources of uncertainty alone is not enough for a decision maker to adequately search the design space for the most preferred solutions; the technical system's model

must be complete and capture all elements of the system that fulfill a particular function.

Microgrid systems must fulfill the function of supplying power, which has two coupled elements: supply and demand. Demand exists to meet a particular function and the supply exists to ensure the demand can be met. A number of factors affect the demand of a microgrid system: building function, use, mechanical systems, controls, envelope, form, and occupancy; presence of auxiliary needs (e.g., plug-in electric vehicles (PEVs), industrial applications) and location. While demand and supply are coupled elements of the power supply function of microgrids it is important to note that not all microgrid design scenarios exhibit joint decision making power over both the supply and demand. For example a regional utility may undertake microgrid planning for several areas under its control, but while the utility may incentivize end-users to reduce demand it has no power to make decisions regarding these end-users. In contrast, Stadler et al. (2014) show that a university with joint decision making power regarding individual building demand and DER technology investments will select more preferred designs when considering demand and supply decision variables simultaneously.

There are a number of microgrid business models that exhibit joint decision making power over both the supply and demand decision variables. This dissertation focuses on these particular business opportunities as the modeling of microgrid systems in these contexts generally lacks both a comprehensive framework for assessing reliability and the ability to experimentally investigate the performance impacts of various design options on both the supply and demand. Section 1.3.1 examines current demand side methods of microgrid investment decision making while Section 1.3.2 focuses on current supply side methods of microgrid investment decision making.

1.3.1 Current Demand Side Design Methods

Architectural domain experts recognize the impact of architectural design on demand and attempts to reduce demand through design has created a vernacular of low-energy architecture. Illustrative examples of this vernacular are movements such as PassivHaus, Net-Zero Energy, Living Building Challenge, Architecture 2030 and others (Adamson and Feist, 1988; Mazria, 2006; Peterson et al., 2015; International Living Future Institute, 2016). Ultra low-energy buildings with the advent of distributed generation give rise to explorations of systems designated as net-zero energy (Marszal

et al., 2011; Sartori et al., 2012). Fortunately, architecture has effectively handled local integration of modern DERs, in particular solar photovoltaics, for decades (Buresch, 1983; Sodha et al., 1986). Demand reducing solutions have in turn emerged for residential buildings as well as commercial and industrial buildings through controls and other design interventions.

Kapsalaki et al. (2012) model a residential building using a modified representation of the equation set of ISO (2008) to evaluate the feasibility of achieving net-zero energy design in a Mediterranean climate. Kapsalaki et al. (2012) define a set of demand interventions for an individual building design and determined the set of interventions that minimized the investment cost to achieve net-zero energy. Similarly, the Building America program has worked to apply demand side optimization techniques to individual residential and single-family buildings (Anderson and Roberts, 2008). The framework followed is to define a base building and demand as well as a set of feasible interventions. The design space is then searched heuristically to determine the combination of interventions that minimizes energy consumption and investment cost.

Dillon and Colton (2014) focus on demand side modeling to determine the optimal parameters of an industrial facility with heavy refrigeration loads. Dillon and Colton (2014) apply a heuristic optimization algorithm to determine the optimal design parameters with a system model built from the bottom-up of non-linear equation modules. Sun et al. (2015) examines an individual building to determine the optimal selection of PV and wind capacities after sizing the HVAC system to meet a desired risk level. Sun et al. (2015) do not include passive measures as retrofit options, but accept the building as built while incorporating physical parameter, design parameter and basic scenario uncertainty.

Demand centric investigations into distributed generation coupled with low-energy buildings share several common characteristics: (1) the work typically explores a common set of supply system options (i.e., photovoltaics, wind, small fuel-powered generators, electric vehicles and electric energy storage), (2) models of the electric power demand are time varying and non-linear, and (3) the models tend to have a high level of fidelity as they are built-up systems of equations that represent individual buildings.

1.3.2 Current Supply Side Design Methods

Current microgrid design methods with an emphasis on the supply side focus on specifying the component capacities of defined DG technologies within a pre-defined microgrid typology. Key microgrid typologies investigated include combined heat and power (CHP), combined cooling heat and power (CCHP), derivatives of CCHP systems with integrated renewable generation technologies and custom investigations of new technology combinations. This research area assumes a given demand profile and very few studies investigate or quantify the demand uncertainty.

Cho et al. (2009) present a key development of optimal CHP design, in which a CHP system is modeled as a set of linear equations to determine both an optimal operation schedule and a component capacity set that maximized the investment value. Li et al. (2014) expand the work of Cho et al. (2009) to determine the trade-off between heat driven and electric driven cooling in a distributed generation system servicing an office building. Gu et al. (2015) investigate another CCHP type system, but include thermal energy storage as an option while also introducing uncertainties regarding the system parameters within the heuristic optimization algorithm. Fuentes-Cortés et al. (2015) address a CCHP system for a collection of residential loads with thermal energy storage and an internal combustion engine, with the problem formulated as a deterministic nonlinear optimization over multiple objectives including investment cost and emissions.

Supply design methods generally model the microgrid performance with a fixed demand, which may be either generated by a building energy simulation tool or from historical data. Modeling the operation of the system is typically achieved by a system of linear equations and constraints and the resolution of the modeling depends on the application of interest. The distinguishing characteristic of this work is that decision variables that affect system performance are constrained to the DER technologies themselves.

1.3.3 Towards Integrated Design of Communities & Distributed Generation

The studies mentioned in Section 1.3.1 and Section 1.3.2 indicate that within the microgrid design literature researchers tend to focus on either selecting demand interventions for a particular building or sizing DGs for a given system type and a known load profile. The modeling tools that have

emerged limit decision making power only to variables that affect either the supply or demand sub-system alone. This section briefly introduces research that begins to address an integrated microgrid design process by modeling the demand and supply sub-systems simultaneously.

Stadler (2009a) recognize the effect that building function has on demand and microgrid design. To further investigate the effects of building function on microgrid design Stadler (2009a) apply the Distributed Energy Resource Customer Adoption Model (DER-CAM) to a suite of individual commercial buildings with different functions. Stadler (2009a) derive the building demand data from observations of thermal and electric power data at the site as well as energy models of two buildings.

Stadler (2009b) attempts to integrate the design of the supply with demand side interventions. A commercial building demand is supplied to the DER-CAM tool for finding the optimal supply system specification, but additional parameters that allowed the demand curve to be shifted or reduced for certain time steps by specific percentages at a defined cost were integrated. This initial attempt at demand side intervention modeling was left aside for further research, which is reasonable given that the method did not relate the demand parameters to the actual functional constraints of the demand.

It is important to note that a number of the supply side focused microgrid design studies investigated the optimal operation of the DER components (Hakimi and Moghaddas-Tafreshi, 2014; Chauhan and Saini, 2014). Optimal operations planning and scheduling is a key part in the design of microgrids as one can not asses the potential operational costs and resilience without establishing a control policy. Modeling the coordinated control of DER components and the demand is difficult as the modeling frameworks best suited for each sub-system do not generally lend themselves to coupled simulation. Sharma et al. (2016) presents a novel integrated control approach, in which the demand and supply sub-systems are both modeled explicitly as a set of linear equations to facilitate optimal control evaluation. The specifics of modeling demand and supply will be addressed in Chapter 2 and Chapter 4, respectively, but for now we simply note that issues of system resilience and control are closely interrelated within the microgrid system design context.

Stadler et al. (2011) focus explicitly on net-zero energy building investigations with DER-CAM by applying a constraint to ensure an annual balance of energy imported and exported for a single

California commercial building. Stadler et al. (2014) demonstrate a true integration of supply and demand design within the microgrid context. Stadler et al. (2014) edit the DER-CAM model to calculate thermal building demand for heating and cooling through a linear model. Results showed that an integrated design process resulted in more preferred solutions than without improvements to the demand. Additional studies demonstrate similar characteristics to the DER-CAM model, but have been applied to optimization of supply specification for groups of office buildings and other communities.

Simpkins et al. (2015) introduce a tool for renewable DG selection that is also a formulation of linear equations to represent the supply system. Simpkins et al. (2015) model the demand of a Alaskan village by summing together outputs of EnergyPlus models. Morvaj et al. (2015) also explore the integrated design problem by demonstrating a theoretical design of a distributed generation system for twelve residential buildings. Morvaj et al. (2015) compare the distributed system design for residential buildings pre- and post- retrofit to determine that low-energy buildings reduced CHP investment costs.

Reviewing the literature of integrated modeling tools to analyze the performance of microgrid systems show that few methods exist. Those that do exist have focused on single buildings yet use building energy models that do not capture common physical modeling assumptions expressed in demand side approaches to microgrid design. In addition, while there is evidence of supply side work that attempts to quantify uncertainty in performance, this work generally does not consider a number of the key uncertainty sources identified in Section 1.3.

1.4 Problem Statement

Performance based design of microgrids is difficult because there are a number of sources of uncertainty to consider in the real system yet current modeling methodologies do not allow decision makers to express quantified uncertainty for important sources. Also, decision making scenarios that exhibit joint decision making power over design variables on both the demand and supply are not fully supported. Tools and methods such as DER-CAM that do allow decision makers to consider such joint scenarios do not use a building energy model that conforms to common thermal modeling assumptions. Additionally, these joint decision making scenarios are not supported as

much research either focuses on demand side only or supply side only interventions, which implies that the strengths of each approach independently are not leveraged. For example, recent work in building energy modeling has greatly advanced understanding of the demand profile uncertainty related to specific demand side interventions yet demand uncertainty quantification at this level of detail is not included in many supply side only microgrid design approaches.

Several existing business cases exhibit joint decision making on the supply and demand side of microgrid design such as university and campus microgrids, co-operatively owned microgrids and single owner microgrids serving the owner's building portfolio. Decision scenarios that are not explicitly treated in the literature related to these business models include: (1) new design or retrofit of an existing community with an installation of a microgrid and (2) expansion of an existing microgrid to include new end-users. In the first scenario two conventional solutions are to either not consider design interventions on the demand side or to minimize the thermal and electric demand of the end-users; however, in neither solution are the implications for these decisions calculated in reference to the final performance of the microgrid system. Similarly, with the second scenario the microgrid owner should evaluate the performance of the system while considering both demand reduction of the proposed new end-users and investment in new DERs.

1.4.1 Hypotheses

Current performance based design methods applied to microgrid investment decision making are insufficient due to limited modeling capabilities. Existing microgrid system models do not (1) incorporate a framework for considering major sources of uncertainty and (2) do not allow decision makers to select design parameters across the interacting technical sub-systems of demand and supply. Existing tools that allow integrated system modeling do not adequately model the building thermal demand and ignores effects due to solar radiation, geometry, air infiltration, occupants, controls and heat capacity. This lack of modeling resolution limits a decision maker's ability to asses passive demand interventions (i.e.,reducing air infiltration, shading, etc.). While the impact of any passive or active demand side intervention is specific to the decision scenario it is important to note that in cases for which these variables affect demand there is no adequate modeling tool. This dissertation proposes three hypotheses related to the modeling of microgrid systems for performance

based design and investment decision making:

Hypothesis 1: An integrated microgrid system model with high resolution demand and supply models will enable decision makers to analyze more design options and decision variables than is possible with currently available tools.

Hypothesis 2: Microgrid system designs selected via the integrated method will be more preferred than solutions determined via specifying decision variables on either the demand or supply side alone.

Hypothesis 3: Defining a resiliency framework for the integrated microgrid system model will enable decision makers to model scenario uncertainty regarding the utility's reliability. As resilience and load control are closely related, this work also shows that the resilience framework may be interpreted as an abstract model of an optimal load control algorithm.

1.5 Significance

This dissertation proposes an integrated model for the performance based design of distributed generation systems that allows decision makers to consider design options that can not be explored with existing tools. The integrated model extends the DER-CAM supply modeling tool, which is a high-resolution, abstract specification of the supply system as a linear set of equations. This dissertation improves modeling of the end-user demand through a co-simulation approach that allows the demand to be modeled as a set of individual building energy models. This dissertation also presents a method for efficiently searching the demand intervention option set directly rather than using average data to approximate the cost constraints of demand side interventions in the modeled community. This dissertation also presents a framework for incorporating a utility's reliability profile and a decision maker's neutrality to unmet demand, through this framework the dissertation advances the DER-CAM tool's uncertainty propagation methodology. This research demonstrates the benefits and efficacy of this modeling improvement in a case study to determine a co-operative microgrid owner's most preferred investment in both supply generation and demand interventions.

1.6 Thesis Structure

Chapter 1 presents background to the problem and outlines the motivation; Chapter 2 reviews demand modeling of both individual buildings and communities and presents the selected modeling methodology; Chapter 3 presents a means of transforming a large discrete, demand side intervention problem into a problem suitable for coupled optimization; Chapter 4 introduces the DER-CAM tool and reviews related supply modeling literature as well as introduces the reliability framework; Chapter 5 introduces the co-simulation methodology and an optimization approach suitable for the coupled model; Chapter 6 presents an application of the improved modeling methodology to a microgrid design case study; and Chapter 7 concludes with reflections on the modeling approach and implications for future work and research.

CHAPTER II

DEMAND MODELING OF ARCHITECTURAL SYSTEMS FOR MICROGRID DESIGN

This dissertation extends the DER-CAM tool developed by LBNL to create an integrated microgrid system model. DER-CAM defines six quantities of interest: electric only demand, electric cooling demand, thermal heating demand, refrigeration electric demand, thermal hot water demand and natural gas demand. The demand must be specified at an hourly resolution with data for typical weekdays, weekends and peak days. Peak demand is an important quantity of interest in microgrid and power system design as it defines the maximum quantity that the microgrid system must supply. Variation in the six components of demand at an hourly resolution is also important as this behavior of the demand will allow the decision maker to characterize the operating characteristics of the microgrid system. The purpose of this chapter is to define a demand generating function that adequately captures the quantities of interest. First, we briefly review several of the common approaches to both individual building and building stock modeling. Then, we identify a building stock model based on the EPC tool that generates our desired quantities of interest. Finally, the proposed methodology is introduced and validated.

2.1 Background

Architectural systems have two types of demand: (1) thermal (i.e., either heat removal or heat addition) and (2) electric. The thermal demand for either heat removal or addition arises from the need to condition the indoor environment to satisfy occupant comfort or other functional criteria and to meet certain process needs. Process needs are quite variable and depend highly on the building function, but examples of process needs includes heat for domestic hot water, heat removal for ice storage and heat requirements for an industrial process like desalination. Electric power as we've previously introduced is required to provide a number of energy related services including lighting, equipment, appliances and heating, ventilation and air conditioning (HVAC).

Building demand modeling is the process of virtually observing realizations of the thermal and electric demand of an architectural system for a desired time period and resolution. Each realization is based on a specification of both the scenario of use and design documents of the system. Building demand modeling is often applied to the design of HVAC systems with some use in the architectural design process. Architectural design is a creative process aimed at client satisfaction as such the degree to which demand modeling is performed during the design formulation stage depends primarily on the desires of the client.

Practical architectural design typically eschews detailed building demand modeling in favor of rules of thumb, professional experience and additional design guidelines. Electric demand reductions are typically achieved by specifying target equipment and lighting power densities. Advanced daylighting controls, however, have begun to allow the use of more complex demand modeling during the architectural design process. Nevertheless, the chief use of demand modeling of architectural systems in practice is to estimate the energy consumption of the HVAC system specified and sized by a mechanical engineer.

Theoretical use of demand modeling has grown primarily due to its use in virtual experiments to predict energy consumption and compare HVAC design options. Demand modeling at its core is driven by the use case and the field of research or application. As such a number of methodologies have been applied throughout the literature, some with impact in practice and others with only theoretical implications. Based on this work's requirement that the demand model be used for co-simulation with DER-CAM tool we may assert the following modeling needs:

1. computationally inexpensive at an hourly resolution
2. representative of a known building population
3. parameterized on decision variables that affect demand
4. directly link decision variables to associated costs
5. scalable level of detail that aligns with available information

2.2 Approaches to Building Demand Modeling

Demand generating functions or models are classified into three broad categories: data driven or statistical, physics driven and hybrid models (Amara et al., 2015). Within each category of modeling there may be differences in how individual buildings are treated versus collections or building stocks. We make note of these key differences where the distinction between indvidual building and building stock modeling approaches is significant.

Data Driven & Statistical Demand Modeling Data driven or "black box" modeling of architectural systems is an approach, in which data for a set of explanatory variables is fed into a chosen model form and the parameters are automatically tuned until the model output matches the observed output within a desired tolerance or similar criterion. Statistical energy models come in a variety of forms such as linear equations, polynomials, transfer functions and neural networks. Amara et al. (2015) notes that data driven models of individual buildings are most often used in system control and error detection as there is no explicit relationship between the model parameters and physical reality. Statistical energy models typically have high predictive validity as model observations are derived solely from the input-output relationship of the studied system.

Tian et al. (2015) study statistical energy modeling applied to building stocks and highlight that an important challenge in statistical energy modeling is to ensure that any correlation between explanatory variables be accounted for prior to assessing the impact of changing any single variable on a quantity of interest. There are numerous examples of building sector meta models with varying output resolution, quantities of interest, explanatory variables and application. Priddle (2015) present the World Energy Model, which is not directly concerned with the features of individual buildings within a stock, but rather the relationship between economic drivers such as GDP, CO_2 prices, technology adoption scenarios and policy scenarios on macro level energy flows, CO_2 emissions and investments.

Rezaee et al. (2015) and Zhao (2012) apply linear meta models of monthly building demand to develop inverse modeling methods to aid design and find retrofits of building stocks, respectively. A limitation of meta models of building stock demand is that they are generally of a coarse

resolution (e.g., monthly), which is not particularly useful for the performance based design of microgrids. Keep et al. (2011) present a high resolution model to study the ability of thermostatically controlled devices with either an on or off state (i.e., "switchable") to provide very short term load services such as either strategically increasing or decreasing aggregate demand. Keep et al. (2011) presents a final top-down model that is an autoregressive moving average (ARX) time series model of an aggregate of switchable refrigerators.

Keep et al. (2011) parameterize the model as a function of the number of refrigerators in an "on" state at a given time, t. Formulating the demand aggregate refrigerator demand on this single parameter is a powerful means of exploring optimal control strategies, however, it does not allow the model user to investigate alternative means of improving the aggregate refrigerators' response performance such as through improvements to the appliance (e.g., better compressor, more insulation). Exploring demand interventions of mass produced refrigerators may be trivial, but this example illustrates how top-down models may be simultaneously powerful yet limited for expanded explorations related to system design. Makarov et al. (2009) present another high-resolution example of a top-down demand model used to simulate the California Independent System Operator (CASIO)'s total generation and demand power. Makarov et al. (2009) model the demand of the system as the sum of a historical demand profile and forecast errors selected from a truncated normal distribution. Parameters of the truncated normal distribution are identified from historical forecast error data.

Statistically based energy models of either individual buildings or building sectors typically demonstrate strong validity in regards to training data, but at times they may lack a direct connection to a design intervention. In addition, these methods, which are also referred to as meta modeling generally have lower computational overhead than physics driven modeling. Three important challenges for developing meta models that generate a demand profile for use in microgrid system design are to determine any correlation between the explanatory variables, ensure there is sufficient data to parameterize a model at the desired resolution of the application and to translate meta model parameters into physical design variables. Researchers may attempt to circumvent limitations of top-down models by developing models based purely on the physical relationships of interest.

Physics Driven Modeling Physics driven modeling is an approach, in which the simulated observations are derived directly from specifications of the underlying processes' governing equations. This modeling approach, often referred to as a "first principles" approach attempts to capture as much of the relevant physical phenomena as possible in order to simulate the system. First principles models are used quite commonly in demand modeling of architectural systems because they are often parameterized on variables with direct relevance to architectural design. For instance, many of these models are structured to receive extremely detailed material property and geometric information for use in various calculation submodules including explicit radiation exchange. The appropriateness of such detailed modeling is a point of ongoing research and is of course dependent on the functional criteria to be evaluated (Hensen and Lamberts, 2012).

Physics driven models are numerous and with different levels of detail available for modeling. It is important to note that no physics driven modeling approach is created without data. In fact, while the physics driven approaches expose a number of physical parameters for decision makers to specify, the underlying model form and equations are generally derived from engineering knowledge and experimental data. These simplifications of the physical interactions gives rise to model form uncertainty as recently investigated by Sun (2014).

Commercially available architectural system simulation engines include EnergyPlus, DOE-2, eQUEST, TRNSYS, Modelica, etc. The Department of Energy's Building Energy Software Tools Directory (EERE) is a more complete directory of the relevant commercial software packages (US D.O.E., 2012). The most notable commercial tools used in both research and practical demand modeling of architectural systems are EnergyPlus, ESP-r, TRNSYS and Modelica. EnergyPlus is a free, stand-alone simulation engine accepted as the current state-of-the-art in the American building simulation market (Crawley et al., 2001). EnergyPlus has been rigorously tested and widely used in both academia and practice via third-party graphical user interfaces; as such EnergyPlus is often defined as the standard by which other demand simulation engines are compared (Henninger et al., 2004).

A number of researchers decide to generate demand models of building stocks from the "bottom-up", which is to say that individual demand end-uses are modeled at an extreme level of physical detail. These individual components are then aggregated together in accordance with the research

aims. There are numerous examples of these types of models and their applications as covered in the reviews of Kavgic et al. (2010) and Swan and Ugursal (2009).

McKenna et al. (2013) review bottom-up demand models within the European Context and conclude there is a need for a bottom-up model applied directly to the German residential housing market as it is underrepresented in their review. The goal of the developed demand model is to assess the potential for design interventions (i.e., retrofits) to meet the energy and emissions related policy goals of the German government. McKenna et al. (2013) seek to project the growth in residential energy demand by considering the growth in the building stock size and the energy consumption of individual buildings according to their vintage based on a review of existing data.

Reinhart and Davila (2016) reviews bottom-up models with an agenda more oriented toward design. Quan et al. (2015) labels these types of urban design models as planning support systems (PSS). PSS are an advanced class of building stock modeling with the aim of capturing as many physical interactions as possible in the modeling. For instance, Robinson (2012) proposes a comprehensive methodology that incorporates agent-based modeling of city occupants, detailed geographical data of urban areas for solar radiation and wind flow calculation as well as building energy use into a single model of the urban area. Zhao (2012) in contrast attempts to capture only the aspects of the building aggregate that are relevant to investment decisions. As such Zhao (2012) modeled the energy use of a collection of commercial buildings through inverse extrapolation of the inputs to the normative energy model described in Section 2.3.

While Zhao (2012) demonstrated that the normative energy model may be expressed as a linear regression model and also represent the energy use of an aggregate of a single building class, Quan et al. (2015) furthers the use of the normative modeling paradigm for aggregate demand modeling. The urban modeling approach is furthered in a number of key ways: (1) the urban context is explicitly modeled (i.e., interactions between buildings, microclimate effects and occupancy), (2) more classes of buildings are identified and modeled via the normative approach. Specifically, Quan et al. (2015) leverages existing databases of typical reference buildings to provide the parameter inputs to the demand simulation models, however, the work did not detail a methodology for iteratively exploring the urban design through design interventions on the building demand.

Hybrid Modeling Many researchers develop demand models that rely on a combination of data and first principles. Such hybrid or "grey box" models achieve some of the advantages of black box models (e.g., improved predictive capabilities) without sacrificing the relationship between model parameters and the physical reality. A common methodology is to deploy an equivalent thermal parameter (ETP) model that represents a building's energy balance as a circuit of resistors and capacitors (Johnson et al., 2014; Li and Wen, 2014; Zhang and Lu, 2013) and calibrate the reduced model to data. ETP models are typically very small networks with limited physical phenomena represented and researchers often scale this methodology upwards to include more resistors, capacitors and calculation submodules (Hu, 2009; Bueno et al., 2015). Alternatively, Zakula et al. (2014) identify a grey box model of a thermally activated building slab for optimal control of a TRNSYS model via transfer functions.

2.3 Simplified Hourly Building Demand Modeling

Detailed physical modeling and hybrid modeling have the disadvantages that these techniques allow modeler's bias and representation errors. In addition, the execution time of many physical modeling tools relative to either hybrid or statistical models is high. While grey box models may have a lower computational overhead they also require information regarding the input-output relationship of the system, which may be unavailable during the design phase. Lee et al. (2013) present the hourly Energy Performance Calculator (EPC), which is a building energy simulation tool that is one of many similar tools that implements the solution methodology ISO (2008). The purpose of the original normative calculation technique is to ensure reproducibility and robustness of performance comparisons, which is achieved by removing modeler's bias, increased calculation transparency and increased modeling simplicity. The EPC tool itself is no longer a normative calculation method as decision makers now select input parameters specific to the building being simulated and the EPC has been used in the literature primarily for demand calculations at the annual, monthly and hourly timescales (Lee et al., 2013; Quan et al., 2015; Rezaee et al., 2015).

In this work we model the demand of building stocks and communities using the EPC. The EPC tool generates four of the six demand inputs to DER-CAM at an hourly resolution; electricity for refrigeration and natural gas profiles must be specified by the decision maker via an external method.

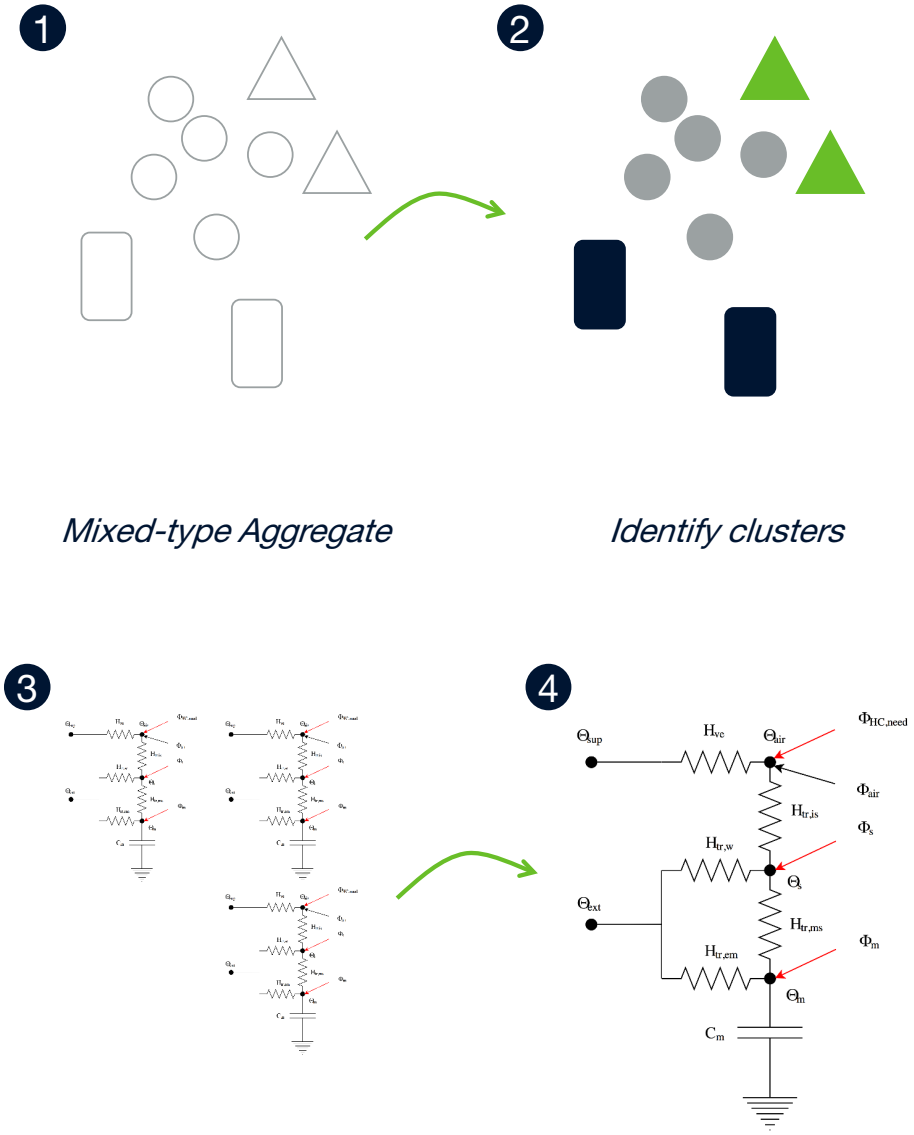

Figure 2: The proposed method decomposes an aggregate of buildings into relevant building clusters, which are then aggregated to form the final model of a "mixed-type" aggregate.

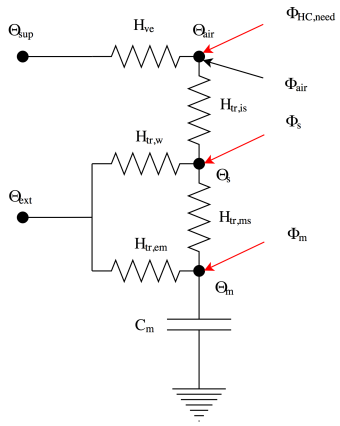

Figure 3: Thermal R-C representation of a building in accordance with ISO (2008).

Of the remaining four demand components, hot water demand and electric only demand are not functions of the building's design parameters, but rather its specified scenario of use. Therefore, we must only consider the adequacy of the EPC tool to generate hourly profiles of the electric demand for cooling and the thermal demand for heating including their peaks. Bueno et al. (2015) present an R-C model that is similar to EPC yet with advanced treatment of solar radiation on façades. Bueno et al. (2015) separately calculate the RMSE of both thermal demand for heating and cooling when comparing hourly output from the R-C model at EnergyPlus for summer (2 W/m2)and winter (1 W/m2) days. Zhao (2012) qualitatively compares the total electric demand of an EPC model to that of an input matched EnergyPlus model at an hourly resolution and concludes that while the EPC appears to follow the EnergyPlus profile well, the peak electric demand values of the EPC were underestimated during Spring by 20% and overestimated in summer by 30%. EPC underestimated peak electric cooling demand on the range of 10-50% during the Summer. Kapsalaki et al. (2012) note that the peak demand estimation of tools based on ISO (2008) is unreliable and apply the peak cooling and heating demand equations from ASHRAE (2009). This dissertation relies on the hourly EPC to simulate the demand of building stocks and communities given the strong agreement of R-C network modeling and EnergyPlus for hourly thermal demand and a peak demand estimation method found in the literature.

Given the weather data and a user defined scenario of use and operation, the EPC calculates for each hour, the average thermal power required for either heating or cooling required ($\Phi_{HC,need}$)

to maintain the temperature set point (Θ_{air}). The building's thermal mass is represented by a single capacitor (C_m), which indirectly interacts with Θ_{air} via conduction heat transfer to the mass surface ($H_{tr,ms}$) and then convection heat transfer to the air ($H_{tr,is}$). Air temperature is affected directly by heat transfer via ventilation air (H_{ve}) that enters at a given supply temperature (Θ_{sup}). The building's mass, C_m, is connected to the external air temperature (Θ_{ext}) via heat transfer through the windows ($H_{tr,w}$) and envelope ($H_{tr,em}$). Solar radiation affects both the building's mass and air temperatures through three inputs: radiation to mass (Φ_m), radiation to mass surface (Φ_s) and radiation to air (Φ_{air}) (Fig. 3). ISO (2008) details the full calculation methodology for each hour.

The method presented here, however, is most similar to Zhao (2012), which presents the concept of *building stocks*. A building stock, which this dissertation refers to as *clusters*, are groups of buildings that are of identical type. More formally, a cluster is a group of buildings identified by the designer, which are *indistinguishable* from each other. Here we define two deterministic models as *indistinguishable* if they have the same input parameter set and identical output for the same design interventions. Fig. 2 illustrates the initial steps of the modeling methodology, which are discussed in more detail below. While the normative model does provide significant improvements for calculation speed, reproducibility and robustness it cannot overcome the base complexity in efficiently searching such a broad design space for preferential design options. This dissertation then proposes an alternative method of aggregate demand modeling that is a hybrid of both bottom-up and top-down approaches. The proposed approach is discussed in the following section in greater detail.

Step 1: Identify the Aggregate to Model The first step in the methodology is to identify the building aggregate to be modeled. The primary data needs to identify are the functional types of each of the buildings and information regarding the building program, use scenario, envelope, mechanical systems and climate. In the case of new design then this information should be sufficient to meet the data requirements of the EPC (Quan et al., 2015). Zhao (2012) identifies EPC model parameters based on actual consumption data. This dissertation focuses on deriving model parameters from reference buildings as done in Quan et al. (2015).

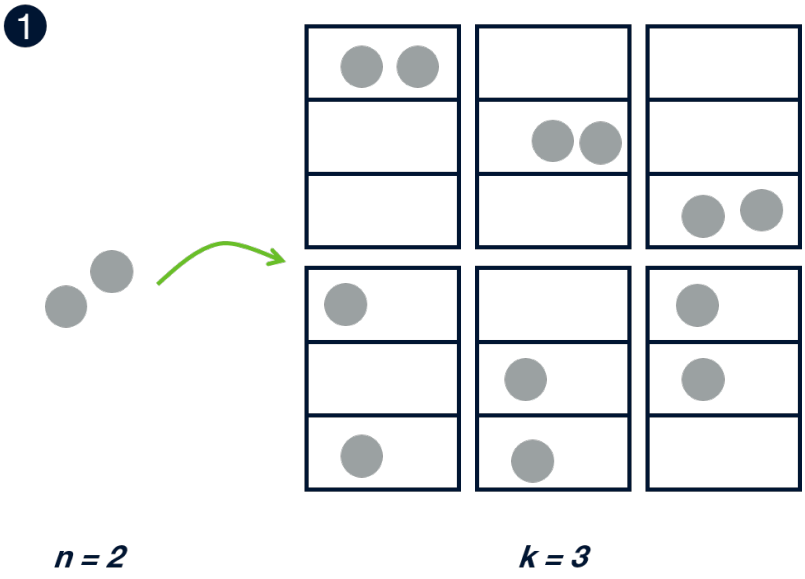

Figure 4: Simple illustration of a cluster model's counting principle. A cluster model parameter is determined by specifying the discrete option level of each building of the same type. Here the number of indistinguishable buildings within the cluster is $n = 2$ and the discrete options for a variable is $k = 3$.

Step 2: Identify Building Clusters Next, the modeler must group the building aggregate into relevant clusters. Clusters are groups of building with the same function, which we assume may be modeled as *indistinguishable* buildings. For instance, a community aggregate may have supermarkets, primary schools, multi-family residences and single-family residences. This dissertation applies existing reference building definitions (Deru et al., 2011). Reference buildings are applied quite often in bottom-up models of building aggregate demand. Best et al. (2015) determined the optimal mix of various building types in a single community based on reference models. Morvaj et al. (2015) explored the impact of low-energy buildings on the sizing of a community CHP system and used several reference models of typical single-family residences in the European context. Reference buildings are not a prerequisite for applying this methodology. An alternative is for the modeler to specify the complete set of input variables for the EPC tool based on a design specification.

Step 3: Aggregate Modeling of Building Clusters The number of clusters identified in Step 2 will determine the initial number of EPC models required. If the clusters align with available

data for reference buildings then this information is used to parameterize the EPC, otherwise the modeler must specify the full set of EPC inputs based on design specifications. Zhao (2012) defines an inverse methodology for identifying EPC model parameters based on consumption data for a specific building cluster, which is recommended in the case of a retrofit scenario.

Step 4: Finalizing the Mixed-Type Building Aggregate Model The final step is to combine each EPC model of a building cluster into a single EPC instance to model the complete building aggregate. The EPC model environment is separated by input types into parameters that define general building characteristics, the mechanical systems for heating and cooling, zone level energy demand, schedules and the building envelope. These variables may be further grouped into normalized metrics, rates and dimensioned variables. This final step creates a single EPC instance that represents all of the clusters defined and modeled in Step 3. To accomplish this the variables of input parameters are combined via area weighted averages in accordance with the a corresponding scaling factor. Rate variables are the exception and these parameters are combined as a simple summation. The general equation used to combine the variables is given as:

$$X_i = \sum_{j=1}^{N} w_{i,j} \cdot x_j \tag{1}$$

where X_i is input parameter i to the mixed-type aggregate model, N is the number of clusters, $w_{i,j}$ is the weighting factor for input parameter i and cluster j and x_j is the corresponding input parameter of cluster j. The scaling factor $w_{i,j}$ depends on the input parameter i, for example the overall roof u-value $[W \cdot m^{-2} \cdot K^{-1}]$ scaling factor for each cluster j is given by:

$$w_{roof,\,j} = \frac{A_{roof,\,j}}{\sum_{j=1}^{N} A_{roof,\,j}} \tag{2}$$

where $A_{roof,\,j}$ is the roof area in m^2 of cluster j then $w_{roof,\,j}$ is denoted the roof area scaling factor. Table 1 presents the scaling factors for each of the EPC inputs.

The schedule values of the aggregate model are also derived from a linear sum. There are three parameters scheduled in the EPC: appliance power, lighting power and the number of people. A modeler defines a peak value for these inputs and an hourly schedule that indicates the fraction of

Table 1: EPC input variables and their corresponding scaling factors to build the mixed-type aggregate demand model.

Variable	Scaling Factor
Gross Floor Area (m2)	Floor Area
Occupancy (people)	Floor Area
Metabolic rate (W/person)	Floor Area
Appliance (W/m2)	Floor Area
Lighting (W/m2)	Floor Area
Outdoor Air (liter/s/person)	Floor Area
DHW (liter/m2/month)	Floor Area
Opaque Wall Area	Wall Area
Roof Area	Roof Area
Below Grade Area	Below Grade Area
Window Area	Window Area
U-value (W/m2/K)	Correspond to construction area of interest
Absorption Coefficient	Correspond to construction area of interest
Emissivity	Correspond to construction area of interest
Solar Transmittance	Correspond to construction area of interest
Total Ventilated Volume	Sum
Building Height	Floor Area
Lighting daylighting factor	Floor Area
Lighting occupancy factor	Floor Area
Lighting constant illumination control factor	Floor Area
Heating System Coefficient of Performance (COP) [KW/KW]	Floor Area
Cooling System Full Load COP [KW/KW]	Floor Area
Mechanical ventilation supply air flow rate (liter/s)	Sum
Mechanical ventilation exhaust air flow rate (liter/s)	Sum
Building air leakage level (Air flow m3/h)	Sum
Specific fan power [W/(l/s)]	Floor Area
Fan flow control factor	Floor Area
Set Point Schedule	Floor Area
Occupancy Schedule	See Eqn. 3
Appliance Schedule	See Eqn. 3
Lighting Schedule	See Eqn. 3

the peak value for each hour. These parameters affect both the delivered energy and the zone air heat balance. The aggregate model should calculate the same watts of appliance and lighting power as well as the same number of people for each hour. This fraction can be analytically determined at each hour with the following equation:

$$Z_h = \frac{\sum_j z_{j,\,h} \cdot b_j}{B} \tag{3}$$

where Z_h is the hourly fraction value for the aggregate model, $z_{j,\,h}$ is the hourly fraction of cluster j of total demand b_j and B is the total aggregate value expected. In the case of lighting or appliance power then b_j is peak watts in the building zone of cluster j and for occupancy then b_j is the peak number of people in the zone.

2.4 Validation

Hypothesis: The proposed single-instance modeling approach estimates the thermal need for heating, electric power demand for cooling and electric power demand for non-HVAC related services within an acceptable error versus the experimental control modeling approach (i.e., modeling multiple EPC instances).

This section will validate the proposed model via comparative testing, in which outcomes from the simulation are compared to the outcomes from a standard formulation. Two identical building aggregates will be generated and evaluated under the same scenarios of use and climate. These two aggregate demands will be modeled via two methods. The first method C_{mass} represents each building as a normative building demand model as described in Section 2.3. The test method $C_{proposed}$ will be used to generate a demand in accordance with Section 2.3.

To evaluate the two models, we will first specify the hypothetical building aggregate and its underlying clusters. The valid model is assumed to be C_{mass}, for which each cluster will be modeled individually. The experimental model is $C_{proposed}$, which will represent the complete aggregate as a single model with inputs derived according to Section 2.3. The modeled thermal demand for heating, electricity only demand and electric cooling demand will each be deterministically compared to the forecast values of $C_{proposed}$. The model performance will be evaluated via the

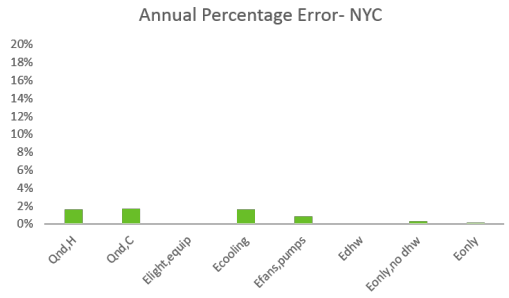

(a) Annual Percentage Error comparing the annual energy use C_{mass} to $C_{proposed}$ for each of the model outputs in Climate Zone 4A.

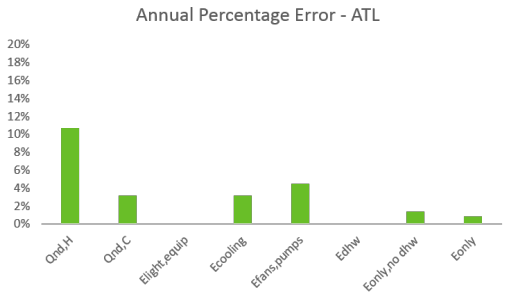

(b) Annual Percentage Error comparing the annual energy use C_{mass} to $C_{proposed}$ for each of the model outputs in Climate Zone 3A.

Figure 5: Percentage error of the annual aggregate energy use of various end-use components of each model.

Mean Absolute Percentage Error (MAPE):

$$MAPE = 100\% \cdot n^{-1} \cdot \sum_{i=1}^{n} \frac{|A_i - F_i|}{|A_i|} \tag{4}$$

where n is the number of time intervals, A_i is the actual value (i.e., C_{mass}) and F_i is the forecast value (i.e., $C_{proposed}$).

Validation Scenario The validation scenario will be completed for ASHRAE Climate Zone 4A (Central Park, NY, NY) and Climate Zone 3A (Hartsfield Jackson Airport, Atlanta, GA) with typical meteorological year (TMY) data (Wilcox and Marion, 2008). In addition we present a hypothetical community with a mixture of building functions. This aggregate includes four small office buildings, five multi-family residences and 15 single family residences. The buildings are all constructed to meet the minimum requirements of ASHRAE 90.1-2013 and additional data regarding the use scenario and mechanical systems are derived from the typical US building stock models of Deru et al. (2011). The use of typical building models is justified as this exercise is done solely to validate the prediction results of the proposed modeling scheme.

The proposed model $C_{proposed}$ compares favorably to C_{mass} at both annual aggregate levels and at an hourly resolution. Fig. 5a details the percentage error of the annual energy consumption of eight different performance indicators for Climate Zone 4A. Results show that annual error is less

Table 2: MAPE comparisons of $C_{proposed}$ to C_{mass} for ASHRAE Climate Zone 4A (Central Park, NY, NY).

	MAPE		
	Annual	Winter Week	Summer Week
$Q_{nd,\ H}$	8.36%	7.05%	0.00%
$Q_{nd,\ C}$	6.73%	0.00%	12.45%
$E_{light,\ equip}$	0.00%	0.00%	0.00%
$E_{cooling}$	6.67%	0.00%	12.30%
$E_{fans,\ pumps}$	5.88%	6.36%	3.38%
E_{dhw}	24.72%	24.76%	27.67%
$E_{only,\ no\ dhw}$	1.86%	3.25%	0.75%
E_{only}	6.37%	4.74%	6.91%

Table 3: MAPE comparisons of $C_{proposed}$ to C_{mass} for ASHRAE Climate Zone 3A (Hartsfield Jackson Airport, Atlanta, GA).

	MAPE		
	Annual	Winter Week	Summer Week
$Q_{nd,\ H}$	9.71%	12.94%	0.00%
$Q_{nd,\ C}$	9.11%	0.00%	9.55%
$E_{light,\ equip}$	0.00%	0.00%	0.00%
$E_{cooling}$	9.03%	0.00%	9.32%
$E_{fans,\ pumps}$	6.63%	9.29%	5.05%
E_{dhw}	24.72%	24.76%	27.67%
$E_{only,\ no\ dhw}$	1.93%	3.98%	1.73%
E_{only}	6.53%	5.12%	6.01%

than 5% for all performance indicators. In particular, the method is able to exactly reproduce the annual energy consumption for both $E_{lights,equip}$ and E_{DHW}. This result is duplicated in Climate Zone 3A as seen in Fig. 5b. The percentage error of $Q_{nd,H}$, however, in Climate Zone 3A is just over 10%, which is the highest error across all performance indicators at the annual level.

Table 2 and Table 3 detail the MAPE at the hourly resolution for three different time periods: annual, winter design week and summer design week. It is important to analyze the hourly resolution of the models as this is the resolution that will be used for designing the supply system. In general, $C_{proposed}$ forecasts C_{mass} well. Note that the MAPE is less than 10% at the annual scale for all performance indicators except the E_{DHW}. E_{DHW} is interesting in that the annual aggregate error is 0% (i.e., the total energy consumed for domestic hot water is identical), but the hourly profiles agree the least among the performance indicators (Fig. 6). The high MAPE is due to the effect

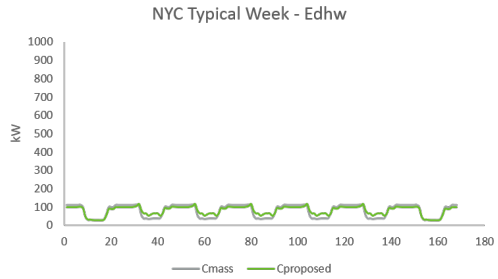

(a) E_{DHW} for a typical week in Climate Zone 4A. See Table 2 for MAPE.

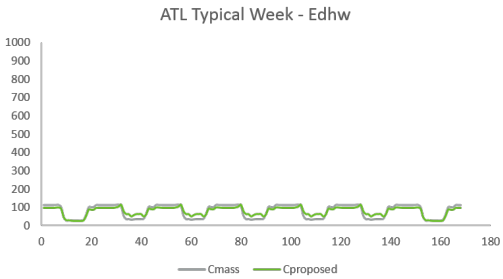

(b) E_{DHW} for a typical week in Climate Zone 3A. See Table 2 for MAPE.

Figure 6: Comparison of electric power for domestic hot water use, E_{DHW}, between C_{mass} and $C_{proposed}$.

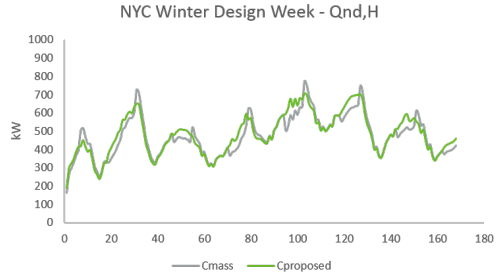

(a) $Q_{nd,H}$ for a typical Winter week in Climate Zone 4A. See Table 2 for MAPE.

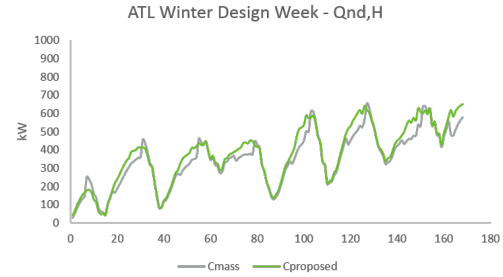

(b) $Q_{nd,H}$ for a typical Winter week in Climate Zone 3A. See Table 2 for MAPE.

Figure 7: Comparison of thermal demand for space heating, $Q_{nd,H}$, between C_{mass} and $C_{proposed}$.

of occupancy schedule weighted averaging and the demand at night tends to be over-predicted by $C_{propsed}$ and similarly under-predicted during the day.

The effect of weighted averaging on the hourly profile is also seen for $Q_{nd,H}$ (Fig. 7). $C_{proposed}$ forecasts C_{mass} at an MAPE of 7% and 13% for winter weeks in Climate Zone 4A (Table 3) and 3A (Table 2), respectively. C_{mass} predicts higher peak values than $C_{proposed}$, while $C_{proposed}$ forecasts higher power demand during the day. The daytime over-prediction should not be considered a shortcoming of the overall modeling methodology, but is rather due to the selection of the mix of the validation model's building types. For example, the single family and multi family buildings have very low use during the day, while the small office has a high use during the day. Similarly, $C_{proposed}$ has higher night time agreement to C_{mass} as the small office use schedule is near zero at night and thus has little effect on the $C_{proposed}$.

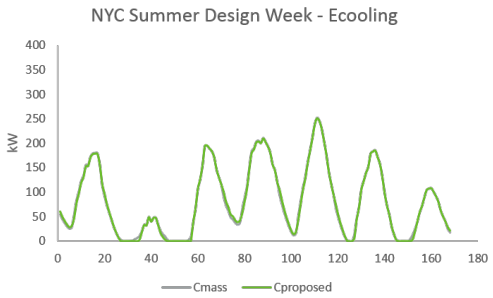

(a) $E_{cooling}$ for a typical Summer week in Climate Zone 4A. See Table 2 for MAPE.

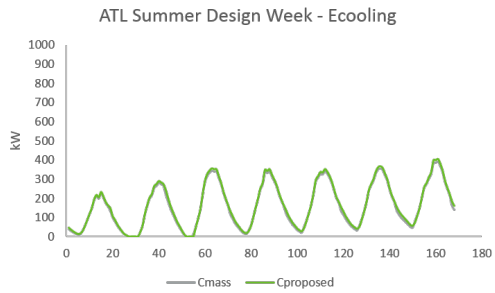

(b) $E_{cooling}$ for a typical Summer week in Climate Zone 3A. See Table 2 for MAPE.

Figure 8: Comparison of electric power for cooling, $E_{cooling}$, between C_{mass} and $C_{proposed}$.

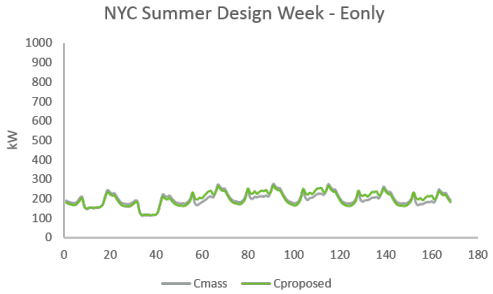

(a) E_{only} for a typical Summer week. See Table 2 for MAPE.

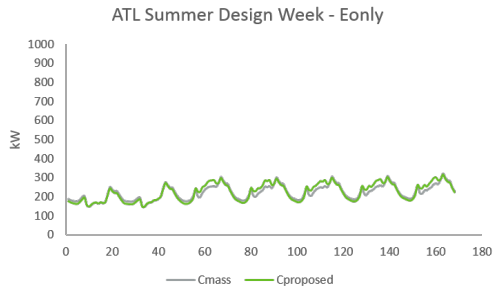

(b) E_{only} for a typical Winter week. See Table 2 for MAPE.

Figure 9: Comparison of total electric power for non-HVAC purposes, E_{only}, between C_{mass} and $C_{proposed}$ in Climate Zone 4A.

$C_{proposed}$ also has strong agreement to the C_{mass} for the non-HVAC related and HVAC related electric power demand. $E_{only,no\ dhw}$ has an annual MAPE of less than 2% for both Climate Zone 3A (Table 3) and Climate Zone 4A (Table 2). Adding in the E_{dhw} signal, however, increases the error, but in both climate zones the annual MAPE is less than 7% (Table 3 and Table 2). There is a correlation between the MAPE in $Q_{nd,H}$ and $E_{fans,\ pumps}$ during winter weeks and a correlation between $Q_{nd,C}$ and both $E_{cooling}$ and $E_{fans,\ pumps}$ for summer weeks. Despite the correlation to error in thermal demand prediction the magnitude of MAPE is reduced for electric power demand calculation. Fig. 10 details the strong model agreement for the summer cooling electric power demand of the building aggregate in Climate Zone 3A and Fig. 9 reveals strong agreement for Climate Zone 4A.

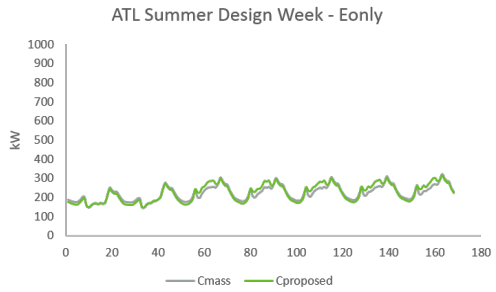

(a) E_{only} for a typical Summer week. See Table 2 for MAPE.

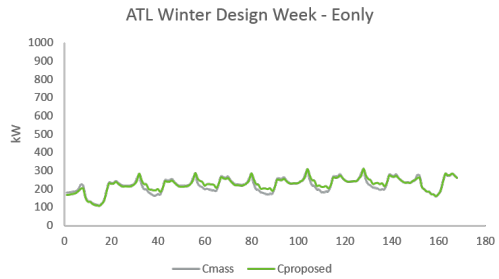

(b) E_{only} for a typical Winter week. See Table 2 for MAPE.

Figure 10: Comparison of total electric power for non-HVAC purposes, E_{only}, between C_{mass} and $C_{proposed}$ in Climate Zone 3A.

We have provided an initial validation for the modeling methodology described in Section 2.3 and our conclusion is that $C_{proposed}$ is an acceptable method for modeling the thermal and electric power demand of aggregate of buildings with mixed types. We arrived at this conclusion by comparing the forecast error of a model $C_{proposed}$ to a model noted C_{mass} to represent the actual demand. Both models are derived from representations of several typical building types: 15 single family residences, 5 multi-family residences and 4 small office buildings. $C_{proposed}$ forecasts the annual aggregate thermal and electrical energy demand with a percentage error less than 10% for all performance indicators of interest (Fig. 5). In addition, an hourly analysis of the MAPE reveals that $C_{proposed}$ forecasts the C_{mass} demand at less than 10% for all performance indicators except E_{dhw} (Table 3 and Table 2). Despite the high MAPE of E_{dhw} the aggregate energy is matched exactly between $C_{proposed}$ and C_{mass} (Fig. 5). Examination of the hourly demand plots suggests that the MAPE of $C_{proposed}$ is not due to a systematic shortcoming of the methodology, but rather in the weighted averaging of the scheduling that works on aggregate, but introduces slight discrepancies at the hourly resolution (Fig. 6, Fig. 7, Fig. 8, Fig. 9 and Fig. 10).

2.5 Hypothesis 1: More Design Options

Hypothesis 1: An integrated microgrid system model with high resolution demand and supply models will enable decision makers to analyze more design options and decision variables than is possible with currently available tools.

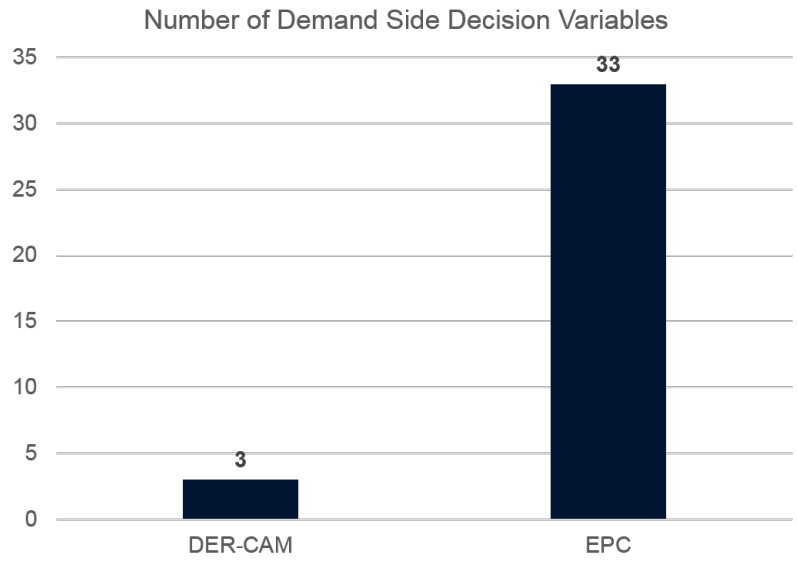

Figure 11: The existing demand modeling within DER-CAM allows only three decision variables versus 33 with the EPC tool.

The first hypothesis of this work is that a integrating a high resolution demand model with a supply side modeling tool will result in an integrated microgrid model with more decision variables than currently available tools. The EPC tool has 33 input variables compared to the DER-CAM demand modeling tool's three (Fig. 11).

2.6 Conclusions

A preliminary step to modeling demand and supply within a microgrid simultaneously as a single system is to have tractable models that represent the performance of the individual sub-systems. In this chapter we reviewed the major developments for the modeling of thermal and electric demand in buildings and building aggregates. The primary problem we identified is that current methods are limited in their scalability in terms of information and computation requirements. This chapter proposed a novel method of building aggregate modeling that advances several key approaches of aggregate demand modeling from the literature. The approach relies on a normative calculation scheme, but is capable of representing a mixed aggregate of buildings within a single modeling instance.

To validate the model we tested our hypothesis that the proposed model would have an acceptable forecast capability as a model of a building aggregate composed of multiple individual model

instances. We confirm our hypothesis that the novel modeling scheme is acceptable for modeling building aggregates for two primary reasons: (1) the annual percentage error for all performance indicators is less than 10% across the investigated climate zones and (2) the MAPE of individual performance indicators at the hourly resolution is within 10% for all metrics except domestic hot water. Based on these findings we accept the proposed model as valid for aggregated demand modeling particularly within the context of the integrated design of microgrid systems.

The proposed model, however, is formulated in terms of discrete specifications of individual buildings and non-linear models with purely discrete variables are inherently challenging to optimize (Murray and Ng, 2002; Arora et al., 1994). Therefore, the next chapter directly address the problems with demand side design optimization given the current modeling framework and proposes a methodology for transforming the problem into one that is more easily optimized while maintaining an equivalent mapping to decision maker preferences.

CHAPTER III

PARETO OPTIMAL COST FUNCTIONS FOR AGGREGATE BUILDING DEMAND OPTIMIZATION

The goal of this dissertation is to demonstrate a methodology for the integrated design of a microgrid system while considering both design interventions on the demand side and supply side simultaneously. To accomplish this requires a flexible formulation of modeling the demand that both captures relevant physical phenomena and maintains a scalable information requirement that can be refined as the design progresses. To that end the method proposed in Chapter 2 relies on a reduced order demand model of a user defined community. The modeling process, however, is difficult to apply to real optimization problems because of the size of the discrete option space, which is detailed in Section 3.1. This chapter details the transformation of the modeling approach from a discrete option space into a continuous option space while maintaining the functional relationship between design interventions and cost. First, this chapter describes the discrete option space spanned by the proposed model. Then the chapter defines a method of searching a continuous parameter space through the use of Pareto optimal cost functions. Finally, an example minimization problem is solved via two methods to demonstrate a validation of the proposed method.

3.1 Modeling a Discrete Option Space

The reduced order demand modeling framework of Chapter 2 facilitates the exploration of a number of demand related decision variables yet the optimization of this model for a decision maker's given preference function is difficult due to the number of discrete options that arise even for a modest number of physical variables. The following sections discuss the theoretical size of the underlying discrete option space and a method to instead optimize over a continuous variable space.

3.1.1 Enumerating the Number of Demand Side Options

The proposed demand model formulation of Section 2.3 allows a decision maker to evaluate the affect of architectural interventions on the performance of a building stock or community. While

the demand model is still a single instance of a reduced order building energy model, its inputs are calculated on the fly. To understand how this calculation occurs lets return our focus to how the single model instance is derived. First, the decision maker groups similar buildings within the community into clusters. In this way each cluster has a distinct number of buildings. After this stage the decision maker has i unique clusters of buildings where each cluster is comprised of k_i *indistinguishable* buildings. *Indistinguishable* is an assumption we make so that all the buildings in a single cluster may be modeled identically.

Now say a decision maker is interested in deciding on j physical parameters of the community, then each cluster must also have j parameters, but as the clusters represent different building types the number of discrete options for the same physical parameter may vary for each cluster. To calculate the community level value of Var_j the decision maker must allocate each of the k_i buildings to a single discrete level of $Var_{i,j}$ (i.e., specify the value of $x_{i,j,k_{i,j}}$ where $x_{i,j,k_{i,j}} \epsilon \{0, 1, ...k_{i,j}\}$) (Fig. 12).

For example, assume that we model a community with two clusters (i.e., i = 2) and we are interested in a single physical parameter (i.e., j = 1) and that each cluster has three discrete options of variable j (i.e., $k_{1,1}$ = $k_{2,1}$ = 3). Then to model a single physical parameter j at the community level introduces six discrete variables from the bottom-up.

We see that despite reducing the problem to a single model instance that by calculating the impact of changes to individual buildings on the fly causes the formulation to become very detailed and the decision maker may evaluate a large number of options. An optimization problem that uses the model of Section 2.3 requires the decision maker to specify an objective function that is a mapping from the aggregate's design options to a metric of performance. This could be formulated with the proposed model as:

$$\textbf{maximize: } J(\mathbf{x}) \tag{5}$$

$$\textbf{subject to: } \sum_{k=1}^{k_{i,j}} x_{i,j,k_{i,j}} = n_i \; \forall \; i, j \tag{6}$$

$$0 \leq x_{i,j,k_{i,j}} \leq n_i \; \forall \; i, j, k \tag{7}$$

where $x_{i,j,k_{i,j}}$ is an integer number corresponding to the number of "C_i -type" buildings at the given

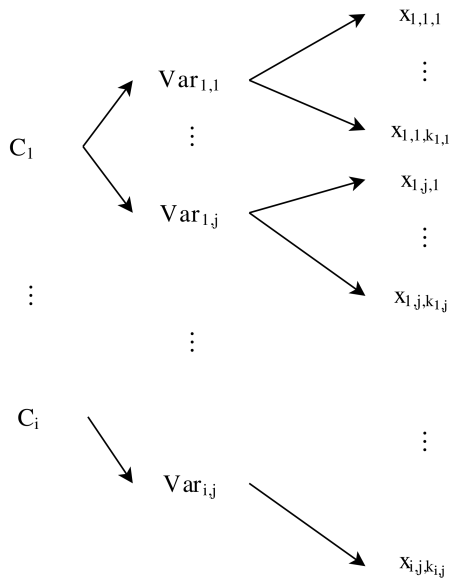

Figure 12: An aggregate model is made of i clusters with j variables and each variable has $k_{i,j}$ discrete levels. $x_{i,j,k_{i,j}}$ is an integer number corresponding to the number of "C_i -type" buildings at the given variable level.

variable level, n_i is the number of buildings in cluster i (Fig. 13). Eq. 6 ensures that the number of buildings specified for each variable is equal to the number of buildings in the cluster. Eq. 7 ensures that the number of buildings at each level for variable j is less than or equal to the maximum number of buildings for a given variable. Formulating an optimization problem, however, in accordance with Fig. 12 is problematic as it introduces a number of discrete variables:

$$N_{var} = \sum_{i} \sum_{j} k_{i,j} \tag{8}$$

where N_{var} is the number of decision variables of the optimization problem, $k_{i,j}$ is the number of levels of variable j for cluster i. The typical formulation of decision variables is not ideal as the goal is to make decisions regarding only j variables yet we have introduced $i \cdot j$ decision variables. An alternative formulation is to optimize the j variables each with discrete values (Fig. 14).

For any given community model we may count the number of possible design options for a single variable. Fig. 13 illustrates the counting method for determining the size of the option space of an aggregate demand model with three clusters, a single variable and three levels of the variable for each cluster. In practice, the number of levels may vary for each cluster. The total count of

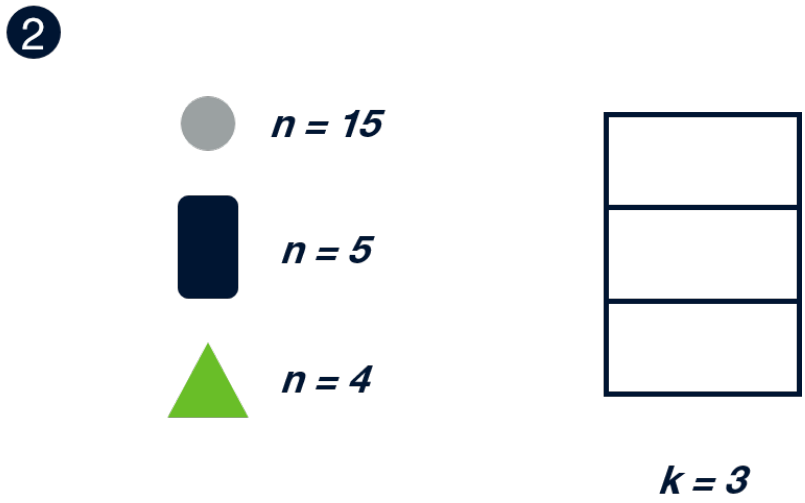

Figure 13: Simple illustration of an aggregate model's counting principle. An aggregate model is comprised of several clusters with n indistinguishable buildings. Here the discrete options for a variable is $k = 3$. By Eq. 9 there are 42840 discrete values of this variable in the aggregate model.

discrete values of the aggregate model for this variable is given by:

$$l_j = \prod_i \binom{k_{i,\,j} + n_i - 1}{n_i} \tag{9}$$

where l_j is the number of design options for variable j, n_i is the number of *indistinguishable* buildings in cluster i and $k_{i,\,j}$ is the number of levels of variable j for cluster i. The notation $\binom{n}{k}$ is short hand for the combinatorial counting problem and is interpreted as n *choose* k. For the particular case illustrated in Fig. 13:

$$\binom{3+15-1}{15} \cdot \binom{3+5-1}{5} \cdot \binom{3+4-1}{4} = 42840$$

Then we may also calculate the size of the complete design option space:

$$N_{total} = \prod_j l_j \tag{10}$$

where N_{total} is the full number of discrete options available on the demand side model with l_j given by Eq. 9. The formulation of Fig. 14 is an improvement over the initial formulation because now the

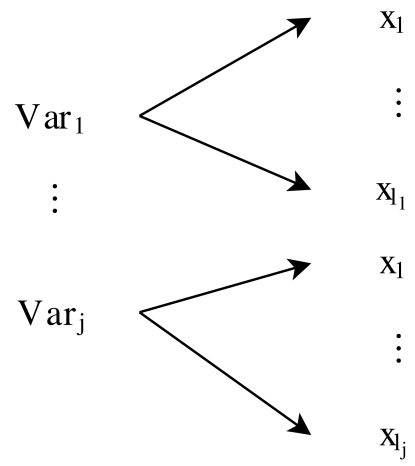

Figure 14: An aggregate demand model formulated in terms j variables rather than i clusters as in Fig. 12. Each variable has l_j discrete values, x_{l_j}. Number of discrete values calculated for each variable via Eq. 9.

optimization problem may be stated in terms of only j decision variables. This solution, however, is still unsatisfactory as the mapping to the cost for each value of x for every variable is not a one-to-one mapping. This result is to be expected: there are a number of possible configurations that result in the same x value, but with a number of different associated costs.

It is important to restate our assumption that buildings within clusters are indistinguishable. This assumption allows to avoid identifying the costs of individual upgrades to different buildings rather we now must only specify the costs of various investment options at the cluster level. Given just the cost information at the cluster level as in Table 5 and an algorithm to enumerate all the possible combinations allows us to generate the complete cost space as in Fig. 17 and Fig. 18. A related approach would be to forgo enumerating the complete cost space of specific clusters in favor of finding average cost data that relates the performance to cost in a similar fashion. In theory, either approach could be applied, but here we use explicit cost data built from cluster data.

For instance, the same window u-value for the overall building aggregate may be achieved by either upgrading more buildings with a mid-level performance window or by upgrading fewer buildings with a very high-performance window. As the high-performance window will tend to be more expensive, this simple hypothetical reveals that there are multiple cost solutions for a single performance level. Another burden is that the number of discrete options will be quite large for

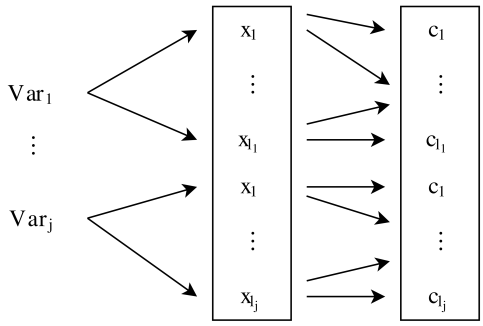

Figure 15: Each discrete value x_l maps to a cost c_l. The mapping, however, is not guaranteed to be 1-to-1 and in practice there will be a number of x values that match to a range of c values.

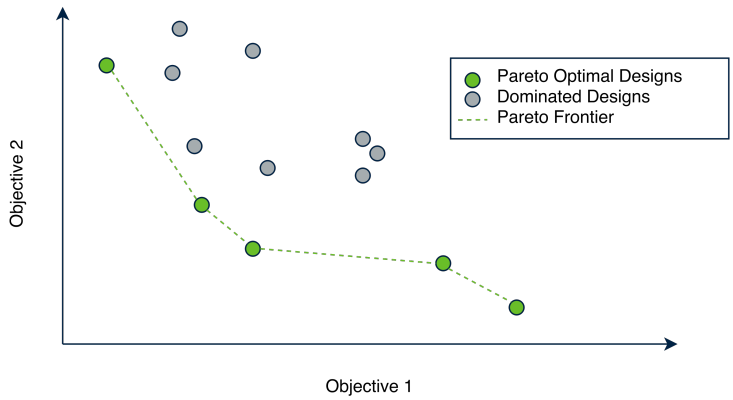

Figure 16: A design problem with Multiple Objectives and the Pareto frontier.

each variable j and thus the optimization problem will become more computationally intensive. To overcome these challenges, this dissertation proposes a continuous formulation of the j variables that explicitly considers the multiple solutions for each level of performance by only considering Pareto optimal cost values. Details of the continuous method follow in Section 3.2.

3.2 Aggregate Demand Model Evaluation with a Continuous Variable Formulation

As we note in the previous section, the modeling of a building aggregate according to Section 2.3 results in a functional relationship between design parameters and option cost that is not a one-to-one mapping (Fig. 15). In this case, it is not possible to maximize a chosen objective function because the relationship between design variables and cost is not a true function. There is an explicit trade-off, however, evident in the relationship between design parameter and cost, which allows a decision maker to evaluate the desirability of certain combinations.

In fact, a number of problems in the fields of engineering, management, social sciences and

design involve trade-offs between multiple preference criteria. In the face of decisions regarding trade-offs it is important to consider a level of efficiency in the selection of design parameters, that is to say we must consider how efficient a design parameter selection is at approaching our preferences regarding specific criteria. Selection of a design parameter that does not allow a competing objective to be improved any further is considered to be Pareto optimal (i.e., Pareto efficient/non-dominated) and all design points that meet this criterion form the Pareto set (Luc, 2008). A Pareto set of optimal design points may theoretically be infinite, which is represented by the Pareto frontier (Fig. 16). A Pareto frontier is the theoretical boundary that defines the feasible set of design points that reach Pareto optimality and in general all points along the Pareto frontier can not be ranked and each combination along the frontier is considered equally acceptable.

Table 4: Parameters of the example community used to determine the cost functions in Fig. 17 and Fig. 18

Building Type	Floor Area $[m^2]$	Roof Area $[m^2]$	Envelope Area $[m^2]$	Window Area $[m^2]$	Count
MultiFamily	2008	785	1256	247	5
Small Office	511	599	209	57	4
Single Family	335	118	202	33	15

3.2.1 Pareto Frontier Based Variable Selection

We apply the concept of a Pareto frontier, but as a means of transforming the one-to-many functional relationship of aggregate building model design parameters and annualized improvement cost into a one-to-one relationship. Since the Pareto frontier of a relationship between two variables is continuous, it is now feasible to model the independent variable of interest as a continuous variable. To accomplish this we assume that all the discrete values of a particular design variable may be enumerated as shown in Fig. 14. Then the complete relationship to cost is determined as suggested in Fig. 15. The final step is to calculate the Pareto set from the data and to model the cost of Var_j as a linear interpolation of the Pareto frontier.

We have defined a sample community to demonstrate the use of the Pareto optimal cost functions. The community parameters and costs are defined in Table 4 and the design option space is

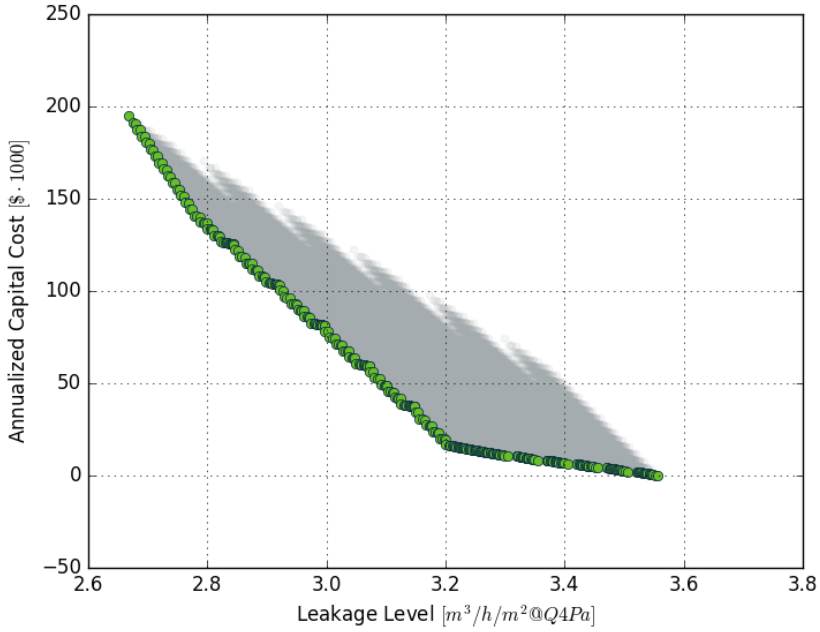

Figure 17: Pareto frontier and discrete options of the Leakage Level parameter of the community defined in Table 5.

defined in Table 5. The community is identical to the one used in the model validation of Section 3.1. In this case we are interested in two decision variables the building leakage level and the roof u-value (Table 5). The specifics of the variables are not of great importance for this exercise, however, the building leakage level defines the level of infiltration and the roof u-value defines the roof's resistance to heat flow. Each of these parameters influence the thermal demand buildings, the magnitude of influence is affected by climate and building function. Nevertheless, these variables are typically of interest during the retrofit decision making process.

We assume that each building's leakage level and roof u-value may assume only one of three possible levels and that each level has an associated cost. The costs in Table 5 are normalized by a corresponding value denoted the "Cost Multiplier" and the exact units are specified under "Cost Unit". In addition, we are interested in the annual cost of ownership. Annual cost is a means of representing the lifetime cost of ownership of an investment considering the rate of inflation (or interest), which is why Table 5 includes a proposed "Lifetime" value.

Section 3.1 showed via Eq. 9 that for a variable with three levels and three building clusters (n_1 = 15, n_2 = 4 and n_3 = 5) there are 42840 discrete options of that single variable. Per Table 5

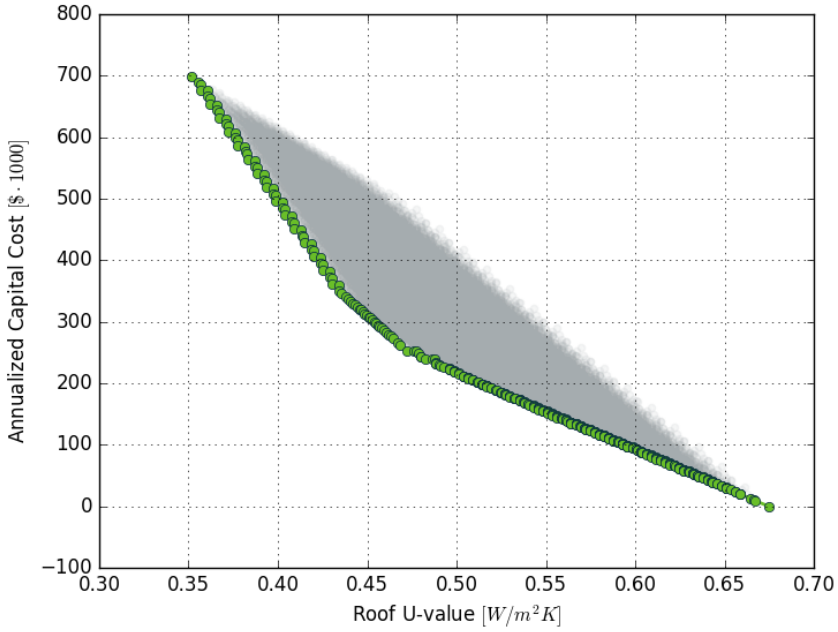

Figure 18: Pareto frontier and discrete options of the Roof U-Value parameter of the community defined in Table 5.

there are two variables with the same characteristics and via Eq. 10 there are 42840^2 options of the building aggregate's leakage level and roof u-value. It is not necessary, however, to consider the entire option space because as we noted previously there are a number of ways to achieve any single value of either roof u-value or building leakage level. Fig. 18 and Fig. 17 illustrate the complete option space for roof u-value and building leakage level, respectively. The figures also highlight the Pareto optimal options, which lie along the curve that minimizes both annual cost and the variable of interest.

The Pareto frontier is a theoretical curve and there are not necessarily any physical solutions that exist along the curve other than at the points that define the "frontier". Fig. 18 and Fig. 17, however, demonstrate that this "frontier" is well defined even for modest building aggregates (i.e., a large number of defining points). We use this feature to justify the transformation of the aggregate model into a function of continuous input parameters. We make the cost function continuous via linear interpolation over the set of points that define the Pareto frontier.

Table 5: Design option space for the generic validation case with three building types and two decision variables each with three discrete levels.

Variable	Building Type	Option Level	Annuity Rate	Lifetime	EPC Variable	EPC Unit	Cost	Cost Multiplier	Cost Unit
Leakage Level	Multi-Family	0	8.5	10	4.3	$[m^3/h/m^2@Q4Pa]$	0	2008	$/floor area
Leakage Level	Multi-Family	1	8.5	10	3.87	$[m^3/h/m^2@Q4Pa]$	1	247	$/sf window
Leakage Level	Multi-Family	2	8.5	10	3.225	$[m^3/h/m^2@Q4Pa]$	2.25	1256	$/sf total envelope
Roof U-value	Multi-Family	0	14.9	20	0.358	$[W/m^2K]$	0	785	$/roof area
Roof U-value	Multi-Family	1	14.9	20	0.2506	$[W/m^2K]$	1.15	785	$/roof area
Roof U-value	Multi-Family	2	14.9	20	0.1969	$[W/m^2K]$	2.3	785	$/roof area
Leakage Level	Small Office	0	8.5	10	2.5	$[m^3/h/m^2@Q4Pa]$	0	511	$/floor area
Leakage Level	Small Office	1	8.5	10	2.25	$[m^3/h/m^2@Q4Pa]$	1	57	$/sf window
Leakage Level	Small Office	2	8.5	10	1.875	$[m^3/h/m^2@Q4Pa]$	2.25	209	$/sf total envelope
Roof U-value	Small Office	0	14.9	20	0.358	$[W/m^2K]$	0	599	$/roof area
Roof U-value	Small Office	1	14.9	20	0.2506	$[W/m^2K]$	1.15	599	$/roof area
Roof U-value	Small Office	2	14.9	20	0.1969	$[W/m^2K]$	2.3	599	$/roof area
Leakage Level	Single Family	0	8.5	10	2.5	$[m^3/h/m^2@Q4Pa]$	0	335	$/floor area
Leakage Level	Single Family	1	8.5	10	2.25	$[m^3/h/m^2@Q4Pa]$	1	33	$/sf window
Leakage Level	Single Family	2	8.5	10	1.875	$[m^3/h/m^2@Q4Pa]$	2.25	202	$/sf total envelope
Roof U-value	Single Family	0	14.9	20	1.81	$[W/m^2K]$	0	118	$/roof area
Roof U-value	Single Family	1	14.9	20	1.267	$[W/m^2K]$	5.5	118	$/roof area
Roof U-value	Single Family	2	14.9	20	0.905	$[W/m^2K]$	18.4	118	$/roof area

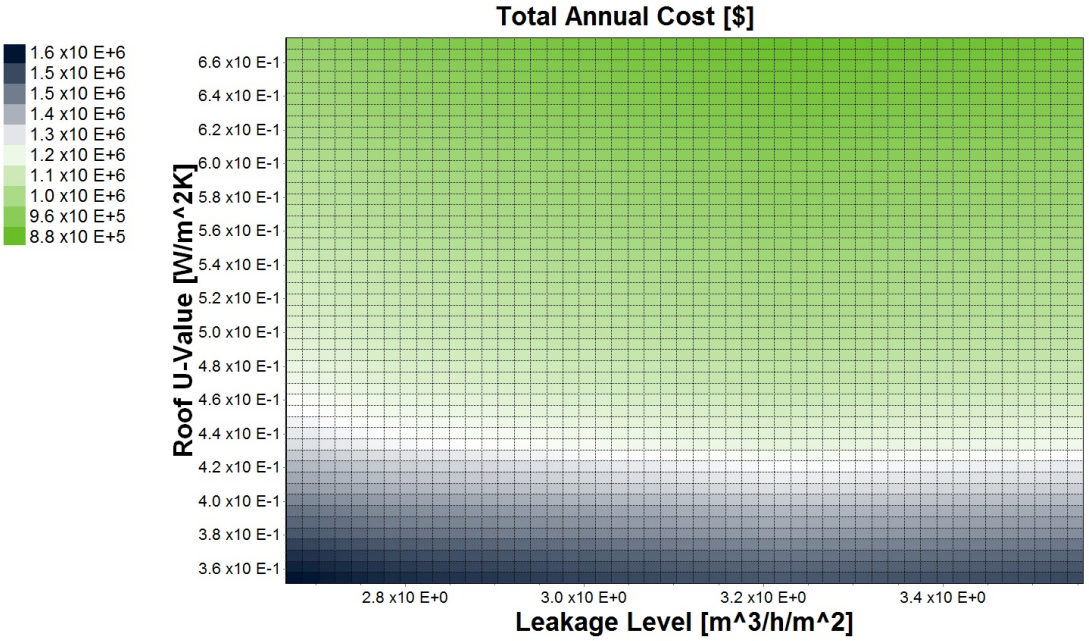

Figure 19: Design of Experiments (DOE) exploration of the total annual cost as a function of roof thermal conductivity and building leakage level.

3.3 Validation

Hypothesis: The proposed continuous optimization approach leads a decision maker to the same decisions as the discrete optimization approach, but in a shorter time, with fewer decision variables and fewer constraints.

To test this hypothesis we will use the aggregate demand model established in Section 3.2. The buildings of interest are 15 single family residences, five multi-family residences and four small office buildings located in Climate Zone 4A (Central Park, NY, NY). In this scenario we assume that the decision maker is an individual or ownership group with the ability to retrofit the complete stock of buildings and their goal is to minimize the annual energy costs of the portfolio at a minimum investment cost. There are two physical parameters of interest: roof thermal conductivity and building leakage level.

The optimization scenario follows the option and parameter spaces defined by Table 5 and Table 4, respectively. The objective function is defined as:

$$\textbf{minimize: } DRC + EC + ARC \tag{11}$$

where DRC is the Annual Demand Rate Charge [\$], EC is the Annual Energy Charge [\$] and ARC is the Annual Retrofit Cost [\$]. We assume for this hypothetical scenario that the ownership group is charged as an aggregate and that this aggregate is under a commercial building like tariff. DRC is a common rate structure where power consumers are charged on their $\$/kW$ demand use. There are a number of complex ways that utilities administer demand charges, for example's sake we assume the decision maker is charged $\$\ 16/kW$ of the highest demand each month regardless of the time of occurrence. We assume the decision maker is charged $\$\ 0.12/kWh$ for energy use and that this value is constant throughout the year. The retrofit costs are annualized via an annuity rate:

$$\text{Annuity Rate Coefficient} = \frac{1-(1+i)^{-n}}{i} \tag{12}$$

where i is the interest rate and n is taken to be the lifetime of a component. Each optimization approach has a unique set of decision variables and constraints. The number of decision variables in the discrete optimization approach is calculated from Eq. 8 and Table 5:

$$\begin{aligned} N_{var,\,discrete} &= \sum_i \sum_j k_{i,j} \\ &= (3+3+3+3+3+3) \\ &= \underline{18} \end{aligned}$$

$k_{i,j}$ is the number of discrete levels for variable j and cluster i. The continuous optimization approach considers two decision variables, which matches the number of physical parameters of interest. The discrete optimization case an upper limit and lower limit constraint on each decision variable and a summation constraint on each variable for each cluster:

$$\begin{aligned} N_{constraints,\,discrete} &= 2 \cdot\ N_{var,\,discrete} + \sum_i N_{var,i} \\ &= 2 \cdot\ 18 + (2+2+2) = \underline{42} \end{aligned}$$

where $N_{var,i}$ is the number of variables with $k_{i,j}$ discrete levels for cluster i. The continuous optimization approach has upper and lower limit constraints on each of the two decision variables for a total of four constraints. Annualized Retrofit Costs in the discrete case are calculated as the inner product of the decision variables, annuity rate, cost and cost multiplier while in the continuous case the costs are linearly interpolated from the Pareto frontier (Fig. 18 and Fig. 17).

Each optimization is started from the same point, which is the minimum of the Design of Experiments (DOE) conducted to map the design space (Fig. 19). The DOE is a full-factorial design with 50 levels for each of the variables of roof thermal conductivity and building leakage level, which is 2500 model executions. The starting points for each optimization are given in Table 6.

Table 6: Starting parameter sets for both the continuous and discrete optimization attempts with the initial total cost.

Objective Function Value		$ 879,486.05
Continuous	$x_{RoofU-Value}$	0.675
	$x_{Leakage\ Level}$	3.21
Discrete	$x_{MultiFamily,\ Leakage\ Level,0}$	0
	$x_{MultiFamily,\ Leakage\ Level,1}$	5
	$x_{MultiFamily,\ Leakage\ Level,2}$	0
	$x_{MultiFamily,\ Roof\ U-value,0}$	5
	$x_{MultiFamily,\ Roof\ U-value,1}$	0
	$x_{MultiFamily,\ Roof\ U-value,2}$	0
	$x_{Small\ Office,\ Leakage\ Level,0}$	0
	$x_{Small\ Office,\ Leakage\ Level,1}$	4
	$x_{Small\ Office,\ Leakage\ Level,2}$	0
	$x_{Small\ Office,\ Roof\ U-value,0}$	4
	$x_{Small\ Office,\ Roof\ U-value,1}$	0
	$x_{Small\ Office,\ Roof\ U-value,2}$	0
	$x_{Single\ Family,\ Leakage\ Level,0}$	2
	$x_{Single\ Family,\ Leakage\ Level,1}$	13
	$x_{Single\ Family,\ Leakage\ Level,2}$	0
	$x_{Single\ Family,\ Roof\ U-value,0}$	15
	$x_{Single\ Family,\ Roof\ U-value,1}$	0
	$x_{Single\ Family,\ Roof\ U-value,2}$	0

3.3.1 Discrete Optimization Approach

The discrete optimization formulation to the optimization problem outlined in Eq. 11 is:

$$
\begin{aligned}
\textbf{minimize:}\quad & DRC + EC + ARC \\
\textbf{subject to:}\quad & 0 \leq x_{multifamily,\ roof,0} \leq 5 \\
& \vdots \\
& 0 \leq x_{smalloffice,\ roof,2} \leq 4 \\
& 0 \leq x_{smalloffice,\ leakage,0} \leq 4 \\
& \vdots \\
& 0 \leq x_{single\ family,\ leakage,2} \leq 15 \\
& \sum_{j} \sum_{k=1}^{k_{multifamily,j}} x_{multifamily,j,k} = 5 \\
& \sum_{j} \sum_{k=1}^{k_{small\ office,j}} x_{small\ office,j,k} = 4 \\
& \sum_{j} \sum_{k=1}^{k_{single\ family,j}} x_{single\ family,j,k} = 15
\end{aligned}
$$

Engineering practice has a number of design problems that both exhibit nonlinear behavior and rely on discrete variables. Although functions of discrete variables have fewer theoretical outcomes, these functions are more difficult either maximize or minimize globally because the response surface is non-convex and disjoint (Arora et al., 1994). Arora et al. (1994) describes the most commonly applied methods for mixed nonlinear programming (MNLP) (i.e., both discrete and continuous input variables): branch and bound methods, integer programming, rounding-off techniques, cutting plane techniques, heuristic techniques, penalty function approach, Lagrangian relaxation approaches and sequential linear programming. Arora et al. (1994) also describes a class of stochastic optimization algorithms known as *genetic algorithms*.

Genetic algorithms follow rules derived from Charles Darwin's theory of evolution; in particular, these algorithms prescribe a "survival of the fittest" type approach to determining feasible combinations of input parameters. Genetic algorithms are computationally expensive and rely on a large number of function evaluations yet this stochastic approach is useful as it does not require any knowledge of the function's derivatives and is a global search approach. Essentially, a set of

initial design parameters is defined and evaluated for their "fitness" (i.e., objective function value). New sets of parameters are selected and evaluated based on functions that define mutations and cross-over among the parameter values; this process ensures that new "generations" result in better evaluations of the objective function. It is essential to note that the genetic algorithm allows constraint violation, but incorporate penalty functions such that "offspring" that violate constraints are less likely to reproduce.

We solve the foregoing discrete problem using the genetic algorithm implemented within ModelCenter (ModelCenter, 2015).

3.3.2 Continuous Optimization Approach

The continuous formulation of the minimization problem defined in Eq. 11 is:

$$\begin{aligned} \textbf{minimize:} \quad & DRC + EC + ARC \\ \textbf{subject to:} \quad & 2.67 \ \leq \ x_{Leakage\ Level} \ \leq \ 3.56 \\ & 0.351 \ \leq \ x_{Roof\ U-Value} \ \leq \ 0.674 \end{aligned}$$

the foregoing minimization problem is still an example of nonlinear programming (NLP), but as the variables are continuous there are more search methods available to solve the problem. Here we apply the pattern search algorithm proposed by Hooke and Jeeves (1961) as implemented in ModelCenter (ModelCenter, 2015). A pattern search algorithm is also a direct search method similar to a genetic algorithm, however, the search pattern is deterministic. In essence the algorithm applies δ's of a prescribed value to the input parameters to monitor changes in the objective function and moves the search in the direction that minimizes the function.

3.3.3 Evaluating the Optimization Approaches

Our hypothesis states that the continuous variable formulation of the problem results in the same decision making as the discrete variable formulation. To evaluate this statement we compare the objective function value and the relationship between the continuous and discrete design spaces. They hypothesis also states that the continuous formulation produces a faster result, with fewer constraints and fewer decision variables. To evaluate this statement we: (1) compare both the clock

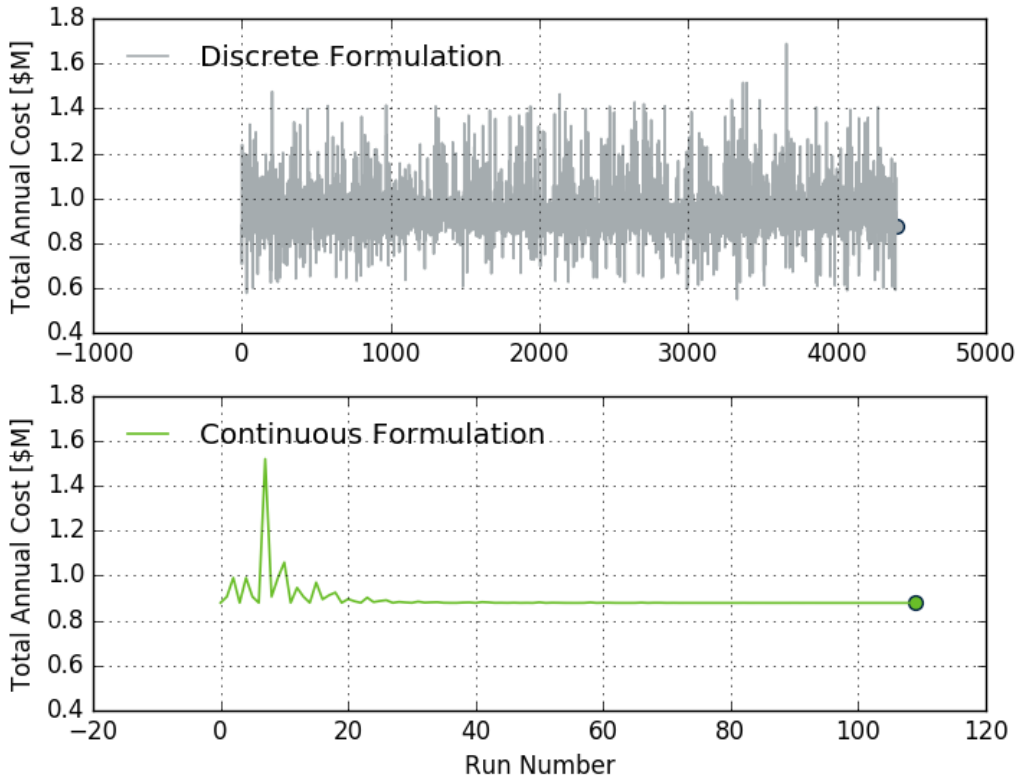

Figure 20: Comparison of the convergence sequence between the Discrete and Continuous formulations. The continuous formulation converges to an identical stopping point, but at fewer runs.

time and function evaluations required to find an optimal solution for each approach given the same start point on the same machine and (2) directly compare the number of variables and constraints between the two methods.

Fig. 20 compares the convergence of both methods. We see that both the continuous and discrete optimization approaches converge to the same minimum value of the Total Annual Cost. We also see, however, that the continuous method converges to the minimum solution in fewer function funs than the discrete formulation. Fig. 20 indicates that the first step of our hypothesis is in fact true, the continuous formulation will result in the same decisions as the discrete process. Furthermore, Fig. 20 indicates that the continuous solution achieves the minimum value in a fewer number of runs. This conclusion is supported by Fig. 21, which details the number of variables and constraints in each problem formulation. The bubble sizes in Fig. 21 are scaled to indicate the total number of function evaluations to reach the minimum objective function value. From Fig. 21 we see that

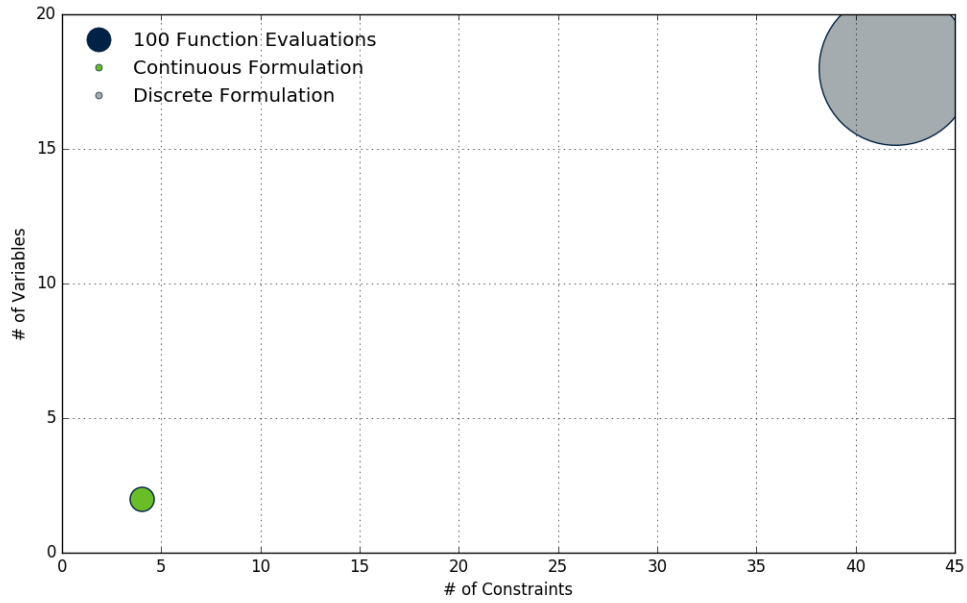

Figure 21: Comparison of the number of variables and constraints for each problem type with the bubbles scaled by the number of function evaluations to reach the minimum point.

the continuous approach has fewer decision variables, fewer constraints and fewer overall function evaluations.

3.4 Conclusions

To achieve our goal of modeling the microgrid system during the design phase in an integrated manner requires methodologies for both modeling and optimization. This chapter has detailed the transformation of the modeling approach defined in Chapter 2 from a discrete option space into a continuous option space. More importantly the transformation proposed maintains the functional relationship between design interventions and cost. This was achieved by applying a Pareto optimal search method that reduces the design space in a logical and preferential way. Finally, this chapter then validated the proposed Pareto optimal search method with continuous parameters by showing that this technique results in the same decision making as a discrete approach yet with fewer overall function evaluations, fewer decision variables and fewer constraints to the problem. As such we recommend the use of the continuous variable formulation over the discrete formulation in the integrated system modeling of a microgrid during the design phase. In the following chapter we

discuss a modeling framework for resilience inclusion during the design of the microgrid supply.

CHAPTER IV

SUPPLY MODELING IN INTEGRATED MICROGRID DESIGN

The goal of this dissertation is to introduce a framework for reliability based design of microgrids that integrates high resolution models of a microgrid's supply and demand sub-systems. The purpose of such an integrated model is both to facilitate more complete uncertainty analysis in microgrid design and support joint decision making efforts in performance based design of microgrids. To that end this chapter briefly reviews linear programming, which is a foundational tool to microgrid design and then introduces the Distributed Energy Resource Customer Adoption Model (DER-CAM) in depth. DER-CAM is a supply side modeling tool that calculates optimal dispatch and capacity sizes of various technologies; the version studied in this work is deterministic with an hourly resolution. Two extensions to this version of the DER-CAM equation set are introduced including a grid availability variable and reliability constraints that allow the decision maker to define preferences with respect to the expected unmet demand of the final microgrid.

4.1 Linear Programming & Microgrid Planning

Linear programming is a mathematical optimization technique that determines either the maxima or minima of an objective function defined as the linear combination of a set of decision variables with linear constraints. The power of linear programming is that a number of common problems in engineering and business can be approximated and modeled as linear equations. In addition this modeling methodology is powerful due to the fundamental theorem of linear programming, which states that if there is no optimal solution then the problem is either infeasible or unbounded. Since linear programming guarantees optimal solutions for feasible and bounded problems, it provides a promising starting ground for the design of a number systems.

The standard form of a linear program is to denote m as the number of constraints and n as the

number of decision variables x_j:

$$\begin{aligned}
\textbf{maximize } & c_1x_1 + c_2x_2 + ... + c_nx_n \\
\textbf{subject to: } & a_{11}x_1 + a_{12}x_2 + ... + a_{1n}x_n \ \leq b_1 \\
& a_{21}x_1 + a_{22}x_2 + ... + a_{2n}x_n \ \leq b_2 \\
& \vdots \\
& a_{m1}x_1 + a_{m2}x_2 + ... + a_{mn}x_n \ \leq b_m \\
& x_1, x_2, ..., x_n \ \geq 0
\end{aligned}$$

The *minimum-cost network flow problem* is a special class of linear programming problem with direct application to microgrid design. This class of problem minimizes the cost of moving a material quantity through a network of nodes and arcs. Mathematically we denote the nodes as $\mathcal{N}$ and the arcs that connect the nodes as $\mathcal{A}$. The corresponding set $(\mathcal{N}, \mathcal{A})$ is denoted either a network or *graph*.

A typical network flow problem must have the supply and demand of a material quantity for each node specified, while each arc has an associated cost of travel. Then b is used to denote the supply or demand from any node and $c_{i,j}$ is the cost to travel along the arc connecting node i to j and the conventional formulation is to ensure that the supply of a material quantity leaving a node equal to the demand at the node:

$$\sum_{i \, \epsilon \, \mathcal{N}} b_i = 0 \tag{13}$$

With the objective to minimize costs stated as:

$$\textbf{minimize: } \sum_{(i,j) \, \epsilon \, \mathcal{A}} c_{i,j}x_{i,j} \tag{14}$$

The *minimum-cost network flow problem* is widely applied throughout the power supply design and operation context under the specific name of the "unit-commitment problem". The unit commitment problem is so ubiquitous due to the fundamental theorem of linear programming, which ensures that the solutions are actually the optimal control of the power supply system. Once a

decision maker specifies the node capacities and the arc costs for a particular system then linear programming is applied to determine the minimum cost of operating the designed system for a given demand at each node.

4.2 Generic Unit Commitment Problem

Padhy (2004) summarizes the general approach to the unit commitment problem within the scope of utility operations scheduling. The generic goal of the unit commitment problem is to determine the commitment schedule (i.e., operation schedule) of a set of power generating or distributed energy resources at either minimum cost or maximum profit. The unit commitment problem does not determine the capacities of the generating unit; it simply calculates the optimal operation given a set of design capacities. Additional objectives for the operation may easily be defined, which may typically include minimize environmental cost. A key constraint in this formulation is that the power output from all units must be equal to the sum of forecast demand and any losses:

$$\sum_{i=1}^{N} (U_{i,t} \cdot \ P_{i,t}) = D_t + losses \tag{15}$$

Where N is the number of time units considered, $U_{i,t}$ is the availability status of unit i during time period t, with $P_{i,t}$ the corresponding power output of the unit. D_t is the demand during the time period t. Padhy (2004) notes an additional constraint: spinning reserve. Spinning reserve is the amount of power that a system holds in reserve throughout operation, which allows the system to increase its output as needed in the existence of a mismatch between actual and forecast demand. Padhy (2004), however, provides very little guidance regarding the spinning reserve and notes that this constraint may be expressed as either increased node capacities or as a reliability measure.

4.3 What is the DER-CAM tool?

The vast majority of microgrid design tools are software modules developed by individual researchers and there is much overlap in the underlying solutions. This overlap is largely due to the common implementation of the microgrid design problem as a linear program as discussed in Section 4.2. Commercial implementations of microgrid design software do exist, one such model

is the Hybrid Optimization Model for Electric Renewables (HOMER), which originated at the National Renewable Energy Laboratory and is now managed by HOMER Energy, LLC (Lilienthal et al., 2005). The HOMER tool, however, is not a true optimization tool rather it is a heuristic analysis methodology that is able to rapidly produce financial information regarding a pre-defined distributed energy resource investment strategy. For instance, HOMER will generate the financial return information for a user specified load and technology set, but will not return an optimum technology set for a known load nor will HOMER determine the optimal operation strategy.

Alternatively, the Distributed Energy Resource Customer Adoption Model (DER-CAM) is a microgrid design and modeling tool that has been developed by Lawrence Berkeley National Laboratory (Stadler, 2008, 2009b; Siddiqui et al., 2005). DER-CAM exists in two-forms either as an operations scheduling or microgrid planning formulation. This separation is needed to facilitate the different decision variables of interest between the two problems. Both problems are formulated as a Mixed Integer Linear Program (MILP) and have been implemented in the General Algebraic Modeling System (GAMS) language (Brooke et al., 1998).

We apply the DER-CAM tool in this dissertation as the supply optimization tool of choice because DER-CAM has no defined preferences for a given technology, calculates both thermal and electric demand recovery and storage, on-site generation and considers both sales and purchases of both electric power. The DER-CAM objective function is multi-objective and minimizes the sum of the normalized total annual cost and CO_2 emissions for meeting a user defined end-use energy demand. The total annual cost is the sum of annualized capital investment, fuel consumption and maintenance costs for distributed energy technologies.

This work applies the DER-CAM planning version of the model, which in addition to determining the optimal operation strategy also defines the optimal technology investment set for a user defined load. The load must be defined at an hourly resolution, but the planning period does not consider each hour of the year. Instead, the user defines three prototypical days for each month. One day representing a typical week day, a typical weekend day and finally a typical peak day. Therefore, the model finds the optimal investment strategy while considering just 36 days of operation throughout the year (Stadler et al., 2014).

While Stadler et al. (2014) incorporates a module for passive investment in demand improvements the authors note that the static building model is an area of needed improvement especially in regards to the assumed correlation between building envelope thermal resistance and cooling load, which is a key motivation for integrating the demand model of Chapter 2 with the DER-CAM tool.

4.3.1 DER-CAM Model Formulation

The full mathematical specification of the DER-CAM tool is proprietary and the author's were granted exclusive rights for use, but not publication of the source code. As such this section will detail the publicly available and high-level formulations of the modeling (Stadler et al., 2013). The DER-CAM objective function is multi-objective and considers the operational cost of providing energy services to a site and the associated CO_2 emissions:

$$\textbf{minimize: } J = w_1 \cdot C_{total}/C_{max} + w_2 \cdot CO_2/CO_{2,max} \tag{16}$$

$$C_{total} = C_{elec} + C_{DER} + C_{fuel} + C_{DR} + C_{EVbat} - V_{sales} \tag{17}$$

$$CO_2 = CO_{2,elec} + CO_{2,fuel} + CO_{2,EV} \tag{18}$$

where C_{total} is the total annual energy costs of the microgrid, C_{elec} are the electricity costs, C_{DER} are the distributed energy resources costs excluding stationary storage, C_{fuel} are the fuel costs for fuel based technologies, C_{DR} are the demand response costs for non-storage technologies, C_{EVbat} are the electric vehicle battery degradation costs and V_{sales} are total revenues from exporting electricity to the grid. The total CO_2 is the sum of the emissions due to electric energy consumption, $CO_{2,elec}$, emissions due to burning fuel, $CO_{2,fuel}$ and the emissions from electric vehicle exchange, $CO_{2,EV}$.

The key constraints on the model are the balance equations and operational constraints:

$$S_{U,m,h} + S_{DER,m,h} + S_{ST,m,h} + S_{EV,m,h} - V_{m,h} = D_{B,m,h} + D_{ST,m,h} + D_{EV,m,h} \tag{19}$$

$$ES_{ST,m,h} = ES_{ST,m,h-1} \cdot (1 - \phi_{ST}) + i_{ST,m,h} - o_{ST,m,h} \tag{20}$$

Eq. 19 is the supply and energy balance where $S_{U,m,h}$ is the electricity supplied by the utility, $S_{DER,m,h}$ is the electricity supplied by distributed energy resources, $S_{STm,h}$ is the electricity supplied by stationary storage, $S_{EV,m,h}$ is the electricity supplied by electric vehicles and $V_{m,h}$ is the

electricity sold to the utility. The demand components are segmented into the microgrid electricity demand, $D_{B,m,h}$, the microgrid demand from stationary storage, $D_{ST,m,h}$, and the electricity demand from electric vehicles, $D_{EV,m,h}$. Similar balance equations are modeled for heating, cooling and natural gas demand. Eq. 20 defines the physical modeling of electricity storage where $ES_{ST,m,h}$ is the energy stored stationary storage, ϕ_{ST} is a self degradation coefficient that model energy losses from stationary storage, while $i_{ST,m,h}$ and $o_{ST,m,h}$ represent the energy input and output, respectively, of the stationary storage. Similar flow equations model the storage in electric vehicles, which are not the focus of this dissertation.

Generators, storage and continuous technologies have constraints on their operation that follow typical assumptions of MILP of microgrid models:

$$gen_{g,m,d,h} + sell_{g,m,d,h} \leq num_g \cdot MaxP_g \tag{21}$$

$$sell_{i,u,m,d,h} = 0 \; \forall u \neq eo \tag{22}$$

where $gen_{g,m,d,h}$ is the energy dispatched by distributed generation source g at month m, day type d and hour h, $sell_{g,m,d,h}$ is the energy sold from distributed generation source g at month m, day type d and hour h, num_g is the integer number of generators of type g and $MaxP_g$ is the rated capacity of generator type g. Eq. 22 ensures end-use u of technology i is not sold back to the grid unless the end-use u is electricity only, eo.

As was stated in Section 1.3 the primary uncertainties within microgrid planning are related to the demand profile, as well as the utility, technology and control reliability. The reduced order demand model of Chapter 2 will facilitate demand side uncertainty propagation within future versions of the integrated microgrid system model; hence, in the following section we outline extensions to the DER-CAM tool itself to facilitate uncertainty propagation of utility reliability and to allow decision makers to specify their risk tolerances. Control failure and reliability is outside the scope of this work, but we do include a discussion on analogous interpretations of risk tolerances and operational load control.

4.4 Modeling Utility Reliability

Resilience and ability to operate in an islanded mode is an important performance criterion of microgrids. Jones (2015) notes several uncertainty sources that contribute to microgrid failure, of

which special focus was placed on the reliability of the grid. Jones (2015) model grid outages and their duration directly by aggregating information about the microgrid site that includes the location of trees and the occurrence rate of various sized storms. Xu et al. (2014) also directly model outages at distribution feeders to study the affects of these failures on the protection procedures of islanded microgrids.

In this work we re-formulate the DER-CAM energy balance limit state to facilitate the future use of quantified uncertainty of grid outages and their duration during microgrid planning:

$$S_{total,m,h} = S_{U,m,h} \cdot Z_{m,h} + S_{DER,m,h} + S_{ST,m,h} + S_{EV,m,h} + S_{Unmet,m,h} - V_{m,h} \cdot Z_{m,h} \quad (23)$$

$$D_{total,m,h} = D_{B,m,h} + D_{ST,m,h} + D_{EV,m,h} \quad (24)$$

Eq. 23 expresses the extended DER-CAM supply-demand limit state. We introduce two new variables: $S_{Unmet,m,h}$, which is the unserved energy at month m and hour h and $Z_{m,h}$, which is a binary input variable indicating the availability status of the grid. It is important to note that $Z_{m,h}$ is an input variable. Therefore a decision maker has additional options for incorporating knowledge of the utility's reliability into the microgrid planning stage. Either the decision maker has quantified the uncertainty in the frequency and duration of grid outages at the microgrid site or the decision maker prefers to specify particular outage scenarios that the microgrid should be prepared to withstand. The former approach requires data to support the underlying quantification and a potential source for such information in the United States is Energy Information Agency (EIA) (2013).

4.5 Enforcing Microgrid System Reliability via Constraints

The previous expression of the DER-CAM supply-demand limit state considered neither grid outages nor the possibility of unmet load as such it modeled the system as 100% reliable (Eq. 19). Such a situation is unrealistic and not modeling potential service interruptions does not allow a decision maker to objectively evaluate the performance of various microgrid design options. For example, unmet demand occurs in real systems if there are combined failures in the due to either a grid outage or technical failure of a DER component. Power system operator seek to balance the supply, S, and demand, D, of electricity at all instants and any imbalances can lead to financial losses for

both the consumer and operator (Makarov et al., 2009; Kjølle, 1996). A typical means of modeling service interruptions in the microgrid design problem is to establish the facility operator's interruption cost function, which is the cost associated with unmet demand given the duration and time of occurrence. Interruption cost functions are a useful means to translate an interruption directly into the cost function yet these functions vary from consumer to consumer. An alternative to defining an interruption cost function is to limit the feasible design space through a reliability constraint. Three important measures of the reliability of a power delivery point are the frequency of service interruptions, the duration of interruptions and the energy not served during the violation. These three measures expressed as normalized performance indicators are:

System Annual Interruption Frequency Index (SAIFI) ratio of total number of interruptions to the number of modeling periods.

System Annual Interruption Duration Index (SAIDI) ratio of total time in failure state to total modeling time period.

Expected Energy Not Served (EENS) ratio of the total energy not served in failure state to total demanded energy during modeling time period.

In this work we opt to introduce reliability constraints to the limit state of Eq. 23 rather than to specify an interruption cost function. In particular we apply a limit to the EENS, which is active over the entire modeling period as well as limit the Power Not Served (PNS) at each hour:

$$\frac{\sum_{m,h} S_{Unmet,m,h}}{\sum_{m,h} D_{total,m,h}} \leq EENS \tag{25}$$

$$S_{Unmet,m,h} \leq PNS_{m,h} \tag{26}$$

where $EENS$ and PNS are set by the decision maker prior to modeling to constrain both the maximum unmet energy and the unmet demand at each hour. When the decision maker specifies their tolerance to unmet energy throughout the modeling period and unmet demand at specific time intervals they are explicitly restricting the feasible design space. Hu and Cho (2014) present an example of ensuring reliability during operation of a CCHP system by reformulated the linear constraints as a set of probability inequalities.

4.6 Interpreting Reliability Constraints

The reliability framework we present in this work is designed to extend the current capabilities of the DER-CAM modeling tool and facilitate the propagation of more advanced levels of uncertainty throughout the microgrid design process. To that aim we have added a binary variable that allows a decision maker to model various utility reliability scenarios and to also define their own levels of power reliability without directly defining an interruption cost function. These points address the primary goal of Hypothesis 3, but we also wish to address the interdependent roles of advanced controls and microgrid reliability.

IEEE Standards Coordinating Committee 21 (2011) note that island capable microgrids require advanced controls, in particular the control, "may be used to balance the load in islanded mode (i.e., via load shedding, load following and load management)". Typically, to model advanced control interactions requires a high fidelity model of both supply and demand as well as the technical subsystems to be controlled. A number of optimal control studies have been undertaken especially within the microgrid context (Meiqin et al., 2008; Pourmousavi and Nehrir, 2012; Chauhan and Saini, 2014). Sharma et al. (2016) model both the demand and supply as a linear program and solve the optimal, centralized control via a model predictive control algorithm. However, the focus of this work is on the design and specification of the system, as such we seek to incorporate important aspects of control without needlessly increasing the modeling burden on decision makers.

An advantage to modeling the problem according to Eq. 25 - 26 is that the proposed integrated modeling framework does not need to model any control interactions between the demand and supply as these equations also define a load shedding policy. Because a decision maker is neutral to losing a specified amount of power at each hour with a limit on the total energy loss, the MILP will seek to optimally dispatch these losses within the constraints.

One plausible example is an electric dimmer switch. Suppose that a light is connected to a dimmer and at a known low power setting it provides enough light to satisfy all potential users for all possible scenarios, but that this setting was below its maximum power threshold. The difference in power between between the upper and lower threshold times the study period gives the maximum energy that can be shed, which then allows the decision maker to calculate the allowed EENS. In

addition, the power difference between the lower and upper thresholds indicates the allowed PNS. While this example may be slightly contrived, it encapsulates the difference between a "shiftable" and "sheddable" load. The sheddable load never has to be made up, as in the energy that is saved by not using the system does not need to be placed back into the system. In contrast, if we attempt to let the temperature of a refrigerator float in accordance with the same logic, at a certain point we must "replace" the energy that was released into the room by running a compressor.

Despite not modeling control actions explicitly a decision maker can evaluate the potential impact of a load shedding controller abstractly as long as the decision maker can determine the requisite reliability constraints. The DER-CAM tool also allows a similar abstract specification of control, in which the decision maker can specify the costs to either shift or shed loads at either a hi, medium or low power level (Stadler, 2009b).

Fig. 22b and Fig. 22a demonstrate the effects of specifying both EENS and PNS on the on the hourly operation schedule of an optimal microgrids. In this case the microgrids are modeled as off-grid. The first case we consider is Scenario 1 with an EENS of 0%, which is the base case design scenario. Fig. 22a details the minimum cost operation in the case of designing without considering grid outages or DER failures and no allowed load shedding. Fig. 22b notes how the load shedding takes place both at day and at night, with intermittent contributions from the generator.

4.7 Conclusions

This chapter discusses the practical aspects of reliability based design of engineering systems with special attention paid to the design of microgrids. The key value added to microgrid owners that arises from investing in supply technologies is the ability to control the reliability of the system; however, a number of supply side design tools do not incorporate a framework for either addressing uncertainties or reliability. The supply side design tool that we will integrate with the reduced order demand model is LBNL's DER-CAM tool, which is impressive for its current level of industry adoption, ability to simultaneously solve the optimal capacity and optimal operation problems of microgrids as well as the large number of technologies that can be modeled within the software. The primary shortcomings of the tool relate to the specification of the demand model and no previous work with either uncertainties or reliability based constraints. We introduce three performance

indicators of reliability that are often applied to electric power systems that address specific criteria of the system including: frequency of interruption, duration of interruption and service level. The purpose of these reliability indicators is to add additional constraints to the DER-CAM tool in order to allow a decision maker to specify their desired level of reliability. In addition, we add a feature to DER-CAM that allows a user to specify the utility's reliability, which is a key step in propagating additional uncertainties through the microgrid design process. This approach improves previous work into the reliability based design of microgrids because it explicitly considers the availability of the external grid via either normative scenarios or user quantified uncertainties. Finally, this chapter examines the importance of control interaction between demand and supply. The decision maker's neutrality to demand losses is actually a means of abstractly representing complex control interactions without having to explicitly model the demand side constraints. In the following chapters we will define the integrated modeling procedure in more detail as well as provide investigate the impact of utility uncertainty on microgrid design outcomes..

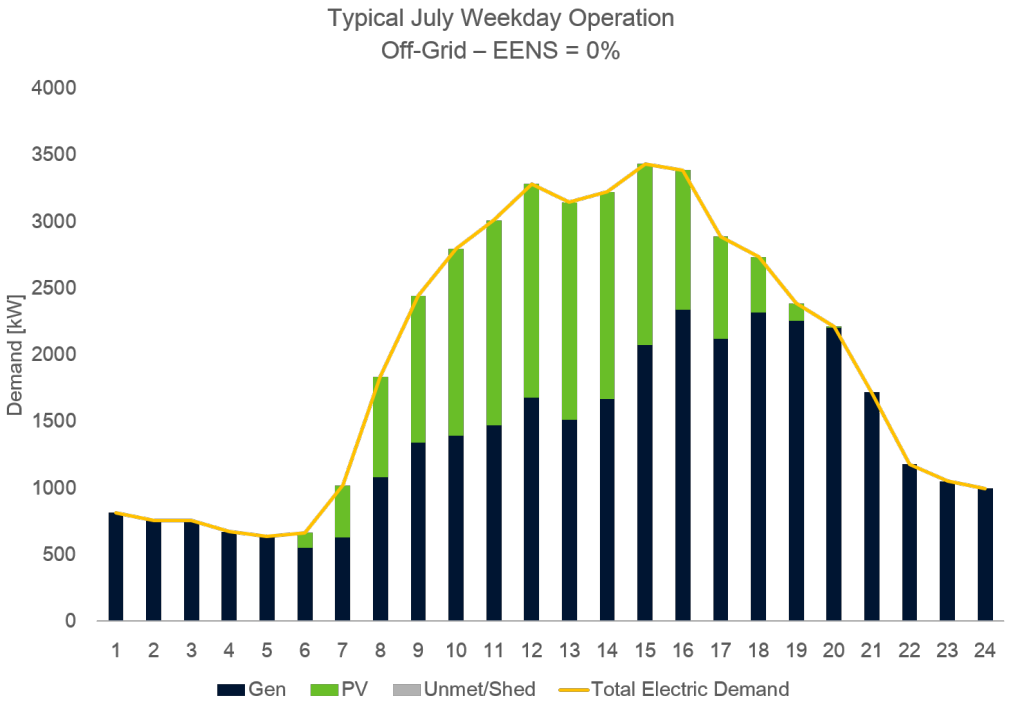

(a) Operation schedule of an optimal microgrid sized for an off-grid scenario with a 0% EENS.

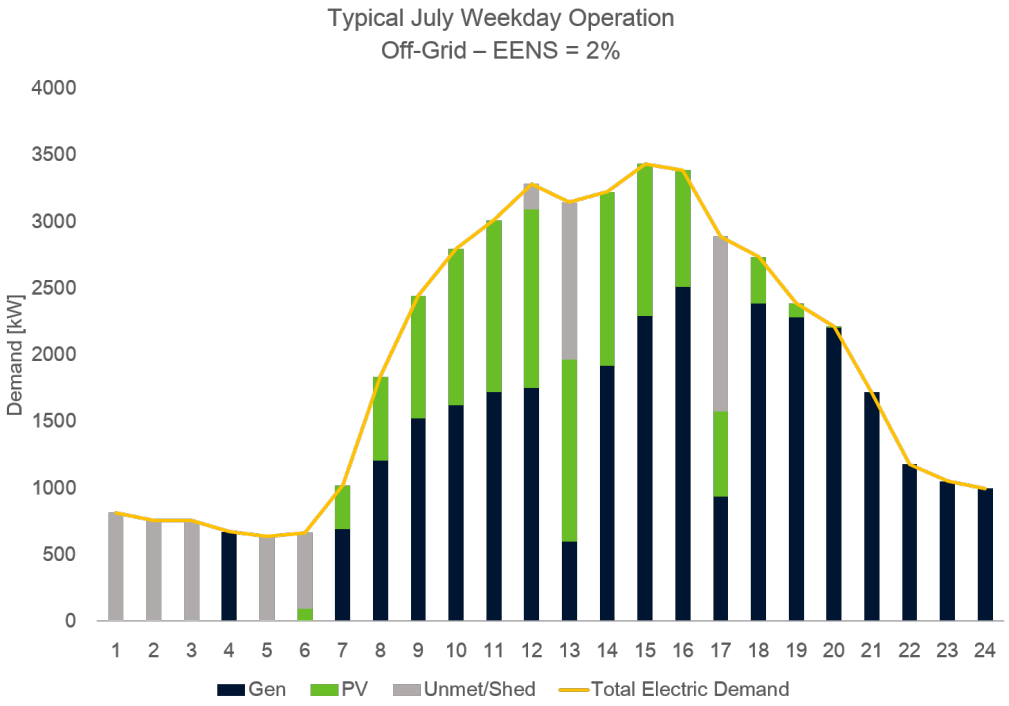

(b) Operating schedule of an optimal microgrid sized for an off-grid scenario with 2% EENS.

Figure 22: Minimum cost dispatch of the optimal supply configuration for off-grid scenarios with a 0% and 2% EENS.

CHAPTER V

INTEGRATED MICROGRID SYSTEM MODELING & OPTIMIZATION

To this point we have methodically developed the sub-components of an integrated microgrid system model. Chapter 2 introduces a framework for modeling building aggregates of mixed building types and Chapter 3 examines a unique way of searching the demand side design space for design parameters that correspond to a decision maker's preferences. Then Chapter 4 describes the process of specifying optimal supply capacities in a microgrid and introduces new concepts regarding the grid availability and a decision maker's neutrality to different amounts of load shedding. The goal of this progression is to achieve an integrated modeling framework of a microgrid that allows decision makers to find optimal design parameters simultaneously on both the demand and supply side of the microgrid system. This chapter specifies the complete framework of integration and co-simulation and introduces the integrated system's optimization algorithm.

5.1 Model Integration & Co-simulation

Modeling the integrated microgrid system is realized through coupled simulation of the defined demand and system models (see Chapter 2 and Chapter 4). The demand sub-model predicts the demand of a building as separate end-uses at an hourly resolution. The supply system model accepts six demand end-uses at the hourly resolution, but does not calculate the optimal capacity sizes and operation for each hour of the demand. Instead the supply system model accepts three day types for each month. These typical day types are a typical weekday, weekend and peak day. Each day type requires 24 hours of demand data across each of the six end-use inputs.

The integrated model's exchange variables are based on the problem formulation of the DER-CAM tool. As we mentioned, DER-CAM accepts six end-use input variables to determine both the optimal supply node capacities and the optimal operation. These six variables are the electric only, cooling electricity, space heating, hot water, natural gas and refrigeration electricity demand. Each demand end-use is specified in kilowatts for each of the hours of each day type for each month. These six end-uses are the variables that connect the demand sub-model to the supply sub-model.

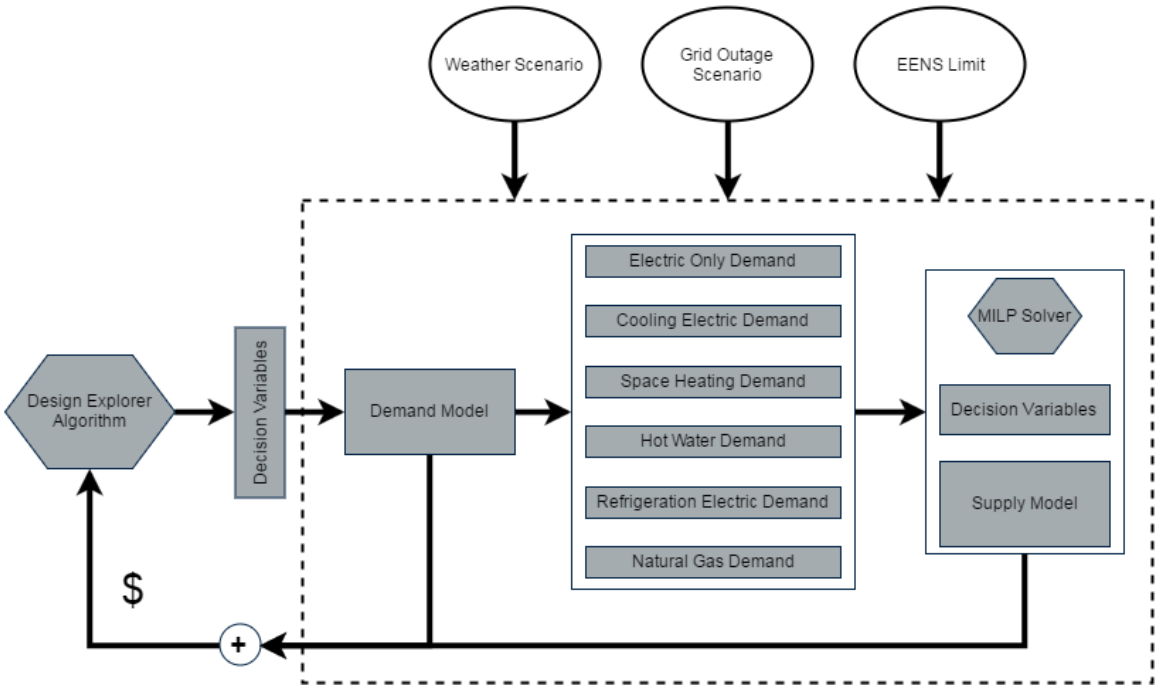

Figure 23: Overview of the integrated optimization framework. DEA searches the decision variable space of the demand model, which interacts with the supply model through six exchange variables. A decision maker defines the weather, grid outage and EENS scenario.

In essence, these variables form the exchange variables (Fig. 23).

The electric only end-use represents the demand due to all non-HVAC and non-refrigeration related power demand. Cooling electricity demand is the electric power required to meet the space cooling demand of the building aggregate under investigation. Space heating demand is the thermal demand in kilowatts required to meet a desired heating set point of the building aggregate. Space heating demand is specified at a thermal demand level because thermal power may be supplied via a number of non-electric related means (i.e., heat recovery from solar thermal systems or CHP). Refrigeration electric demand is the electric power to meet any of the specific non-space cooling related demand, which may be dramatic for microgrids with vaccine facilities for example. Finally, the natural gas demand is the required fuel input for non-heat generating processes such as cooking.

In general, the term co-simulation applies to a "master" simulation module that exercises any number of "slave" modules (Blochwitz et al., 2011). Typically, co-simulation occurs at the "time-step" level, which means that outcomes from one model are integrated with the input of another model for each calculation step because said outputs define either a boundary or start condition (Hensen,

1995). The integrated model that we propose is different in that there is no time-step level coupling of input and output. Instead, the demand model is executed for one year at an hourly resolution. Data from the demand model remains at the hourly resoultion, but is transformed via post-processing into a format that the supply model can use. The supply model solves the MILP defined in Chapter 4, for which the demand at each of the day types for each end-use is the output of the demand model.

5.1.1 Post-Processing Demand Model Output to Supply Model Input

In Section 5.1 we note that the demand model output is a time series of hourly demand values. Each of DER-CAM's required end-use components is output by the demand model, but the values must be post-processed in order to match the demand data input format specified by this version of DER-CAM. The primary issue is that the output end-use time series are not segmented into typical day types. The three day types are weekday, weekend and peak. DER-CAM requires that each month have one of the typical day types defined. There are two obstacles to overcome: (1) specifying a typical weekday and weekend for each month and (2) defining the peak day.

Weekdays and weekends are quite easily segmented from hourly demand data. We considered two potential options for defining the typical weekday and weekend for each month. The first option is to find the average day by averaging across each hour of either each weekday or each weekend. The next option for the microgrid design scenario is to find the day with highest demand for each end-use type and to select that day as the typical day for the supply design modeling. We selected the peak day sizing option as this is most aligned with typical HVAC sizing, which seeks to find the peak possible thermal demand and to then specify equipment that can satisfy this demand. The averaging approach may result in undersized systems.

Defining a peak day type is more open-ended than for weekdays and weekends. We considered two options. The first option was to create a second instance of the schedule values solely to define a peak day as is often done in the HVAC sizing. This method is not as readily scalable as it requires a second model instance with a separate scheduling to determine the end-uses during peak scheduling. The second method is to apply a scaling factor to the end-use data for weekday day types and define this new end-use data as the peak. The only need is to then specify an appropriate scaling factor that may also be dynamic if need be, but allows a single modeling instance. We derived the scaling

factor from Kapsalaki et al. (2012), who note that the normative building model of Chapter 2 does not adequately account for the peak demand level and thus use the peak calculations of Handbook (2009):

$$\alpha_{Ph} = kW_{Ph}/kW_{Max} \tag{27}$$

$$kW_{Ph} = [U_{walls} \cdot A_{walls} + U_{roof} \cdot A_{roof} + U_{glz} \cdot A_{glz} + C_s \cdot \dot{V}] \cdot \Delta T_{design} \tag{28}$$

where α_{Ph} is the heating scaling factor, which we apply to each hour of a weekday day type to generate the peak day type data for the space heating end-use. T_{design} is the difference between the indoor design set point and the outdoor design temperature that corresponds to the 99.6% annual cumulative frequency of occurrence in the heating season, C_s is the sensible heat factor assumed to be $1.23{*}10^3$ $W/(m^3/s \cdot K)$, $\dot{V}$ is the total building airflow in m^3/s, A_i is area i in m^2 and U_i is thermal resistance i in W/m^2K. The peak heating load is calculated assuming no internal gains and no gains from solar while the peak cooling load incorporates these two aspects:

$$\alpha_{Pc} = (kW_{Pc}/COP_c)/kW_{Max} \tag{29}$$

$$\begin{aligned} kW_{Pc} = [&U_{walls} \cdot A_{walls} + U_{roof} \cdot A_{roof} + U_{glz} \cdot A_{glz} \\ &+ C_s \cdot \dot{V} + q_i \cdot A_{floor} + SHGC \cdot I_{max} \cdot A_{glz}] \cdot \Delta T_{design} \end{aligned} \tag{30}$$

where g_i are the total internal gains in W/m^2, $SHGC$ is the solar heat gain coefficient, I_{max} is the peak total solar radiation on the windows and A_{glz} is the total glazed window area. T_{design} is the temperature difference between the cooling set point and the 99.6% annual cumulative frequency of occurrence for the cooling season and COP_c is the modeled cooling system's coefficient of performance. The cooling scaling factor α_{Pc} is multiplied by the weekday cooling electricity type data to create peak data for these segments. The remaining end-uses are modeled with equivalent weekday and peak day data. Once each of the end-uses have been transformed the total integrated model may now be optimized according to the decision maker's preferences. The following section discusses the search algorithm deployed to efficiently search the decision variables to find extrema of the microgrid system performance.

5.2 Optimization Approach

In Chapter 3 we compared two optimization approaches to searching the demand search space: the Darwin algorithm and a pattern search method developed by Hooke and Jeeves (1961). Chapter 4 introduces the MILP problem as formulated in the supply optimization module DER-CAM. The integrated modeling framework requires a global optimization approach that is efficient and able to incorporate a problem formulated in two distinct stages. For that reason we introduce an additional optimization approach that reduces the overall number of model evaluations while still maintaining many of the advantages of a direct search approach in finding the global minima of a solution space.

5.2.1 The Design Explorer Algorithm

Global optimization algorithms are a class of search techniques that seek to find the highest maximum or lowest minimum achievable by a defined objective function rather than accepting one of a number of possible "local" either maxima or minima (i.e. extreme values located in limited regions of the domain spanned by the input parameters). Global optimization theory and algorithms are important as many real-world problems exhibit a functional relationship between design parameters and the objective function with a number of extreme values. In addition, this functional relationship may be non-linear, non-differentiable or have unknown derivatives (Hazelrigg, 2012; Storn and Price, 1995). Algorithms for finding extrema of these complex functions are typically categorized as direct search approaches, which includes the algorithms of Hooke and Jeeves (1961), Nelder and Mead (1965), evolutionary algorithms (Back, 1996) and genetic algorithms (Golberg, 1989) (Storn and Price, 1995).

A direct search approach explores a design space by generating a set of alternatives and evaluating the analysis function at the generated points. Each direct search approach must have a means of deciding whether to accept or reject a generated set of points, which is typically done by ensuring that a parameter set must minimize the objective function value. This is known as the greedy criterion of direct search. The greedy criterion despite leading to fast convergence can also lead to the return of local extrema. The various classes of direct search algorithms therefore seek to strike a balance between speed and accuracy in finding the global extrema. Speed of convergence is especially important in the field of model-based systems engineering where the number of calls to

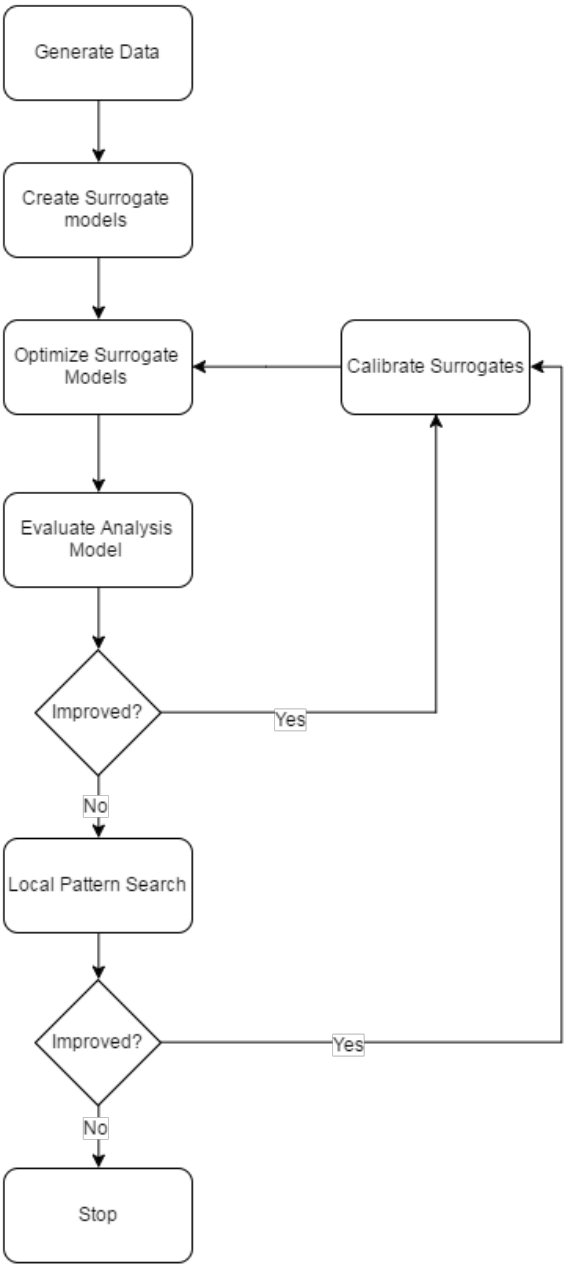

Figure 24: An overview of the Design Explorer algorithm (ModelCenter, 2015).

the underlying simulation or black-box functional model should be limited due to potentially long model runtimes. The multiple performance criteria of direct search algorithms lead directly to the development of the Design Explorer algorithm, which relies on a number of important qualities of deterministic simulations to efficiently explore a design space at a minimum number of function calls.

The Design Explorer algorithm is a direct search approach that limits the number of model evaluations through surrogate modeling of the true analysis function. To start a set of points is constructed from the design parameter space such that the design parameter space is evenly filled with potential points. This initial set of design parameter points is then evaluated via the system analysis model and a surrogate functional model is fit to the results. The surrogate model is generated such that it is smooth and continuous (i.e., differentiable everywhere). The newly created surrogate function is then searched and rapidly evaluated for multiple extrema via sequential quadratic programming (SQP). Extrema returned via the SQP search are evaluated via the original analysis model and if a better value is returned by the analysis function then the surrogate model is recalibrated with the new points and SQP is done again. This process is iterated until the analysis function does not return a better solution. A local pattern search algorithm is applied from the current optimum point to determine if there is anyway to improve the solution with the analysis model via a nearby point. If yes, the surrogate models are again updated and iteration is restarted between SQP and analysis function, otherwise the optimum is found (Fig. 24).

Step 1: Generate Analysis Model Inputs via Orthogonal Sets Let a computer simulation be defined over the set X such that $Y = f(X)\ \epsilon\ R$ where f is the analysis function or simulation. An approximation of f could be found then that is orders of magnitudes faster to evaluate than the underlying simulation itself, but an initial set of points is required to evaluate the simulation before any approximations of f may be determined. The Design Explorer algorithm generates the original sample of points X, at which to evaluate f via a method of orthogonal arrays (ModelCenter, 2015). Alternative sampling methods include random approaches such as Latin Hypercube Sampling, which generalizes to Monte Carlo sampling. While LHS was designed to maximally cover the ranges of random variables and improve convergence over direct Monte Carlo sampling, it has

been shown to miss points in the "corners" of bivariate pairs (Owen, 1992). $OA(n, k, q, t)$ is an orthogonal array with strength t represented as an n row by k column matrix with values taken from q symbols or levels. An important characteristic of orthogonal arrays is that if there are q distinct levels for each variable k then each subset of t variables of a $t - strength$ orthogonal array is a grid (Booker, 1998). Therefore, ModelCenter (2015) applies the special case of a 2-strength orthogonal array, which ensures qxq grids for all bivariate combinations of the design parameters in the optimization.

Step 2: Generate Surrogate Models The Design Explorer algorithm then interpolates observations of the analysis function evaluated at the points within the orthogonal array via kriging models (i.e., model fitting with the assumption that observations are the result of a Gaussian process) (Booker, 1998; ModelCenter, 2015). The predicted values for points in the independent variables space are then the function of a correlation function, the set of observations, the observation points and correlation parameters (Booker, 1998). Correlation parameters of the correlation function are determined using maximum likelihood estimation (MLE). This method allows new observations and observation sites to be added to the MLE formulation and leads to an interpolated model that may be quickly calibrated as new data are added from further analysis function runs (Booker, 1998; ModelCenter, 2015). Response models are created for the objective function and each of the constraints.

Step 3: Optimize the Surrogate Models The Design Explorer optimization continues by finding a set of extrema from the interpolated surrogate models via sequential quadratic programming (SQP) (Nocedal and Wright, 2006). SQP is not a global optimization approach therefore a number of SQP optimizations from a variety of start sites are evaluated, which is now feasible as the optimization is applied on surrogates of the true analysis function (ModelCenter, 2015).

Step 4: Evaluate the Analysis Function A new round of analysis function evaluations is performed using the unique extrema found in **Step 3**. Observations of the analysis function are then compared to the extrema observed via the surrogate models. This is an important step as the surrogate models may not be an appropriate fit to the analysis model. A comparison is made between

surrogate models and analysis model output for the objective function and constraints.

Step 5: Refine Surrogates If the surrogate models' observations did not match the analysis model's observations then the proposed optimal values are rejected. The surrogate models are refined and calibrated to the expanded observation set.

Step 6: Iterate The Design Explorer optimization algorithm iterates through Steps 3, 4 and 5 until a stop criterion is satisfied. If the Design Explorer optimization algorithm passes the threshold for consecutive search steps without an improvement then the current point is advanced to a Step 7 to undergo a local search.

Step 7: Localized Pattern Search The last step in the global optimization algorithm is to perform a local pattern search at either the best design point or least infeasible point found through Step 6. The search begins centered at the selected point and each design parameter is modified by a defined delta. The analysis function is executed for each perturbation of the design parameters. If the perturbed point is an improvement over the starting point then the algorithm updates the surrogate models and moves back to Step 3. Otherwise, the original point is perturbed in the negative direction and the analysis function is evaluated again. If the local pattern search advances through all of the design parameters without finding an improved solution than the starting point is returned as the optimum value and is guaranteed to be at least a local minima.

5.3 Design Explorer Algorithm and the Global Optimum

The optimization problem defined in this chapter is a constrained, non-linear program and the objective function is determined by calls to a "black box" routine defined by the combined results of the demand model and supply optimization. The necessary and sufficient conditions of solution optimality in non-linear programming only refer to either local maxima or minima and there are generally no guarantees to finding a global optimum. This limitation is due to the lack of information that non-linear programming methods have available to search the problem space, which is typically limited to information a point in the design space $\mathbf{x}$, the objective function value at the point $\mathbf{x}$, values of the constraint functions at $\mathbf{x}$ and information regarding the gradient and second

derivative at **x** (Chinneck, 2006).

The Design Explorer Algorithm itself is a class of general constrained optimization based on filter methods, which is to say that the search problem is divided into SEARCH and POLL steps (Booker, 1998; Audet and Dennis Jr, 2004). A SEARCH step refers to the process of globally searching the variable space for extrema based on approximations or surrogates of the underlying subroutines and the POLL step locally explores the variable space near incumbent solutions. Audet and Dennis Jr (2004) refer to Stephens and Baritompa (1998) who note that it is impossible to guarantee a global optimum in scenarios that do not include global information regarding the underlying function; hence, the Design Explorer Algorithm itself can not guarantee a globally optimal solution.

Many practical engineering problems face the same problem of being unable to guarantee a global optimum; however, Booker et al. (1999) and Booker et al. (1998) show that the Design Explorer Algorithm, which is a class of algorithms following the Surrogate Management Framework (SMF), does guarantee "global convergence". An optimization is "globally convergent" if any generated variable sequence converges to a point for which a necessary condition of optimality holds (Lanckriet and Sriperumbudur, 2009).

5.4 Conclusions

State-of-the-art performance based design approaches to the design of microgrids are limited in their ability to evaluate all criteria of a decision maker. This is because current modeling paradigms do not integrate adequate sub-models of demand and supply into a true systems model. In contrast, this chapter addresses the limitations in the state-of-the-art by presenting a co-simulation approach of the demand and supply. The integrated model may then be evaluated by a decision maker through a two-stage optimization approach that allows a decision maker to specify investment parameters that pertain to both demand reduction and supply capacity. The two-stage optimization problem is directed at the top level by the Design Explorer Algorithm, which is a global optimization approach that maximizes its efficiency over other direct search approaches through the use of surrogate models. The supply capacity and operation sub-problem, which is solved each time the integrated system

model is executed, relies on conventional branch and bound techniques common to linear programming. We have presented an integrated microgrid modeling framework comprised of two mutually-exclusive and completely exhaustive sub-models and in the next chapter we investigate applications of this model to microgrid investment decisions that allow simultaneous decisions regarding both supply and demand.

CHAPTER VI

APPLICATIONS

This work has presented a model for the performance based design of distributed generation systems that allows decision makers to consider design options that can not be explored with existing tools. In addition, this work has extended the DER-CAM microgrid planning tool to allow a decision maker to specify both the utility's reliability profile and a level of neutrality to unmet demand. The integrated system model is co-simulated via an interface of six demand components and allows decision makers to evaluate microgrid design options that incorporate decision variables in both the supply and demand sides simultaneously. This chapter attempts to generalize these modeling features and presents two separate scenario analyses.

First, we examine the affect of the utility's reliability scenario on investment decisions and then we apply the integrated optimization framework to demonstrate that joint decision making leads to more preferred design decisions. We introduce a hypothetical case study to facilitate our application of the modeling tool. In particular, we focus on a New York community with an interest in investing in a microgrid for increased reliability.

6.1 Case Description

The NY Prize is a $40 million competition created by the New York State Energy Research & Development Authority (NYSERDA) with the mission to increase microgrid penetration throughout the state of NY by assisting communities via grants that will facilitate partnerships between a number of community groups interested in modernizing the electric grid. The competition awards grants at three phases. Stage 1 grants are directed toward feasibility studies, Stage 2 grants allow more detailed engineering design and business planning while Stage 3 grants are earmarked for project construction and post-operation monitoring. In July 2015, the NY Prize has awarded $100,000 in funding to 83 feasibility studies throughout the state; as of July 2016, approximately 40% of the feasibility reports have been returned to the NYSERDA for review.

NY Prize grants typically were awarded to the most vulnerable communities with a strong showing of partnerships among the community and with industry. As such a number of the communities granted feasibility study funds were greatly affected by outages due to the Super Storm Sandy. Sandy was an incredibly destructive and powerful storm that struck the East Coast of the United States with extreme intensity and left millions of homes and business without power, shrank coast lines and caused shortages for key resources like gasoline (Halverson and Rabenhorst, 2013). Two Bridges, Manhattan, New York, NY was a town affected by Sandy and awarded a feasibility study grant through the NY Prize. Due to Two Bridges' proximity to the East River and location at the lower side of Manhattan, the community experienced widespread power outages and flooding (Fig. 25).

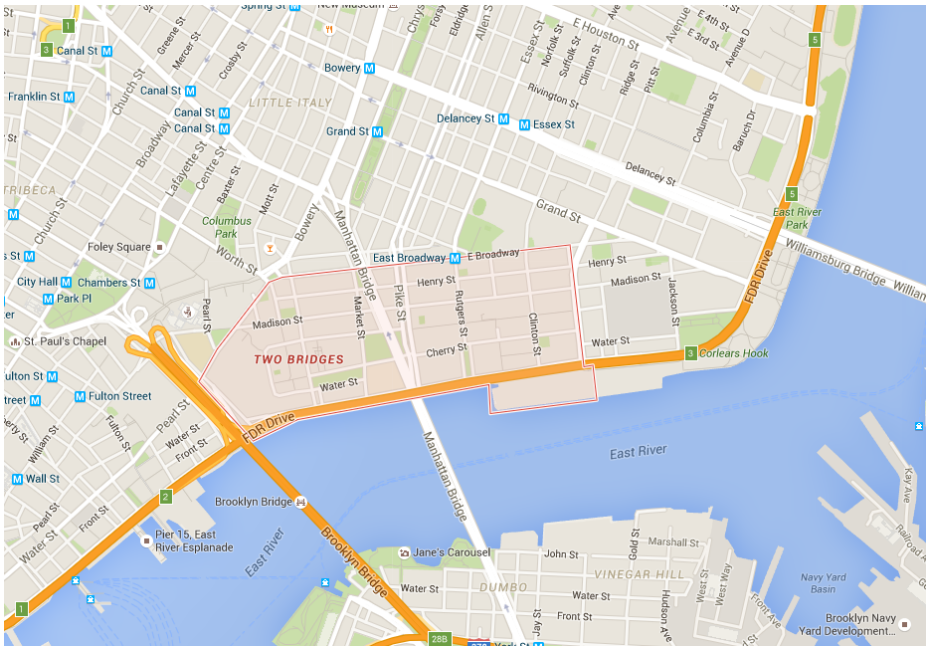

Figure 25: An aerial view of the Two Bridges community detailing its proximity to the East River and location along the southern end of Manhattan. This community experienced wide spread power outages and flooding in the aftermath of Hurricane Sandy.

Sandy had a number of effects on the Two Bridges community. Community members formed a coalition of investors, project managers and community representatives in response to these adverse effects. The coalition proposed the idea of a projected titled *Beyond the Grid*, which seeks to, "consider the social and economic context of the community served and will have positive impacts on quality of life and availability of critical services." As such the coalition decided to establish *Beyond*

Table 7: Microgrid ownership models as detailed in Razanousky and Hyams (2010).

Model		Description
Landlord/Campus	I	Single non-utility owner operates a system and installs private wires and generation technologies on site to meet thermal and electric demand of buildings privately owned by the microgrid owner.
	II	Identical to Type I except some infrastructure may cross public streets or a utility franchise (i.e., NYU in Manhattan).
	III	Identical to Type II except that previously unaffiliated neighboring building owners may be allowed to enter into the microgrid service area through contracts.
Joint Ownership/Co-Op		Multiple owners or unrelated firms may collectively own and operate a microgrid to service thermal and electric loads. Infrastructure may cross the public domain and previously unaffiliated building owners may be allowed to enter into the microgrid service area through contracts.
Independent Provider		A strictly commercial business model. An independent, non-utility microgrid owner sells electricity and/or thermal energy to multiple unaffiliated customers. New customers added via contracts. Infrastructure may cross public domain.

the Grid as a non-profit entity with multiple objectives including financial return to the members served in the proposed power co-operative, improved resiliency and more renewable power integration.

It is important to discuss the decision making scenario and identify who has the authority to make decisions during the microgrid planning process. There are a variety of microgrid business models and the planning team behind the Two Bridge's microgrid denotes their business model as an "urban cooperative", which they model on conventional electric power co-operatives (Table 7). A democratically elected Board of Directors oversees management of the facility and other needs of governance and the microgrid is agreed to operate at cost. The Board of Directors then theoretically aggregates the desires of individual building owners into a single collective strategy. At the same time, however, there are differential impacts of failures and there are different levels of retrofit available to individual buildings. The integrated optimization approach handles the reliability at the aggregate scale and does not examine power reliability to individual buildings. Instead the Board of Directors must specify the reliability constraints defined in Section 4.5. The benefit of using the integrated optimization approach and the demand model specified in Chapter 2 is that results will reflect the best changes required for each type of building within the building stock. Since each

building of the same type, however, is modeled as indistinguishable, then the Board of Directors can address all owners of a specific type and determine which owners are willing to undergo retrofits. In addition to meeting their own demand, the generation facilities are eligible to sell power to Con Edison of New York (ConEd) through a power purchase agreement. Financing for the proposed microgrid is projected to come from private investment, government loads and subsidies, energy incentives from ConEd and member equity.

We will analyze the Two Bridges case given the Board of Director's interest in financial return to co-op members, improved resilience and more renewable power integration. While results of the feasibility study have been published, there is not detailed demand level information about the proposed site. Instead a few general classifications of building functions have been defined broadly. Given the location of the site, cursory demand data and a general sense of the objectives of the Board of Directors we will make assumptions about the demand level and preferences in order to analyze this case within the integrated modeling framework proposed in Chapter 5.

6.2 Analysis Goals

There are two primary research questions with a broader bearing on general integrated microgrid design research:

1. What effect does an integrated design methodology have on the total annual cost and annual CO_2 emissions for various weighs on economic and environmental value?

2. What are the effects of different utility reliability scenarios on the total annual cost and annual CO_2 emissions of the optimal microgrid system design for various weights on economic and environmental value?

These two research questions are derived from the two driving hypotheses:

Hypothesis 2: The proposed integrated modeling framework reveals more preferred solutions than a design approach that does not consider demand interventions during the design phase.

Hypothesis 3: Defining a resiliency framework for the integrated microgrid system model will enable decision makers to model scenario uncertainty regarding the utility's reliability.

The method to answer each of the questions is to first develop models of the assumed building types. Next, we analyze the building aggregate to determine a suite of demand interventions, which are translated into cost functions in accordance with Chapter 3. Then, we define the specific parameters of the supply system components including costs, the utility rate structure, the outage scenarios and the decision maker neutrality to loss. Once these preliminaries are completed the method to solve each individual question diverges.

To address Hypothesis 2 we first define a base scenario known as the "Do Nothing" case, in which the co-op does not invest in either DERs on the supply side or demand side interventions. The "Do Nothing" case represents the cost to simply operate the facilities connected to the utility grid. We then define two conventional design approaches to compare to the integrated optimization approach. "Supply Only" is a design approach that only optimizes the selection of DERs for the "as is" building demand. "Demand First" is a design approach, in which the co-op owners decide to first invest in demand side interventions by determining the minimum cost investment to reduce thermal demand by 25%. Next, the co-op owners then optimize the selection of DERs for the building stock with a 25% reduced demand. "Integrated Optimization" is the integrated optimization approach, in which the co-op decision makers have the ability to select decision variables across the supply and demand sub-systems simultaneously. Each Scenario is simulated multiple times to examine the effect of varying weights in the cost function as the DER-CAM tool minimizes a multiobjective function of both economic and environmental value.

Finally, Hypothesis 3 is intended to demonstrate the effect of utility outages on the optimal sizing of a microgrid. This is important to illustrate because an aspect model that intends to evaluate the reliability performance of a microgrid must be able to propagate multiple sources of uncertainty including the utility reliability. The rational approach to propagating the utility's reliability profile

is to first quantify the uncertainty in both mean time between failures and outage duration length given the microgrid location. Once this uncertainty is quantified a decision maker may generate random samples of the grid outage and downtime for the design location to quantify the impact on the microgrid system's reliability. We present a truncated version of this, in which we define two scenarios of the grid reliability: a minimum and maximum reliability. In the maximum reliability scenario the grid is available for all operating hours while in the minimum reliability scenario the grid is out for all operating hours. We then simulate each scenario for multiple combinations of the weighting parameters in the cost function. All other realizations of the utility's reliability profile should lie within these extreme cases.

6.3 Case Analysis

The Two Bridges microgrid case scenario is an example of the optimal design of a grid-connected, commercial and residential community under a demand rate tariff structure with a peak demand < 10 MW. We assume that the Board of Directors is charged as a single utility node in accordance with other large power consumers. In this way the Board of Directors is seen as the ultimate decision maker both with the ability to invest in new power generation technologies and improvements to buildings owned by members of the co-operative.

Demand rate tariffs are a common tool applied by utilities to penalize consumers for power demand as well as energy consumption. This rate structure exists because meeting high demand is expensive for supply systems. By charging a premium for demand, these rate tariffs reduce the peak consumption that must be met by the utility.

6.3.1 Defining the Demand Side

Literature released regarding the Two Bridges project notes that the microgrid will serve a mix of public and private residential, institutional and commercial sites including three public schools, a community center, pharmacy, supermarket and a variety of apartment buildings. We used this as a basis for defining a potentially similar community, but with a focus on single-family residential rather than multi-family as this may have greater generality. We therefore identified five prototype building models to represent the community: 60 single family residential, 1 supermarket, 2 stand alone retail, 2 primary school and 1 secondary school. We will model the building aggregate in

Climate Zone 4A, which contains New York City. In particular, we use the Central Park TMY3 weather data.

We selected five design parameters for the aggregate demand model based on the results of a sensitivity analysis. As this is a heating dominated climate the most important variables to consider are the building air leakage level, window, roof and wall thermal resistance and the lighting power density. For each building type we defined a set of options and design improvements along with an associated cost for each variable level (Table 8). From this information we generated the Pareto Optimal cost curves for each variable as in Chapter 3 (Fig. 28).

Table 8: Discrete option space for the demand side decision making. Each building has discrete levels for five input variables.

	Primary School (2004)	Secondary School (2004)	Single Family (2007)	Supermarket (2004)	Stand Alone Retail (2004)
Leakage Level	4.3	2.5	2.5	3.8	7.41
$[m3/h/m2]$	3.87	2.25	2.25	3.42	6.669
	3.225	1.875	1.875	2.85	5.5575
Lighting Power Density	21.99	12.38	1.7	16.72	19.29
$[W/m2]$	18.6915	10.523	1.275	12.54	14.4675
	16.4925	9.285			
Roof U-value	0.358	0.358	1.81	0.36	0.36
$[W/m2K]$	0.2506	0.2506	1.267	0.2506	0.2506
	0.1969	0.1969	0.905	0.1969	0.1969
	0.1611	0.1611		0.1611	0.1611
Opaque U-value	0.704	0.704	0.35	0.86	0.86
$[W/m2K]$	0.5984	0.5984	0.2975	0.62	0.62
	0.4928	0.4928	0.25	0.5	0.5
	0.4224	0.4224			
Window U-value	3.236	3.236	1.99	3.24	3.24
$[W/m2K]$	2.427	2.427	1.4925	2.43	2.43
	1.618	1.618	1.194	1.62	1.62

6.3.2 Define the Supply Side

There are a number of costs related to operating a microgrid. The most important costs are the initial investment capital in generation technologies, the utility rate tariff and the fuel consumption volume and price for operating the generator. Microgrids may also generate revenue through either direct sales of produced power or via incentives and tax reductions due to different technology selections.

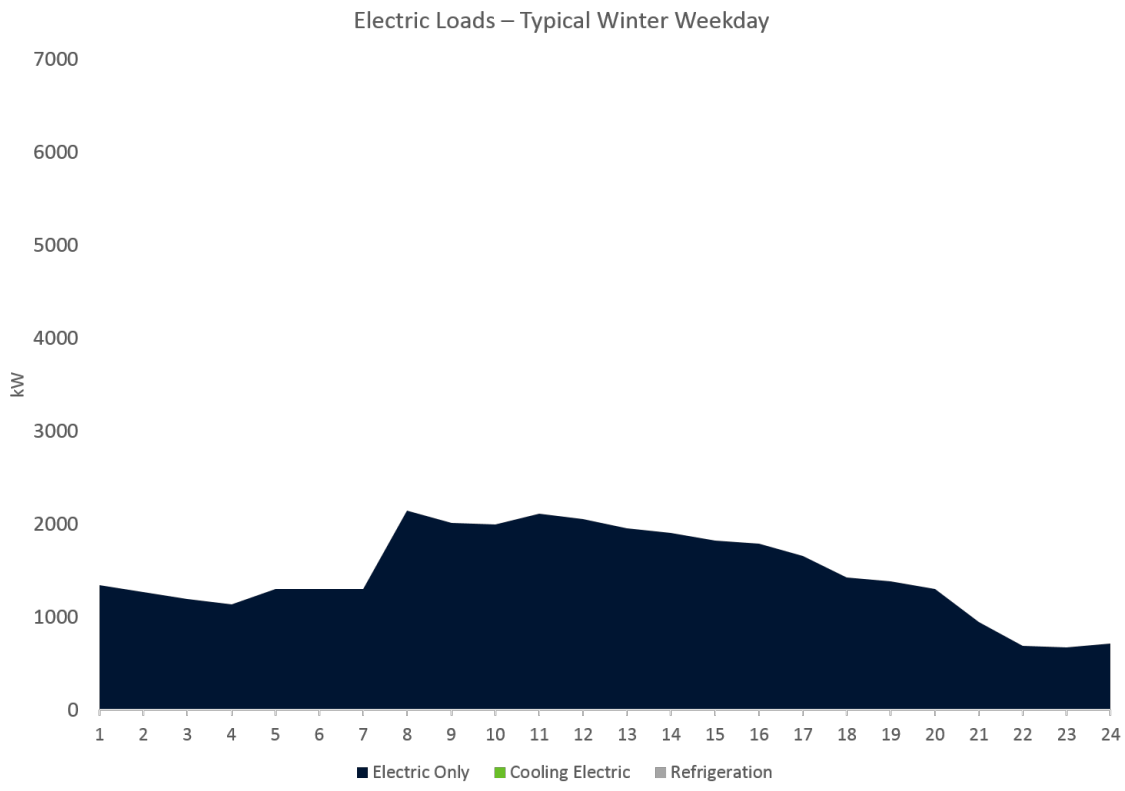

(a) Electric demand of the case study building aggregate for a typical Winter day separated by end-use.

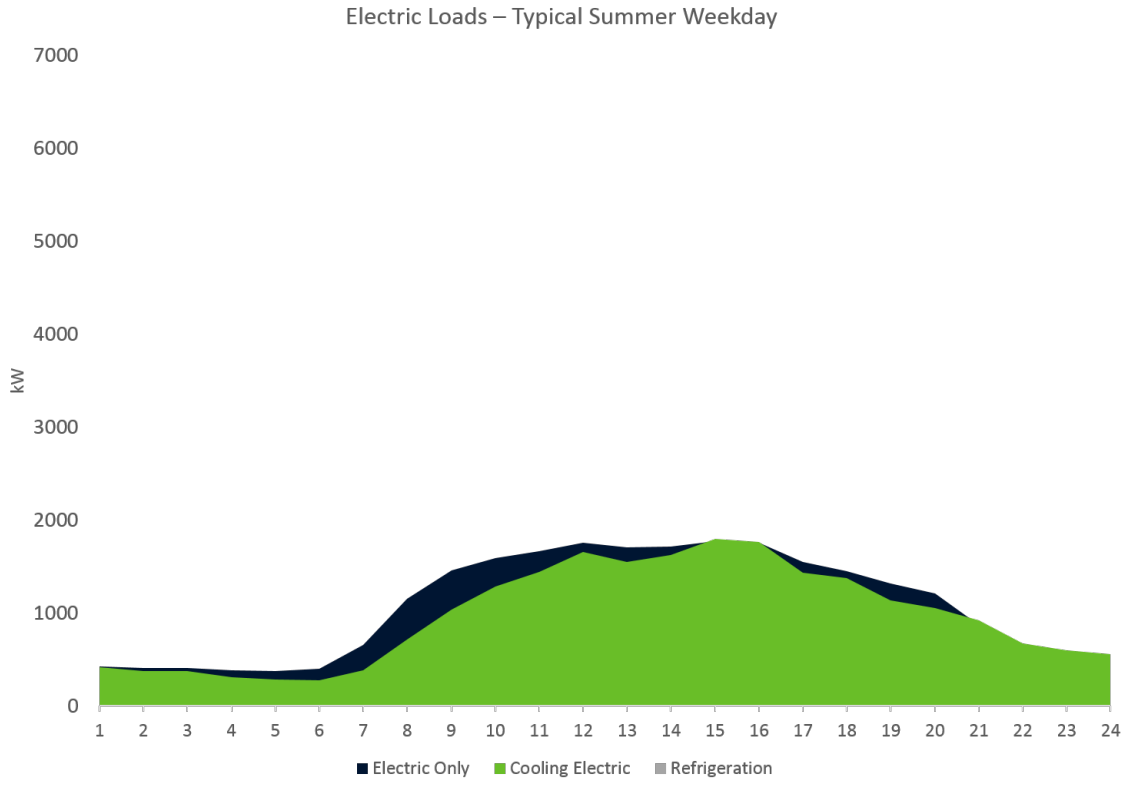

(b) Electric demand of the case study building aggregate for a typical Summer day separated by end-use.

Figure 26: The modeled electric demand during both the Summer and Winter of a proposed micro-grid in lower Manhattan.

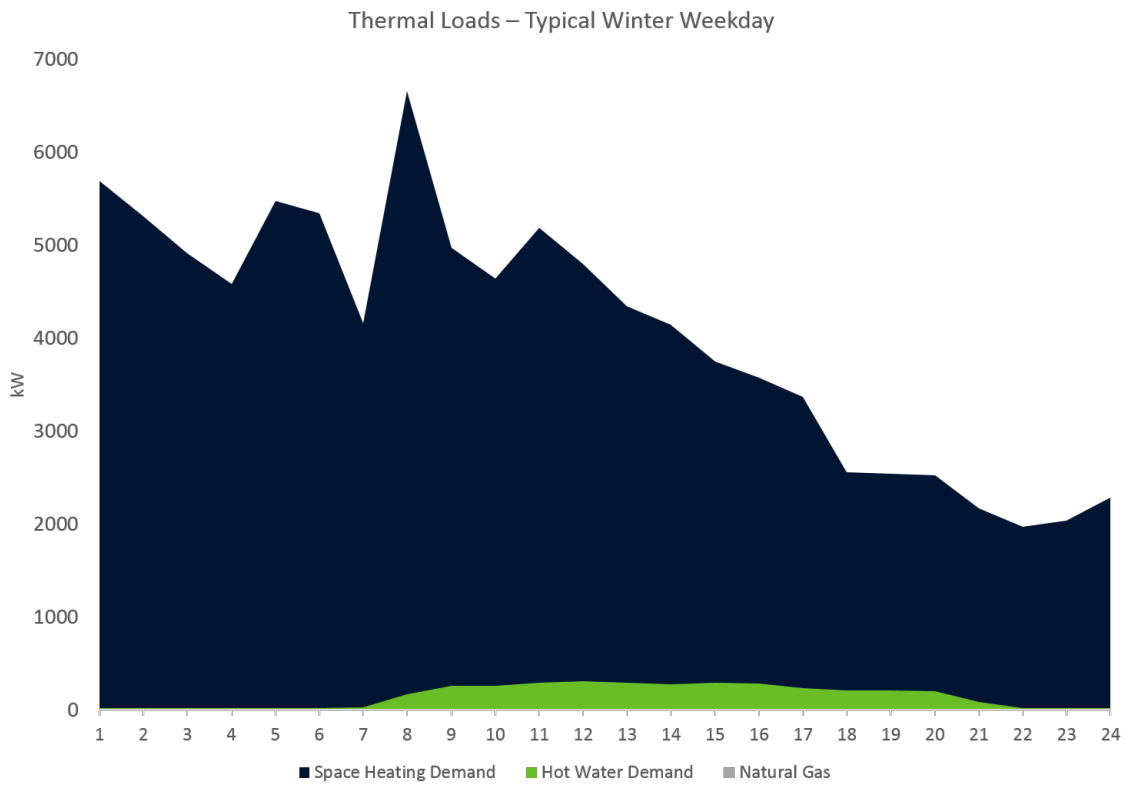

(a) Thermal demand of the case study building aggregate for a typical Winter day separated by end-use. Thermal demand is dominated by Space Heating needs in Winter.

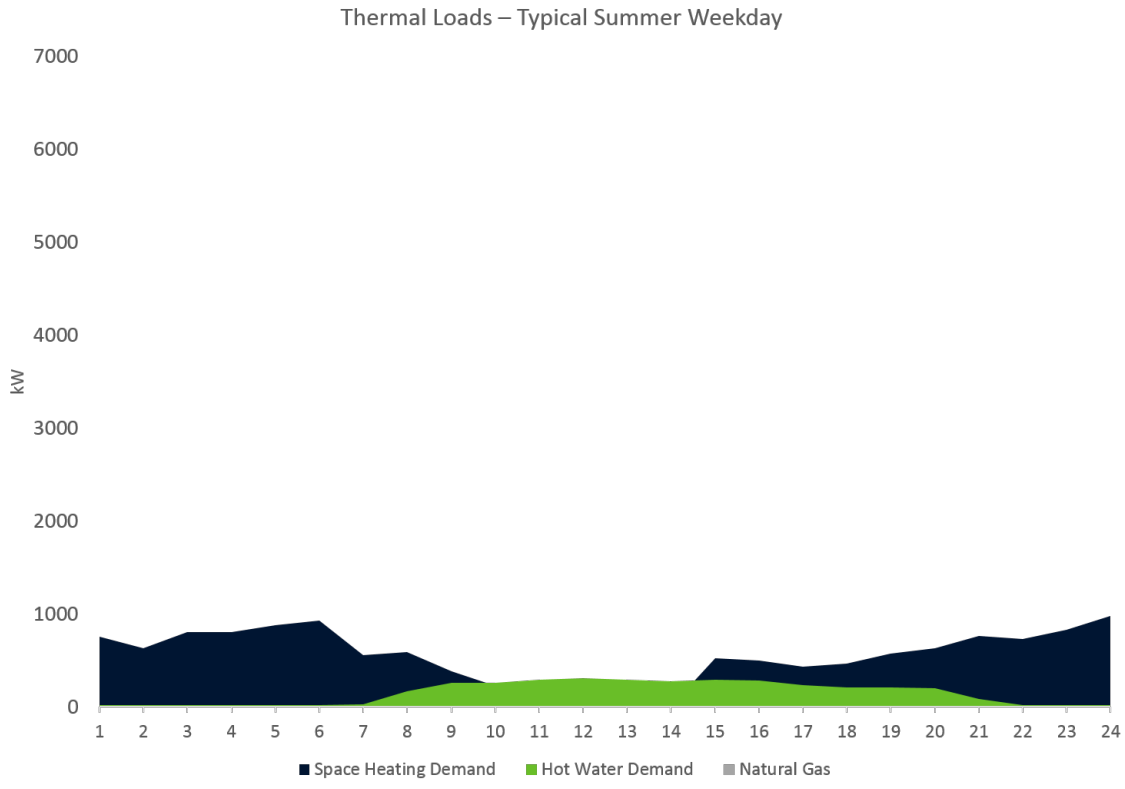

(b) Thermal demand of the case study building aggregate for a typical Summer day separated by end-use.

Figure 27: The modeled thermal demand during both the Summer and Winter of a proposed micro-grid in lower Manhattan.

Table 9: Demand rate structure assumed for the design study in $\$/kW$.

	Non-Coincident	On-Peak	Mid-Peak
January	11.88	0	0
February	11.88	0	0
March	11.88	0	0
April	11.88	0	0
May	11.88	0	0
June	11.88	19.49	5.46
July	11.88	19.49	5.46
August	11.88	19.49	5.46
September	11.88	19.49	5.46
October	11.88	0	0
November	11.88	0	0
December	11.88	0	0

In this section we first describe the assumed utility rate structure, then we introduce a number of technologies and their associated costs due to both operations and investment.

We assume the utility charges for both demand and energy. The demand charges are listed in Table 9. There are three specific charges listed in $\$/kW$ for demand: Non-coincident, on-peak and mid-peak. Non-coincident peak demand is a customer's maximum power demand during a utility defined period, typically the period of time is a month, which is what we assume. In this case, the utility charges $11.88/kW of the maximum monthly non-coincident demand. On-peak and mid-peak are similarly defined as the customer's peak demand during a specific time interval. In this case we assume that the on-peak versus mid-peak distinction is only made during the summer months with separate timing for weekdays, peak days and weekends. More specifically, the weekday and peak on-peak periods are between the hours of 13:00 and 18:00 and there are no on-peak or mid-peak periods on weekend days. Mid-peak hours are from 09:00 to 12:00 and 19:00 to 24:00 on weekdays. Further pricing for these day types is in Table 9.

Utilities also charge an energy rate in $\$/kWh$. Our assumed energy rates are detailed in Table 10. The decision maker has also entered into a power purchase agreement with the utility. The ask price for electricity is also governed by the time of use, which is detailed in Table 11. Again there are no on-peak times considered during the winter. Also, the mid-peak and off-peak times mirror those presented for the demand rate charging.

Table 10: Assumed electricity charges in $\$/kWh$ with on-peak, mid-peak and off-peak rates.

	On	Mid	Off
January	0	0.07505	0.0498
February	0	0.07505	0.0498
March	0	0.07505	0.0498
April	0	0.07505	0.0498
May	0	0.07505	0.0498
June	0.10323	0.08078	0.05407
July	0.10323	0.08078	0.05407
August	0.10323	0.08078	0.05407
September	0.10323	0.08078	0.05407
October	0	0.07505	0.0498
November	0	0.07505	0.0498
December	0	0.07505	0.0498

Table 11: Assumed buy back rate agreement for power purchases between the customer and utility.

	On	Mid	Off
January	0	0.040329	0.036663
February	0	0.040329	0.036663
March	0	0.040329	0.036663
April	0	0.040329	0.036663
May	0	0.040329	0.036663
June	0.152651	0.065993	0.065993
July	0.152651	0.065993	0.065993
August	0.152651	0.065993	0.065993
September	0.152651	0.065993	0.065993
October	0	0.040329	0.036663
November	0	0.040329	0.036663
December	0	0.040329	0.036663

The decision maker has a number of supply side generation technologies to consider. The generation technologies are separated into two classes either continuous or discrete. The energy capacity of the electric storage and generation capacity of the photovoltaics are modeled as continuous variables. The unit sizes for these technologies are generally small relative to the actual load and thus can be considered to be continuous. Design parameters of the continuous parameters are noted in Table 12. The costs in Table 12 for electric storage is given in $\$/kWh$ and $\$/kW$ for PV and lifetime is in years.

Alternatively, the generator capacity and CHP capacity are modeled as discrete units. We consider seven generator set types and six generator sets with heat recovery (i.e., CHP) (Table 13). We

Table 12: Continuous parameters modeled on the supply side including photovoltaics and simple electric energy storage. Variable costs listed in $\$/kW$.

	C_{Fix}	C_{Var}	Lifetime	OM_{Fix}
Electric Storage	295	193	5	0
PV	3851.25	3237	30	0.25

consider three main types of generators: internal combustion engine (ICE), microturbine (MT) and fuel cell (FC). Each generator varies based on its conversion efficiencyi, initial capital cost, variable costs and lifetime (Table 13).

Table 13: Generator options considered for the microgrid design case study.

	P_{max}	Lifetime	C_{Cap}	OM_{Fix}	OM_{Var}	η
ICE-small-30	60	20	1587	0	0.021	0.29
ICE-med-30	250	20	865	0	0.015	0.3
GT-30	1000	20	1932	0	0.011	0.22
MT-small-30	60	10	1410	0	0.017	0.31
MT-med-30	150	10	1148	0	0.017	0.33
FC-small-30	100	10	3605	0	0.033	0.46
FC-med-30	250	10	2889	0	0.033	0.46
ICE-HX-small-30	60	20	2088	0	0.021	0.29
ICE-HX-med-30	250	20	1271	0	0.015	0.3
GT-HX-30	1000	20	2647	0	0.011	0.22
MT-HX-small-30	60	10	1584	0	0.017	0.31
MT-HX-med-30	150	10	1290	0	0.017	0.33
FC-HX-small-30	100	10	4192	0	0.033	0.46

6.4 Results

6.4.1 Hypothesis 2: Integrated Design Optimization

Fig. 29 presents the results of the three design scenarios and the "Do Nothing Case" as described in Section 6.2. The "Supply Only" design case is a design method, in which the decision maker leaves the building stock *as is* and only specifies the DER investments. "Demand First" is the method, in which the decision maker first determines the minimum cost demand side investment to produce a 20% savings in thermal demand for heating and then determines the optimal DER investments. Finally, "Integrated Optimization" are designs that result from using the integrated modeling methodology introduced through this dissertation. Fig. 29 shows CO_2 emissions versus

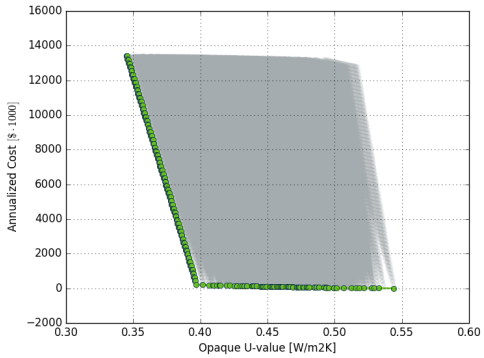

(a) Annualized investment cost $[\$]$ *versus opaque wall thermal resistance* $[W/m^2K]$.

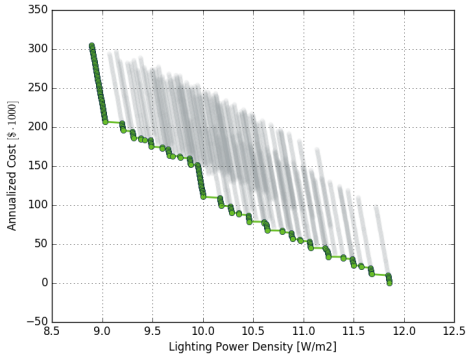

(b) Annualized investment cost $[\$]$ *versus lighting power density* $[W/m^2]$

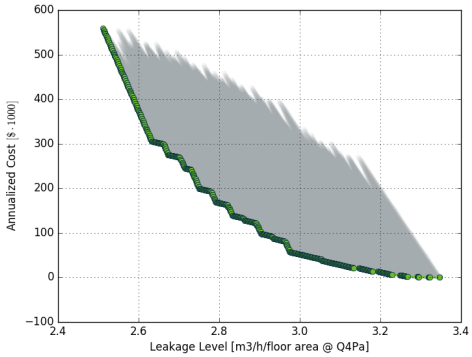

(c) Annualized investment cost $[\$]$ *versus building air leakage level* $[m^3/hm^2]$

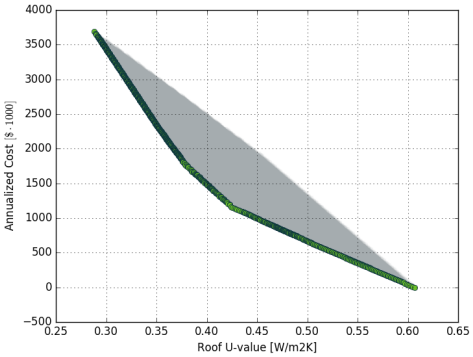

(d) Annualized investment cost $[\$]$ *versus roof thermal resistance* $[W/m^2K]$

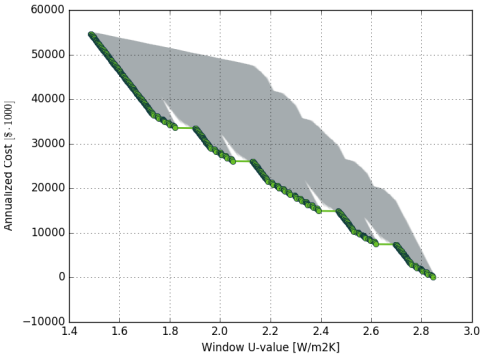

(e) Annualized investment cost $[\$]$ *versus window thermal resistance* $[W/m^2K]$

Figure 28: Corresponding Pareto frontier for each of the five investigated demand parameters capturing variation in performance versus cost for the complete building aggregate.

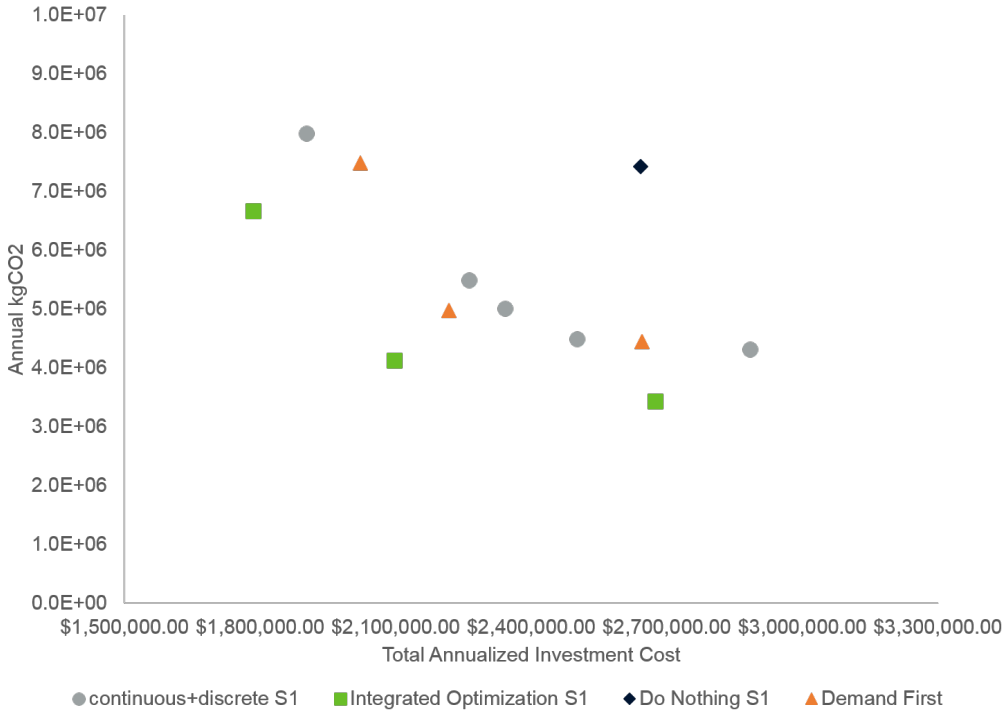

Figure 29: Plot of the CO_2 emissions versus Total Annualized Investment Cost results for multiple weights of the $wCost$ and three different approaches to microgrid system design: IO, DF and SO. Results show that the IO approach proposed in this dissertation results in more preferred microgrid designs than the two conventional, dis-jointed design approaches.

Total Annualized Investment cost for multiple weights of the $wCost$ parameter in Eq. 16 as it is a multi objective function with CO_2 and Total Annualized Costs as the two objectives of interest.

In each scenario the DER investment options available are listed in Table 13 and Table 12. The demand side options are shown in Table 8 and the corresponding cost functions for each variable are in Fig. 28. Each design scenario considers the a grid that always operates and that the decision maker requires that no demand be unmet (i.e., 0% EENS).

From Fig. 29 we immediately see that each of the microgrid designs determined by the integrated design method "dominates" all other solutions. That is to say that for the same weighting of cost and environmental value, that a decision maker applying the integrated modeling methodology to their microgrid design problem will find a more preferential solution that doing either of the conventional design methods. At $w_{Cost} = 0.2$ the "Integrated Optimization" design results in a 1% higher annual cost compared to the "Demand First" method, but a 7% reduction in annual cost compared to the "Supply Only" method. Carbon dioxide emissions of the "Integrated Optimization" case are 23% and 20% less when compared to the "Demand First" and "Supply Only" methods, respectively (Table 14). The minimum cost solution is interesting in that the Integrated Optimization approach results in a 12% annual cost reduction versus the "Demand First" approach and 6% annual cost reduction compared to the "Supply Only" method.

Another observation to note is that while the IO case achieves the lowest total annual cost ($1.78M) the smallest range of annual costs actually belongs to the DF case ($2.02M - $2.64M). By pre-selecting the demand side interventions the maximum savings of either annual cost or emissions are effectively capped as we see that the DF case also has the tightest range on CO_2 emissions. The results in Fig. 29, Table 14 and Table 15 support the hypothesis that the proposed integrated

Table 14: Percent change in economic and environmental value for the Integrated Optimization versus the Supply Only and Demand First methodologies at the same reliability level.

	Supply Only		Demand First	
w_{Cost}	Total Annual Cost	CO_2	Total Annual Cost	CO_2
0.2	-7%	-20%	1%	-23%
0.6	-10%	-18%	-6%	-17%
1	-6%	-17%	-12%	-11%

modeling framework reveals more preferred solutions than a design approach that does not consider demand interventions during the design phase. The integrated modeling solution also reveals more preferred solutions than a design approach that begins with a target demand savings prior to optimally selecting the DERs.

6.4.2 Hypothesis 3: Effects of Utility Reliability

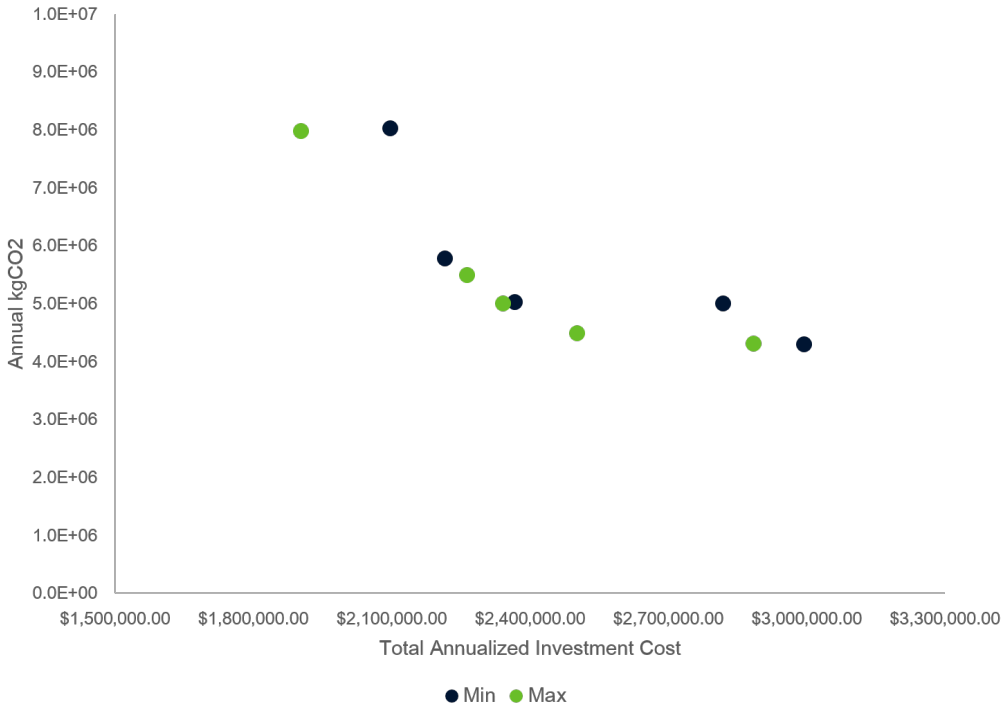

Figure 30: Comparing the annual emissions and total investment cost in the microgrid for various combinations of the weighting parameters. The two green points are results from the integrated system optimization with either pure cost minimization or pure emissions minimization.

Table 15: Demand side interventions and investments for the base case, Integrated Optimization and Demand First methodologies.

		0.2	0.6	1	
	Base	IO	IO	IO	DF
Roof U-value [W/m2K]	0.61	0.38	0.39	0.45	0.47
Opaque U-value [W/m2K]	0.54	0.48	0.51	0.49	0.51
Window U-value [W/m2K]	2.85	2.83	2.85	2.85	2.73
Leakage Level [m3/h/m2]	3.35	2.78	2.79	2.71	2.83
Lighting Power Density [W/m2]	11.86	10.57	11.36	11.44	11.45
Annualized Upgrade Cost		$ 96,087.45	$ 69,943.69	$ 27,224.96	$ 61,937.02

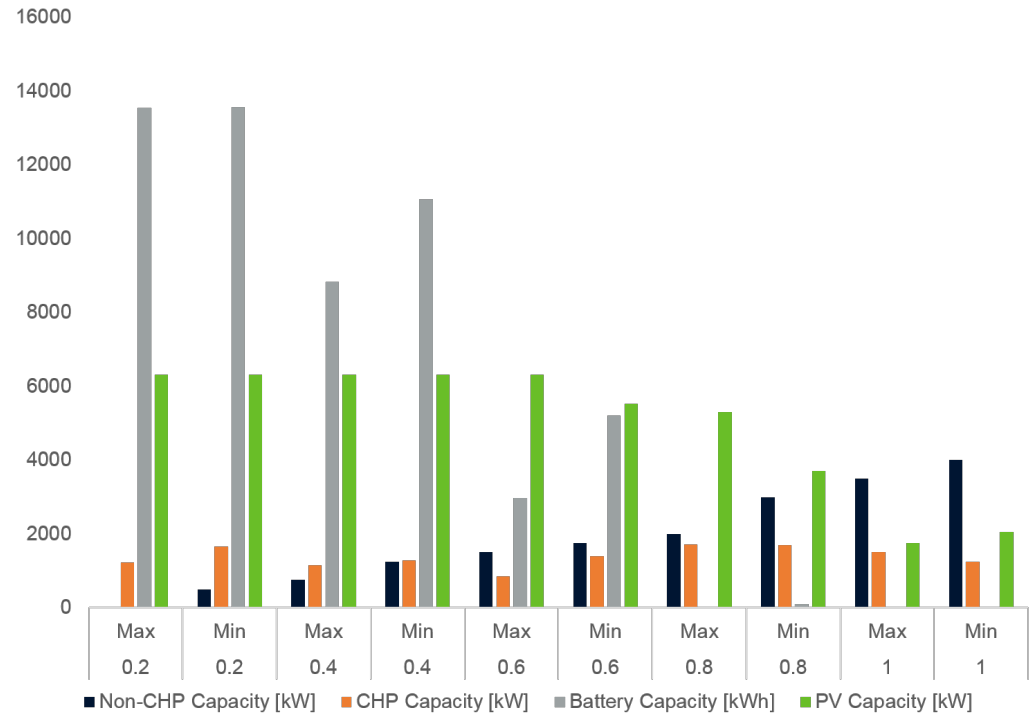

Figure 31: Analysis of the microgrid design parameters for a maximum and minimum grid reliability scenario.

Fig. 30 and Fig. 31 summarize the optimal microgrid designs for two utility reliability scenarios. The first effect that we notice is that the spread in total annual cost between the two scenarios is not as large as expected ($0.98M versus $0.89M). At $w_{Cost} = 0.6$ and $w_{Cost} = 0.8$ the total annual costs are within 5% of each other and carbon emissions are also within 5% of each other. At the extremes (w_{Cost} = 1.0 and w_{Cost} = 0.2), however, it is respectively 10% and 13% more costly to design microgrids for utilities with high levels of outages. Generally, it seems that for the minimum utility reliability cases that more investment should be guided towards CHP capable DERs.

The lack of sensitivity of the microgrid design to the utility reliability is counter intuitive, but not surprising. We should expect that if we don't incorporate the failure rate of DERs within the microgrid and assume perfect operation that most cost variation will be attributed to differences in operation strategies. The primary takeaway from this study is that the extension to the DER-CAM tool now allows decision makers to quantify utility outages and incorporate this uncertainty in the decision making process.

We can also compare the results of Fig. 31 to the actual Two Bridges microgrid plan, which

includes 350 kW of PV, 8.4 MWh of electric storage and 1665 kW of generation with 65 kW of CHP. Although we did not attempt to strictly model the Two Bridges community, but rather use the suggested peak demand as a reference point we will look at the discrepancy in PV sizing. Manhattan has generally a constrained footprint available for installing PV and the 6 MW system may not be feasible in such a constrained environment. The standard method for rating the capacity of a PV system is to calculate the output power at a reference solar irradiance of 1 kW/m^2:

$$\eta_{maximum} = \frac{P_{max}}{I_{reference} * A_{System}} \tag{31}$$

In DER-CAM we assume a 15% efficient panel. The actual area available to cover in the Two Bridges community is actually several factors less than what is modeled in this chapter as the solar panels cover the roofs of just eight buildings. We can determine the roof area of the Two Bridges community if we assume the same panel efficiency, which gives 2288 m^2 (i.e., 350 kW/0.153). Our total roof area is based on the commercial reference building models and not the buildings from the actual Two Bridges community and thus our area is 41351 m^2. Due to this difference between modeling choice and reality, we consider about 18 times more roof area. Our maximum solar capacity of 6300 kW is exactly 18 times the 350 kW noted in the actual study results.

6.5 Conclusions

This chapter sought to answer two primary questions:

1. What effect does an integrated design methodology have on the total annual cost and annual CO_2 emissions for various weighs on economic and environmental value?

2. What are the effects of different utility reliability scenarios on the total annual cost and annual CO_2 emissions of the optimal microgrid system design for various weights on economic and environmental value?

Hypothesis testing with the integrated system modeling framework allows us to answer the first question and say that the integrated design methodology has a preferential effect on microgrid designs, which is to say that this method finds solutions that are both lower in total cost and produce

fewer emissions. More specifically, the work in this chapter suggests that this integrated approach is better than two conventional design approaches.

The first conventional design approach is to not consider improvements to the demand side and to simply optimize the selection of DERs in accordance with one's preferences (i.e., Supply Only). The second conventional design approach is to define a desired level of thermal demand reduction and to invest in the demand side parameters via the minimum cost solution. Once the minimum cost solution for a desired demand reduction is attained the next step is typically to then simply optimize the selection of the DERs for the new demand (i.e., Demand First). Fig. 29 shows that the integrated design optimization approach results in microgrid system designs that dominate solutions from both conventional microgrid design approaches. Due to this evidence we recommend that the integrated system modeling framework should be used in decision making scenarios that allow interventions on both the demand and supply side of microgrid design. This recommendation is supported by these additional observations:

1. Optimization results of the integrated system model return solutions on average exhibit an 8% total annual cost reduction and 18% reduction in CO_2 emissions versus the Supply Only case. Similarly, the results on average reduce total annual cost by 5% and annual emissions by 17% for the Demand First case.

2. The integrated system model explores a more complete demand option space that is at least an order of magnitude larger within an existing framework (Chapter. 2).

3. Investment in demand side improvement measures determined by the integrated modeling methodology average less than 5% of the overall investment cost.

Next, we were able to examine the effect that a utility's reliability profile has on the optimal microgrid designs. We approach this problem for two primary reasons: (1) to demonstrate that new extensions to the DER-CAM tool now allow propagation of utility uncertainty and (2) to identify extrema in the microgrid design outcomes. To that end we devised two scenarios, a maximum and minimum reliability scenario. In the maximum reliability scenario the grid is always available while for the minimum reliability scenario the grid is never available. Modeling these two extreme cases

will indicate the solution envelope for the impact that utility uncertainty may have on microgrid design and microgrid performance.

Results from the utility's reliability scenario testing reveal that the total annual cost and annual emission performance of the microgrid is somewhat insensitive to this parameter. For example, at w_{Cost} = 0.8 and w_{Cost} = 0.6 the total annual cost difference between the two scenarios was less than 5%. However, at certain extreme values the maximum reliability did save costs as expected. Further examining the reasons behind this insensitivity further motivates the study of uncertainty propagation in integrated microgrid design. This is because the current studies did not consider failure rates of the DER equipment itself and thus the main separation in cost between the scenarios was due to operational differences. At w_{Cost} = 0.4, however, the minimum reliability design invested in roughly 35% more electric energy storage than the maximum reliability case. Overall, we concluded from this testing that the integrated modeling technique and extension of DER-CAM have successfully enabled propagation of an additional source of uncertainty, but that more work should be done to both quantify this uncertainty and introduce the remaining sources into the model.

Answering these questions via an application to the Two Bridges community revealed that a primary limitation of this integrated modeling framework is that it is a two-stage optimization. The Design Explorer algorithm specifies a set of design variables, which must in turn be executed within the MILP sub-problem of the framework. In comparison, both the Supply Only and Demand First methods that we compared the framework to require only a single execution of the MILP subproblem. A typical successful optimization over the integrated modeling framework requires 200-300 MILP function evaluations. As computational power continues to increase this may not cause as much overhead, but in the short term there is added complexity that will fundamentally require more evaluations than conventional design approaches.

CHAPTER VII

CONCLUSIONS

7.1 Summary & Conclusions

Stakeholders have always experienced the need to maintain critical functions such as refrigeration of vaccines, power to servers and power to critical wings of hospitals. Yet the realities of climate change and sever storms are driving the desire for increased power reliability and resiliencey to new heights. Demand for local power generation is growing at such a rate that industry best estimates predict this market to grow to $40B in revenue globally by 2020. Microgrids, both physical and virtual, which are small-scale systems of loads and DGs that can operate independent of the utility grid are a technology poised to help overcome many of the challenges related to power reliability and resilience.

While the objectives of microgrid design appear simple, rationally evaluating microgrid design options is difficult for several reasons. Primarily, it is evaluating the multiple criteria of performance that make this task difficult. In addition to satisfying multiple criteria, microgrid designers must handle a large number of uncertainty sources that affect system performance. Uncertainty exists across the two coupled, technical sub-systems of demand and supply.

Given the number of current obstacles to performance based design of microgrids we argue that current methods are insufficient due to limited modeling capabilities. Existing microgrid system models do not (1) incorporate a framework for considering major sources of uncertainty and (2) do not allow decision makers to select design parameters across the interacting technical sub-systems of demand and supply. Existing tools that allow integrated system modeling do not adequately model the building thermal demand and ignores effects due to solar radiation, geometry, air infiltration, occupants, controls and heat capacity. In this work we addressed three primary hypotheses related to the modeling of microgrid systems for improved performance based design:

Hypothesis 1: An integrated microgrid system model with high resolution demand and supply models will enable decision makers to analyze more design options and decision variables

than is possible with currently available tools.

Hypothesis 2: Microgrid system designs selected via the integrated method will be more preferred than solutions determined via specifying decision variables on either the demand or supply side alone.

Hypothesis 3: Defining a resiliency framework for the integrated microgrid system model will enable decision makers to model scenario uncertainty regarding the utility's reliability. As resilience and load control are closely related, this work also shows that the resilience framework may be interpreted as an abstract model of an optimal load control algorithm.

This dissertation addresses the main hypotheses by first defining a reduced order demand sub-model as a core component of the integrated system model. To create a tractable optimization problem we also introduce a means of optimizing over the expanded set of demand side investment options. Next, we defined the gaps in resilience based modeling of microgrids generally with particular focus on the DER-CAM tool, which we apply within our integrated system model with additional constraints. Finally, we introduce a framework for co-simulating the two sub-models as well as present a design application focused on a hypothetical mixed use residential area in Manhattan. Based on these studies we conclude that the integrated system model is indeed adequate for modeling several microgrid decision scenarios in both accuracy and computation efficiency. As such we offer several modeling recommendations:

Conclusion 1: Model building aggregate as a reduced order demand model. Multiple building stock modeling studies focus on modeling each building as a single instance (Reinhart and Davila, 2016; Quan et al., 2015). This is computationally expensive and requires a lot of upfront data regarding each building (Quan et al., 2015). Zhao (2012) showed that the normative modeling approach of ISO (2008) is sufficient for modeling individual buildings with the same input parameters. Zhao (2012) then used clusters of the same building type to identify the parameters of a building portfolio. We extend this work by modeling a collection of mixed building types as a single reduced order model instance. This method, however, is not without limitations. For example, there are documented deficiencies in estimating the peak load. The decision to model a building stock as a single reduced order model instance was made to facilitate the co-simulation of demand with the

DER-CAM tool and the output of this single instance model is within 10% of MAPE at an hourly resolution for all performance indicators. In addition, the demand modeling tool requires limited levels of information and generally the complexity of the tool matches the level of information at earlier stages of design. Promising advances to this methodology are high-resolution, statistical energy models especially in light of the work of Tian et al. (2015) to identify correlations between explanatory variables.

Conclusion 2: Model the design parameters of the building aggregate as continuous variables with Pareto efficient cost functions. One implication of modeling a building aggregate is that the design parameters are discretely valued. Then if a decision maker models each building within an aggregate individually and considers multiple levels and multiple design parameters for each building the design option space grows to a size that is impractical to search via many common algorithms. A common means of overcoming optimization problems with many discrete variables is to use modified direct search techniques, which include stochastic methods like genetic algorithms.

One reason that these design spaces are impractical to search is that typical direct search techniques are not efficient in how they specify the design combinations to evaluate. When it comes to the retrofit or design of a community, it is apparent that a number of different design parameter combinations can result in the same cost. We overcome the inefficient search processes that do not account for this one-to-many relationship by generating cost functions based on linear interpolation of the Pareto efficient design combinations. This method is an improvement over a genetic algorithm as it results in the same final decision, but in an order of magnitude fewer function evaluations when starting from the same search point.

This method is analogous to modeling the building stock's meta parameters with cost functions derived from average data regarding the various physical components; however, this method explicitly determines the relationship between the specific options defined by a decision maker and their cost.

Conclusion 3: Specify outage scenarios and percentage of demand that can be unmet without penalty. The typical microgrid design for the grid connected case will specify enough gas driven generation to meet the peak demand of the site. In addition, the decision maker will specify a number of desired hours of protection and then a battery is sized such that it can meet the

peak demand for the requested number of hours. This conventional method is capital intensive. We propose a method that allows the decision maker to specify the expected outage scenarios, which is an improvement over the current methods because it finds the optimum investment choice while accounting for actual hourly operations.

In addition, a decision maker is neutral to unmet demand in certain situations. For instance, in an off-grid facility or in a facility with controllable loads that can be shed to optimize performance the decision maker is neutral to these loads being lost. Prior work has not addressed the ability of the decision maker to define a level of required resilience in early stage design as an abstraction of optimal control modeling. We add a resilience constraint to the DER-CAM modeling tool that allows a decision maker to specify which percentage of the annual demand is non-critical and can be shed at no cost; this method leads to microgrid designs that require less initial investment capital in generation.

Conclusion 4: Model an integrated microgrid system via the co-simulation methodology introduced in this work for joint decision making scenarios with decision making power over both supply and demand Testing our hypothesis via a sample case study shows that an integrated modeling framework allows a decision maker to find more preferential investment decisions over two conventional methods. The integrated optimization approach results in better decision making than either reducing demand of the building stock to a pre-defined level and then specifying the DER investments (Demand First) and better than simply accepting the building stock as is and then finding the optimal DER investments for the given resilience requirement (Supply Only). This recommendation is supported by these additional observations from a sample case:

1. Optimization results of the integrated system model return solutions on average exhibit an 8% total annual cost reduction and 18% reduction in CO_2 emissions versus the Supply Only case. Similarly, the results on average reduce total annual cost by 5% and annual emissions by 17% for the Demand First case.

2. The integrated system model explores a more complete demand option space that is at least an order of magnitude larger within an existing framework.

3. Investment in demand side improvement measures determined by the integrated modeling

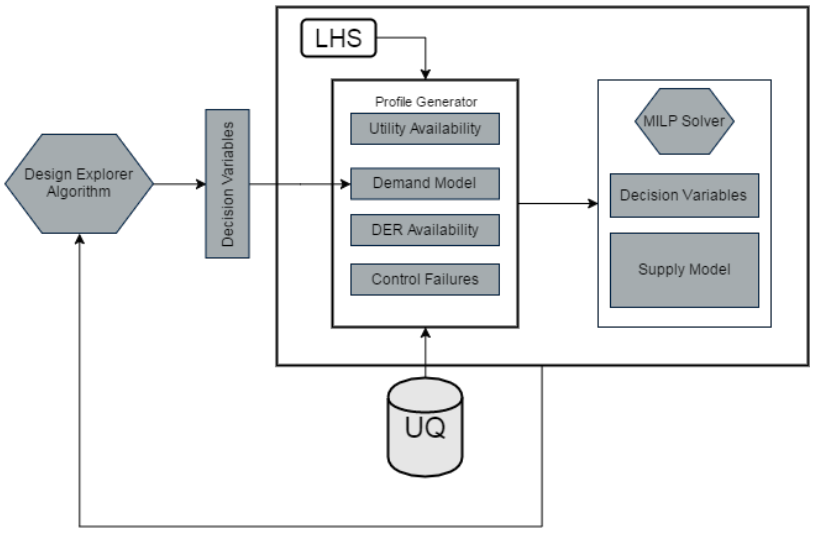

Figure 32: Work in this dissertation has established a framework for propagating uncertainties through an integrated microgrid system model, but future work should build this framework out and include generators of random processes.

methodology average less than 5% of the overall investment cost.

Applying this integrated modeling methodology to an example microgrid design case we confirm that the methodology is indeed an improvement over conventional design methods. While the Pareto efficient search method undoubtedly reduced the problem to a tractable form it is important to note that a limitation of the integrated approach is the increase of function evaluations required to determine an optimal microgrid design. This is due to the two-step formulation of the optimization, which must execute the DER-CAM tool for each new design variant generated by the Design Explorer algorithm. Overall, we find the approach satisfactory and recommend its use in a number of joint decision scenarios.

7.2 Recommendations for Future Work

Prior to looking forward, it's best to briefly summarize where we have come from and where we currently stand in regards to our knowledge of microgrid system design at the conclusion of this work. Chiefly, we have shown that a feasible implementation exists to model the demand and supply of a microgrid system at a high-resolution. By feasible we mean that the implementation does not require more information of the decision scenario than a decision maker has available, the implementation does not over burden current levels of computational power and most importantly

the methodology discussed in the previous chapters opens doors to further exploration in the field.

The integrated microgrid model we have presented had three primary goals: (1) allow decision makers simultaneous access to decision variables on both the supply and demand side of microgrid models, (2) establish a framework for deeper studies into reliability and resilience based design of microgrids and (3) facilitate the use of demand uncertainty research in microgrid design. To that aim we have succeeded on several fronts, but recognize there is more to be desired.

Demand Modeling The simplified demand model introduced in this work upholds the fundamental physical assumptions required to accomplish basic energy modeling of buildings. It has advanced the previous thermal demand generator of DER-CAM to a great degree simply by accounting for building geometry, solar radiation and thermal mass effects. Simplified schedules, the ability to model air infiltration and other tuning parameters that allow more advanced building representations go a long way in brining this integrated system model on par with the state-of-the-art in building energy modeling. One aspect, however, that did not receive the attention it deserved is the impact of peak demand modeling on the final microgrid designs. Microgrid design in practice is often presented in extremely simplified terms, in which the generator capacity is sized to be 110% of the historical peak electric demand. Given the known shortcomings of simplified heat balance methods to capture true peak demand it is important for future work to attempt to quantify the additional model form uncertainty added due to these simplifications.

Specifying Risk Preferences In this work we grapple with placing a value on reliability and resilience. Service interruptions in real systems have real costs, which may or may not be explicitly known by a decision maker. Utility companies, large industrial power consumers and some commercial consumers make it their job to know the cost of service interruptions. The cost of a given interruption arises from the magnitude of lost demand, specific outage costs, outage duration and outage frequency. This information may be culled into a customer specific damage function and then outages may be translated directly into a monetary equivalent. In this work we took a different approach and instead of translating outages into monetary equivalents we decided to constrain the sizing problem such that systems that did not meet a desired level of reliability could not be designed. To that end we incorporated a constraint within the DER-CAM tool that allows the decision maker to specify both the upper limit of total demand not met in a year as well as the maximum

amount of demand not met in a given hour. While this works to an extent, there are other important constraints we missed such as frequency and duration, which have been discussed within the context of the generic unit commitment problem before. The challenge here is to evaluate which approach is more useful: specifying more constraints or specifying damage functions.

Modeling Controls Advanced controls are transforming the microgrid industry. In this dissertation, however, we do not model the controls within the microgrid explicitly. There is a growing need to understand the various impacts that the supervisory control of the building and microgrid have on design sizing of systems. While researchers have developed optimal control strategies with embedded building models typically of data driven formulations, there is still room to better understand the role of controls modeling during design. For instance, modeling a demand response control during design may indicate to a decision maker that less generation capacity is required yet if the controller fails in reality and the system is now undersized was it a rational decision to incorporate controls modeling in the design?

Siemens completed a recent study of two 2 MW CHP generators servicing a microgrid and found several interesting control actions that conflicted with typical control approaches (Wood, 2016a). Overall, control investment constitutes approximately 15% of the microgrid investment compared to 50% due to generation technology. Results of the control study revealed that the sizes of the two CHP generators were not optimized for the building's demand profile and more money could have been saved during operations and initial investment. Therefore there is a need to critically examine the trade off between different control strategies and initial investment costs, which can potentially be achieved through more explicit modeling techniques.

To explicitly model the possible control interactions between supply and demand requires high fidelity models that can communicate at the simulation time step. Sharma et al. (2016) illustrates such a setup, but in this work we wished to avoid the additional complexity required to establish this modeling approach. Instead we reinterpret the resilience constraints as analogous to specifying an optimal controller, but in this case the decision maker knows the load loss levels at which constraints on the building side are violated. By having the decision maker denote this information as a supply modeling constraint we circumvent the need to explicitly model damage functions on the demand side, but this is an area that could use additional research and exploration.

Uncertainty Quantification and Optimization Under Uncertainty There are a number of real sources of uncertainty in microgrid operation: thermal and electric power demand profiles, the utility's reliability (i.e., failure frequency and duration), power generation from renewable sources, reliability of DERs, control system reliability, construction issues and maintenance. As we mentioned in the introduction these uncertainties produce a number of design challenges and one example of the ongoing challenges are the lack of performance guarantees and insurance in the microgrid space.

Uncertainty quantification with respect to these identified sources is largely under-represented in the microgrid design literature. We feel that this work will be a launching point for incorporating uncertainty sources in microgrid design. This work focuses on a deterministic optimization, but Fig. 32 details a framework for microgrid optimal design under uncertainty with particular focus on the database of quantified uncertainty. This approach relies on a sampling methodology to generate reliability traces of the utility, DER technologies and the demand given a base design parameter set. This approach is similar to stochastic unit commitment problems defined in the literature, which are commonly solved by executing a deterministic simulation for a number of enumerated scenarios.

Jones (2015) acknowledge that one of the more difficult aspects of uncertainty to capture in microgrid performance is the frequency of control failures. For that reason we include control failures in the diagram and consider it a pressing issue for further research. Overall Fig. 32 represents a potentially comprehensive approach to uncertainty propagation throughout integrated microgrid design. Such a methodology could be used to further the emergence of performance contracts in microgrids and potentially usher in more reliable systems. In conclusion, there are a number of open questions remaining within the field of microgrid design especially in regards to performance guarantees and it is the goal of this work to provide a starting point for more advanced study into more complete uncertainty quantification throughout the design process.

REFERENCES

Ackermann, T., Andersson, G., and Söder, L. 2001. Distributed generation: a definition. *Electric power systems research*, 57(3):195–204.

Adamson, B. and Feist, W. 1988. Passivhaus. *Passivhaus Institut, Darmstadt, Germany*.

Amara, F., Agbossou, K., Cardenas, A., Dubé, Y., and Kelouwani, S. 2015. Comparison and simulation of building thermal models for effective energy management. *Smart Grid and Renewable Energy*, 6(04):95.

Anderson, R. and Roberts, D. R. 2008. *Maximizing residential energy savings: Net zero energy home technology pathways*. National Renewable Energy Laboratory.

Arora, J., Huang, M., and Hsieh, C. 1994. Methods for optimization of nonlinear problems with discrete variables: a review. *Structural optimization*, 8(2-3):69–85.

ASHRAE 2009. *Handbook – Fundamentals*. ASHRAE.

Audet, C. and Dennis Jr, J. E. 2004. A pattern search filter method for nonlinear programming without derivatives. *SIAM Journal on Optimization*, 14(4):980–1010.

Back, T. 1996. *Evolutionary algorithms in theory and practice: evolution strategies, evolutionary programming, genetic algorithms*. Oxford university press.

Best, R. E., Flager, F., and Lepech, M. D. 2015. Modeling and optimization of building mix and energy supply technology for urban districts. *Applied Energy*, 159:161–177.

Blochwitz, T., Otter, M., Arnold, M., Bausch, C., Clauß, C., Elmqvist, H., Junghanns, A., Mauss, J., Monteiro, M., Neidhold, T., et al. 2011. The functional mockup interface for tool independent exchange of simulation models. In *8th International Modelica Conference, Dresden*, pages 20–22.

Booker, A. J. 1998. Design and analysis of computer experiments. *AIAA paper*, (1998-4757).

Booker, A. J., Dennis Jr, J., Frank, P. D., Serafini, D. B., Torczon, V., and Trosset, M. W. 1999. A rigorous framework for optimization of expensive functions by surrogates. *Structural optimization*, 17(1):1–13.

Booker, A. J., Frank, P. D., Dennis Jr, J., and Moore, D. W. 1998. Managing surrogate objectives to optimize a helicopter rotor design further experiments aiaa mdo 98-4717.

Brooke, A., Kendrick, D., Meeraus, A., Raman, R., and America, U. 1998. The general algebraic modeling system. *GAMS Development Corporation*.

Bueno, B., Wienold, J., Katsifaraki, A., and Kuhn, T. E. 2015. Fener: A radiance-based modelling approach to assess the thermal and daylighting performance of complex fenestration systems in office spaces. *Energy and Buildings*, 94:10–20.

Buresch, M. 1983. Photovoltaic energy systems: Design and installation.

Campbell, R. J. 2012. Weather-related power outages and electric system resiliency. Congressional Research Service, Library of Congress.

Chauhan, A. and Saini, R. 2014. A review on integrated renewable energy system based power generation for stand-alone applications: Configurations, storage options, sizing methodologies and control. *Renewable and Sustainable Energy Reviews*, 38:99–120.

Chinneck, J. W. 2006. Practical optimization: a gentle introduction. *Systems and Computer Engineering), Carleton University, Ottawa. http://www. sce. carleton. ca/faculty/chinneck/po. html*.

Cho, H., Mago, P. J., Luck, R., and Chamra, L. M. 2009. Evaluation of cchp systems performance based on operational cost, primary energy consumption, and carbon dioxide emission by utilizing an optimal operation scheme. *Applied Energy*, 86(12):2540–2549.

Crawley, D. B., Lawrie, L. K., Winkelmann, F. C., Buhl, W. F., Huang, Y. J., Pedersen, C. O., Strand, R. K., Liesen, R. J., Fisher, D. E., Witte, M. J., et al. 2001. Energyplus: creating a new-generation building energy simulation program. *Energy and Buildings*, 33(4):319–331.

Deru, M., Field, K., Studer, D., Benne, K., Griffith, B., Torcellini, P., Liu, B., Halverson, M., Winiarski, D., Rosenberg, M., et al. 2011. Us department of energy commercial reference building models of the national building stock.

Dillon, K. and Colton, J. 2014. A design methodology for the economic design of vaccine warehouses in the developing world. *Building and Environment*, 82:160–170.

EIA, U. 2011. Annual energy review. *Energy Information Administration, US Department of Energy: Washington, DC* `www.eia.doe.gov/emeu/aer`.

Energy Information Agency (EIA) 2013. Electricity - annual disturbance events archive. `http://www.eia.gov/electricity/data/disturbance/disturb_events_archive.html`.

Fuentes-Cortés, L. F., Ávila-Hernández, A., Serna-González, M., and Ponce-Ortega, J. M. 2015. Optimal design of chp systems for housing complexes involving weather and electric market variations. *Applied Thermal Engineering*.

Golberg, D. E. 1989. Genetic algorithms in search, optimization, and machine learning. *Addion wesley*, 1989:102.

Gu, W., Tang, Y., Peng, S., Wang, D., Sheng, W., and Liu, K. 2015. Optimal configuration and analysis of combined cooling, heating, and power microgrid with thermal storage tank under uncertainty. *Journal of Renewable and Sustainable Energy*, 7(1):013104.

Hakimi, S. and Moghaddas-Tafreshi, S. 2014. Optimal planning of a smart microgrid including demand response and intermittent renewable energy resources. *Smart Grid, IEEE Transactions on*, 5(6):2889–2900.

Halverson, J. B. and Rabenhorst, T. 2013. Hurricane sandy: the science and impacts of a superstorm. *Weatherwise*, 66(2):14–23.

Handbook, A. F. 2009. American society of heating, refrigerating and air-conditioning engineers. *Inc.: Atlanta, GA, USA*.

Hansen, J., Sato, M., Hearty, P., Ruedy, R., Kelley, M., Masson-Delmotte, V., Russell, G., Tselioudis, G., Cao, J., Rignot, E., et al. 2016. Ice melt, sea level rise and superstorms: Evidence from paleoclimate data, climate modeling, and modern observations that 2 c global warming could be dangerous. *Atmospheric Chemistry and Physics*, 16(6):3761–3812.

Hazelrigg, G. A. 2012. *Fundamentals of Decision Making For Engineering Design and Systems Engineering*.

Henninger, R. H., Witte, M. J., and Crawley, D. B. 2004. Analytical and comparative testing of energyplus using iea hvac bestest e100–e200 test suite. *Energy and Buildings*, 36(8):855–863.

Hensen, J. 1995. Modelling coupled heat and airflow: ping pong vs. onions. In *DOCUMENT-AIR INFILTRATION CENTRE AIC PROC*, pages 253–253. Citeseer.

Hensen, J. L. and Lamberts, R. 2012. *Building performance simulation for design and operation*. Routledge.

Hooke, R. and Jeeves, T. A. 1961. "direct search"solution of numerical and statistical problems. *Journal of the ACM (JACM)*, 8(2):212–229.

Hu, H. 2009. *Risk-conscious Design of Off-grid Solar Energy Houses*. PhD thesis, Georgia Institute of Technology. `http://hdl.handle.net/1853/31814`.

Hu, M. and Cho, H. 2014. A probability constrained multi-objective optimization model for cchp system operation decision support. *Applied Energy*, 116:230–242.

IEEE Standards Coordinating Committee 21 2011. Ieee guide for design, operation, and integration of distributed resource island systems with electric power systems.

International Living Future Institute 2016. The living building challenge. `http://living-future.org/lbc`.

ISO, E. 2008. 13790: Energy performance of buildings–calculation of energy use for space heating and cooling (en iso 13790: 2008). *European Committee for Standardization (CEN), Brussels*.

Johnson, B. J., Starke, M. R., Abdelaziz, O. A., Jackson, R. K., and Tolbert, L. M. 2014. A method for modeling household occupant behavior to simulate residential energy consumption. In *Innovative Smart Grid Technologies Conference (ISGT), 2014 IEEE PES*, pages 1–5. IEEE.

Jones, R. 2015. How reliable is your microgrid? *Public Utilities Fortnightly*, pages 26–36.

Kapsalaki, M., Leal, V., and Santamouris, M. 2012. A methodology for economic efficient design of net zero energy buildings. *Energy and Buildings*, 55:765–778.

Kassakian, J. G., Schmalensee, R., Desgroseilliers, G., Heidel, T. D., Afridi, K., Farid, A., Grochow, J., Hogan, W., Jacoby, H., Kirtley, J., et al. 2011. The future of the electric grid. *Massachusetts Institute of Technology, Tech. Rep*.

Kavgic, M., Mavrogianni, A., Mumovic, D., Summerfield, A., Stevanovic, Z., and Djurovic-Petrovic, M. 2010. A review of bottom-up building stock models for energy consumption in the residential sector. *Building and environment*, 45(7):1683–1697.

Keep, T. M., Sifuentes, F. E., Auslander, D. M., and Callaway, D. S. 2011. Using load switches to control aggregated electricity demand for load following and regulation. In *Power and Energy Society General Meeting, 2011 IEEE*, pages 1–7. IEEE.

Kjølle, G. H. 1996. Power supply interruption costs: Models and methods incorporating time dependent patterns. Technical report, Norges Teknisk-Naturvitenskapelige Univ.

Lanckriet, G. R. and Sriperumbudur, B. K. 2009. On the convergence of the concave-convex procedure. In *Advances in neural information processing systems*, pages 1759–1767.

Lee, S. H., Zhao, F., and Augenbroe, G. 2013. The use of normative energy calculation beyond building performance rating. *Journal of Building Performance Simulation*, 6(4):282–292.

Li, L., Mu, H., Gao, W., and Li, M. 2014. Optimization and analysis of cchp system based on energy loads coupling of residential and office buildings. *Applied Energy*, 136:206–216.

Li, X. and Wen, J. 2014. Review of building energy modeling for control and operation. *Renewable and Sustainable Energy Reviews*, 37:517–537.

Lilienthal, P., Gilman, P., and Lambert, T. 2005. *HOMER® Micropower Optimization Model*. United States. Department of Energy.

Luc, D. T. 2008. Pareto optimality. *Pareto optimality, game theory and equilibria*, pages 481–515.

Makarov, Y. V., Loutan, C., Ma, J., and de Mello, P. 2009. Operational impacts of wind generation on california power systems. *Power Systems, IEEE Transactions on*, 24(2):1039–1050.

Marszal, A. J., Heiselberg, P., Bourrelle, J., Musall, E., Voss, K., Sartori, I., and Napolitano, A. 2011. Zero energy building–a review of definitions and calculation methodologies. *Energy and Buildings*, 43(4):971–979.

Mazria, E. 2006. The 2030 challenge. *Architecture*, 2030.

McGlade, C. and Ekins, P. 2015. The geographical distribution of fossil fuels unused when limiting global warming to 2 [deg] c. *Nature*, 517(7533):187–190.

McKenna, R., Merkel, E., Fehrenbach, D., Mehne, S., and Fichtner, W. 2013. Energy efficiency in the german residential sector: a bottom-up building-stock-model-based analysis in the context of energy-political targets. *Building and Environment*, 62:77–88.

Meiqin, M., Chang, L., and Ming, D. 2008. Integration and intelligent control of micro-grids with multi-energy generations: A review. In *Sustainable Energy Technologies, 2008. ICSET 2008. IEEE International Conference on*, pages 777–780. IEEE.

ModelCenter, P. 2015. 11.0. blacksburg, va, usa: Phoenix integration. *Inc.(http://www. phoenix-int. com/)*.

Morvaj, B., Evins, R., and Carmeliet, J. 2015. The impact of low energy buildings on the optimal design of distributed energy systems and networks. In *14th Conference of International Building Performance Simulation Association*.

Murray, W. and Ng, K.-M. 2002. Algorithms for global optimization and discrete problems based on methods for local optimization. In *Handbook of global optimization*, pages 87–113. Springer.

Nelder, J. A. and Mead, R. 1965. A simplex method for function minimization. *The computer journal*, 7(4):308–313.

Nocedal, J. and Wright, S. J. 2006. Sequential quadratic programming. *Numerical Optimization*, pages 529–562.

Owen, A. B. 1992. Orthogonal arrays for computer experiments, integration and visualization. *Statistica Sinica*, pages 439–452.

Padhy, N. P. 2004. Unit commitment-a bibliographical survey. *IEEE Transactions on power systems*, 19(2):1196–1205.

Peterson, K., Torcellini, P., and Grant, R. 2015. A common definition of zero energy buildings. `http://energy.gov/sites/prod/files/2015/09/f26/bto_common_definition_zero_energy_buildings_093015.pdf`.

Pourmousavi, S. A. and Nehrir, M. H. 2012. Real-time central demand response for primary frequency regulation in microgrids. *Smart Grid, IEEE Transactions on*, 3(4):1988–1996.

Priddle, R. 2015. World energy outlook 2015. *International Energy Agency*, 1.

Quan, S. J., Li, Q., Augenbroe, G., Brown, J., and Yang, P. P.-J. 2015. Urban data and building energy modeling: A gis-based urban building energy modeling system using the urban-epc engine. In *Planning Support Systems and Smart Cities*, pages 447–469. Springer.

Razanousky, M. and Hyams, M. 2010. Microgrids: An assessment of the value, opportunities, and barriers to deployment in new york state. `http://www.nyserda.ny.gov/-/media/Files/Publications/Research/Electic-Power-Delivery/microgrids-value-opportunities-barriers.pdf`. [Online; accessed 21-November-2015].

Reinhart, C. F. and Davila, C. C. 2016. Urban building energy modeling–a review of a nascent field. *Building and Environment*, 97:196–202.

Rezaee, R., Brown, J., Augenbroe, G., and Kim, J. 2015. Assessment of uncertainty and confidence in building design exploration. *Artificial Intelligence for Engineering Design, Analysis and Manufacturing*, 29(04):429–441.

Robinson, D. 2012. *Computer modelling for sustainable urban design: Physical principles, methods and applications*. Routledge.

Sartori, I., Napolitano, A., and Voss, K. 2012. Net zero energy buildings: A consistent definition framework. *Energy and Buildings*, 48:220–232.

Sharma, I., Dong, J., Malikopoulos, A. A., Street, M., Ostrowski, J., Kuruganti, T., and Jackson, R. 2016. A modeling framework for optimal energy management of a residential building. *Energy and Buildings*.

Siddiqui, A. S., Marnay, C., Edwards, J. L., Firestone, R., Ghosh, S., and Stadler, M. 2005. Effects of carbon tax on microgrid combined heat and power adoption. *Journal of Energy Engineering*, 131(1):2–25.

Simpkins, T., Cutler, D., Hirsch, B., Olis, D., and Anderson, K. 2015. Cost-optimal pathways to 75% fuel reduction in remote alaskan villages. In *Technologies for Sustainability (SusTech), 2015 IEEE Conference on*, pages 125–130. IEEE.

Sodha, M. S., Bansal, N., Bansal, P., Kumar, A., and Malik, M. 1986. Solar passive building.

Stadler, M. 2008. Distributed energy resources on-site optimization for commercial buildings with electric and thermal storage technologies. *Lawrence Berkeley National Laboratory*.

Stadler, M. 2009a. Effect of heat and electricity storage and reliability on microgrid viability: a study of commercial buildings in california and new york states. *Lawrence Berkeley National Laboratory*.

Stadler, M. 2009b. Optimal technology investment and operation in zero-net-energy buildings with demand response. *Lawrence Berkeley National Laboratory*.

Stadler, M., Groissböck, M., Cardoso, G., and Marnay, C. 2014. Optimizing distributed energy resources and building retrofits with the strategic der-camodel. *Applied Energy*, 132:557–567.

Stadler, M., Kloess, M., Groissböck, M., Cardoso, G., Sharma, R., Bozchalui, M. C., and Marnay, C. 2013. Electric storage in californias commercial buildings. *Applied Energy*, 104:711–722.

Stadler, M., Siddiqui, A., Marnay, C., Aki, H., and Lai, J. 2011. Control of greenhouse gas emissions by optimal der technology investment and energy management in zero-net-energy buildings. *European Transactions on Electrical Power*, 21(2):1291–1309.

Stephens, C. and Baritompa, W. 1998. Global optimization requires global information. *Journal of Optimization Theory and Applications*, 96(3):575–588.

Storn, R. and Price, K. 1995. *Differential evolution-a simple and efficient adaptive scheme for global optimization over continuous spaces*, volume 3. ICSI Berkeley.

Sun, Y. 2014. *Closing the Building Energy Performance Gap By Improving Our Predictions*. PhD thesis, Georgia Institute of Technology. http://hdl.handle.net/1853/52285.

Sun, Y., Huang, P., and Huang, G. 2015. A multi-criteria system design optimization for net zero energy buildings under uncertainties. *Energy and Buildings*, 97:196–204.

Swan, L. G. and Ugursal, V. I. 2009. Modeling of end-use energy consumption in the residential sector: A review of modeling techniques. *Renewable and sustainable energy reviews*, 13(8):1819–1835.

Tian, W., Choudhary, R., Augenbroe, G., and Lee, S. H. 2015. Importance analysis and meta-model construction with correlated variables in evaluation of thermal performance of campus buildings. *Building and Environment*, 92:61–74.

US D.O.E. 2012. Building energy software tools directory. https://buildingdata.energy.gov/cbrd/resource/705.

Wilcox, S. and Marion, W. 2008. *Users manual for TMY3 data sets*. National Renewable Energy Laboratory Golden, CO.

Wood, E. 2015. How fast is the microgrid market growing, really? https://microgridknowledge.com/how-fast-is-the-microgrid-market-growing-really/. [Online; accessed 3-August-2016].

Wood, E. 2016a. The role of the advanced microgrid controller in microgrid financing. http://microgridknowledge.com/advanced-microgrid-controller/. [Online; accessed 17-July-2016].

Wood, E. 2016b. What would you pay for energy resiliency? http://microgridknowledge.com/energy-resiliency/. [Online; 23-April-2016].

Xu, X., Mitra, J., Wang, T., and Mu, L. 2014. Evaluation of operational reliability of a microgrid using a short-term outage model. *IEEE Transactions on Power Systems*, 29(5):2238–2247.

Zakula, T., Armstrong, P., and Norford, L. 2014. Modeling environment for model predictive control of buildings. *Energy and Buildings*, 85:549–559.

Zhang, Y. and Lu, N. 2013. Demand-side management of air conditioning cooling loads for intra-hour load balancing. In *Innovative Smart Grid Technologies (ISGT), 2013 IEEE PES*, pages 1–6. IEEE.

Zhao, F. 2012. *Agent-based Modeling of Commercial Building Stocks for Energy Policy and Demand Response Analysis*. PhD thesis, Georgia Institute of Technology.